Rheology of Pure Ionic Liquids and Their Complex Fluids

A Review

Shakeel, Ahmad; Mahmood, Hamayoun; Farooq, Ujala; Ullah, Zahoor; Yasin, Saima; Iqbal, Tanveer; Chassagne, Claire; Moniruzzaman, Muhammad

DOI
10.1021/acssuschemeng.9b02232

Publication date
2019

Document Version
Final published version

Published in
ACS Sustainable Chemistry and Engineering

Citation (APA)
Shakeel, A., Mahmood, H., Farooq, U., Ullah, Z., Yasin, S., Iqbal, T., Chassagne, C., & Moniruzzaman, M. (2019). Rheology of Pure Ionic Liquids and Their Complex Fluids: A Review. *ACS Sustainable Chemistry and Engineering*, *7*(16), 13586-13626. https://doi.org/10.1021/acssuschemeng.9b02232

ACS Sustainable Chemistry & Engineering

Perspective

Cite This: ACS Sustainable Chem. Eng. 2019, 7, 13586−13626

pubs.acs.org/journal/ascecg

Rheology of Pure Ionic Liquids and Their Complex Fluids: A Review

Ahmad Shakeel,*[,†,‡] Hamayoun Mahmood,[‡] Ujala Farooq,[‡] Zahoor Ullah,[§] Saima Yasin,[‡] Tanveer Iqbal,[‡] Claire Chassagne,[†] and Muhammad Moniruzzaman[∥]

[†]Department of Hydraulic Engineering, Faculty of Civil Engineering and Geosciences, Delft University of Technology, Stevinweg 1, 2628 CN Delft, The Netherlands

[‡]Department of Chemical, Polymer & Composite Materials Engineering, University of Engineering & Technology, KSK Campus, Lahore, 54890 Pakistan

[§]Department of Chemistry, Balochistan University of Information Technology, Engineering, and Management Sciences, Quetta, Pakistan

[∥]Department of Chemical Engineering, Universiti Teknologi PETRONAS, 32610 Bandar Seri Iskandar, Perak, Malaysia

ABSTRACT: Ionic liquids (ILs) are liquid salts at ambient or lower temperatures and consist of ions and short-lived ion pairs. They are potential alternatives to toxic, hazardous, highly flammable, and volatile solvents for preparing solutions, dispersions, gels, composites, and polymeric melts. ILs have some very interesting and unique characteristics like good chemical and thermal stability and very low vapor pressures. They have good solvation interactions with a wide range of organic, inorganic, and polymeric compounds. They can enhance colloidal stability and the elasticity range of polymers. ILs are environmental friendly, easily recyclable, and structurally similar to the conventional solvents. For optimal performance, it is necessary to fully understand the rheological properties of ILs and their different systems for academic interests such as understanding the ability of ILs as processing aids particularly in film casting, fiber spinning and spraying, comprehension of thermodynamics and dynamics of polymer chains in ILs, analyzing the hydrodynamic volume of dispersed polymer, polymer−ILs interactions, characterizing the viscoelastic properties and nanophase−ILs interactions in nanocomposite systems, analyzing the plasticization efficiency, and the final properties of the composite system. The rheological analysis is also important for industrial purposes particularly for designing processing techniques and suitable operating conditions for IL based systems. The aim of this review is to give an overview of the rheological properties of pure ionic liquids and solutions, dispersions, gels, composites, and melts based on ionic liquids.

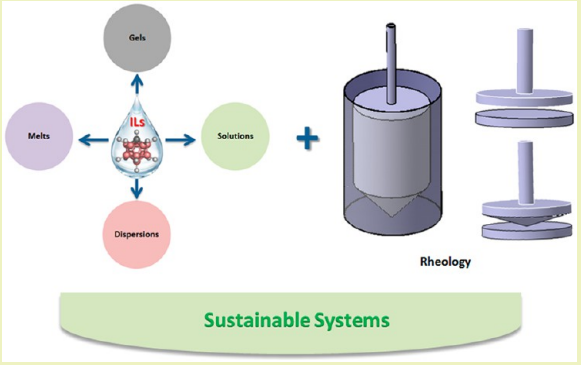

KEYWORDS: *Ionic liquid, Rheology, Gels, Solutions, Dispersions, Plasticizer*

INTRODUCTION

Ionic liquids (ILs) entirely consist of ions and are liquid at room temperature or below ambient temperatures.[1,2] Several unique features of ILs such as low vapor pressures,[3,4] excellent chemical and thermal stability,[5] higher solvation interactions with organic and inorganic compounds,[6,7] broad electrochemical windows, and excellent ionic conductivities make ILs good candidates as alternatives to volatile and toxic solvents for numerous applications.[8] Moreover, different physicochemical properties of ILs including their viscosity, density, polarity, solute solubility, etc. can be manipulated by selecting different combinations of cations and anions as well as substituent groups to meet particular needs.

ILs are typically composed of organic cations and organic or inorganic anions. The physical and chemical properties of ILs usually depend on the cation (e.g., its nature, symmetry, and length of substituent groups) and anion (structure and magnitude of charge delocalization).[9] Anions are accountable for their reactivity and chemical characteristics. ILs are capable of dissolving many compounds which are either insoluble or partially soluble in typical organic solvents, due to the presence of hydrogen bond acceptors such as Cl^-, $[Ac]^-$, and $[NO_3]^-$ in ILs.[10,11] Generally, the physical properties (i.e., viscosity, melting points, and density) of ILs are controlled by their cations. Indeed, the length and size of the cation molecules in ILs is the main controlling factor for the rheology of ILs.[12,13] This shows that unlike conventional molecular solvents, the ILs can be tweaked to optimize their properties and hence the overall economics of the process.[14] These properties make them suitable for a wide range of applications such as inorganic and organic synthesis and catalysis,[15−18] extraction and separation,[19−21] nanomaterial synthesis,[22,23] microreactors,[24] lubricants,[25] membrane preparation,[26] energy and sensors,[27] metal−organic frameworks,[28] food and bioproducts,[29] pharmaceut-

Received: April 22, 2019
Revised: July 17, 2019
Published: July 28, 2019

DOI: 10.1021/acssuschemeng.9b02232
ACS Sustainable Chem. Eng. 2019, 7, 13586−13626

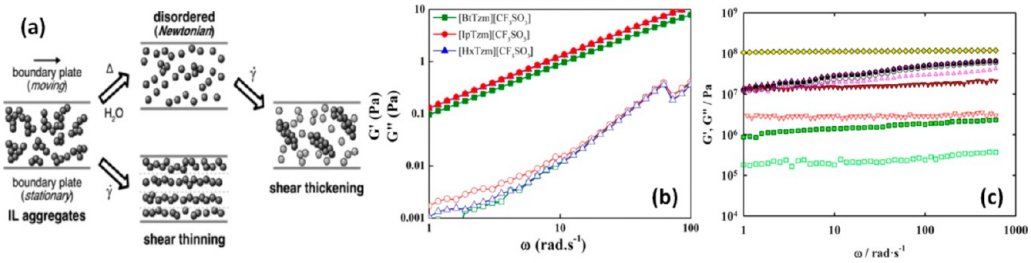

Figure 1. (a) Schematic representation of shear thinning and shear thickening behavior of IL as a function of shear rate and water addition, respectively [Reprinted with permission from ref 52. Copyright 2010. The Royal Society of Chemistry]. (b) Storage (open symbols) and loss (closed symbols) moduli as a function of angular frequency for different ILs [Reprinted with permission from ref 12. Copyright 2016. American Chemical Society]. (c) Storage (solid symbols) and loss (empty symbols) moduli as a function of angular frequency for: square, $[C_4C_1pyr][N(C_4F_9SO_2)_2]$; inverted triangle, $[C_4C_1pyr][C_4F_9SO_3]$; circle, $[C_8C_1im][C_4F_9SO_3]$; triangle, $[C_6C_1im][C_4F_9SO_3]$ and diamond, $[N_{4444}][C_4F_9SO_3]$ [Reprinted with permission from ref 65. Copyright 2017. American Chemical Society].

icals,[30] and polysaccharide processing.[31] In particular, the effective selective extraction of different components from polysaccharides is now possible by dissolving them in ILs, as shown by the studies from the last 10−15 years.[32] Many lignocellulosic and biopolymeric fibers regenerated from ILs solutions showed higher thermal and processing stability.[33]

The inspiration for performing rheological analysis comes from the idea that the numerous characteristics of materials witnessed in commercial applications can be interrelated with some easily investigated rheological properties. Several applications of rheology can be summarized as (i) rheological analysis of the material could provide some parameters which can be helpful to understand the physical or chemical structure of the material, (ii) rheological studies can provide a comparative analysis of similar materials but do not answer the question of whether the investigated material is good or bad, (iii) modeling the dynamic behavior and flow of materials using obtained rheological properties, (iv) analyzing the special rheological phenomena like solid−liquid transition, Weissenberg effect, etc. which can be important for some commercial applications.[34,35]

Rheological analysis of pure ionic liquids and their different systems like gels, dispersions, solutions, etc. is substantial for their efficient processing, design of appropriate equipment and process conditions, and manipulation of their properties for final application. The relaxation dynamics and structure−property relationships in ILs have been extensively investigated using rheological measurements.[36] The viscosity analysis as a function of temperature and shear rate enables the study of the ionic interactions and rotations within ILs.[37] Steady and dynamic rheological methods are also useful tools to assess the quality of ILs as solvents for polymeric materials in different processes such as film casting, fiber spinning, and spraying. Moreover, rheology can also provide a strong base to comprehend polymer−IL interactions, polymeric chain mobility, and hydrodynamic volume of polymer dispersed in ILs.[38,39] The aggregation behavior of surfactant based IL solutions can also be probed using rheology as an interesting tool.[40] Rheological characterization is complementary to other techniques in understanding the physical and structural changes such as phase separation, gelation, melting, viscoelasticity, and mechanical strength of the ionogels.[41] The rheological investigation of IL based suspensions enables manipulation of the viscoelastic properties of the resultant system by adjusting the concentration and surface functionalization of the dispersed phase in addition to the polarity of ILs.[42] Three types of dynamic tests can be performed to get the rheological properties of ILs based systems: (1) Frequency sweep tests in which storage modulus (G') and loss modulus (G'') are obtained as a function of frequency (ω) at fixed temperature and shear stress or shear strain according to the linear viscoelastic region identified in a stress/strain sweep test, (2) temperature ramp tests (or time cure tests) in which G' and G'' are determined as a function of temperature at fixed ω and applying a stress/strain within the linear viscoelastic region, and (3) time sweep tests in which G' and G'' are obtained as a function of time at fixed ω, temperature, and stress/strain.

A key element for the development of sustainable systems is the accessibility to the novel and unique chemical solvents[43,44] that allow fine-tuning of their physicochemical properties for particular applications through alterations/variations in chemical or physical parameters. ILs proved to be the evolving novel green solvents that provide such fine-tuning and alterations in physical and chemical properties.[45] Rheology is a convenient tool to study the influence of different physical and chemical parameters on the properties of complex systems.[46] Rheology also helps to verify the suitability of materials before their production and utilization on a larger scale. The principle objective of this study is to provide a brief overview of the current state-of-the-art on rheological characterization of pure ionic liquids and various ILs based systems including gels, suspensions, and polymeric solutions. Therefore, we believe that this study provides the crucial information about the fine-tuning of ILs (rheological) properties to efficiently develop sustainable systems for various applications.

RHEOLOGY OF PURE IONIC LIQUIDS (ILs)

Pure ionic liquids (ILs) belong to a class of materials that have fascinating properties that can be assessed by studying their structure−property relationships. In particular, quite a number of studies have focused on the relaxation dynamics of ILs in the vicinity of glass transition temperature (T_g) using rheological measurements. Viscosity and its dependence on both temperature and shear rate can, for instance, provide useful information about ionic interactions within ILs.[37,47]

Smith and co-workers reported the rheological analysis of five different protic ionic liquids (PILs) and their mixtures.[48] Ammonium based ILs displayed Newtonian behavior at low shear rates whereas they showed pseudoplastic shear thinning behavior at higher shear rates. They showed that the IL nanostructures (resulting from the strong electrostatic and hydrogen bonding attractions between ions which drive a solvophobic segregation of the nonpolar alkyl chains) was the controlling parameter for the shear thinning behavior whereas the viscosity was affected by both the hydrogen bonded network

DOI: 10.1021/acssuschemeng.9b02232
ACS Sustainable Chem. Eng. 2019, 7, 13586−13626

and the nanostructure. In another study, the rheological analysis of different protic ionic liquids demonstrated that the viscosity in the non-Newtonian regime is a function of stress and temperature.[49] The influence of alkyl chain length of cations and different anions on the rheological behavior of ILs was also investigated.[50] The shear-thinning behavior occurs at higher shear rates for longer alkyl chains. Likewise, a shear thinning behavior of ILs at higher shear rates was also reported by Gusain et al. which was linked to the disruption in interactives forces of ILs.[51] This disruption was even observed at lower shear rates for [N8888][BScB] whereas other studied ILs displayed almost Newtonian behavior at lower shear rates. This shear thinning behavior of ILs is highly dependent on the temperature which reduced/diminished at higher temperatures or shifted toward the higher shear rates due to the reduction in aggregates.[52,53]

Shear thickening behavior was also observed in the literature for ILs which was attributed to their ionic packing and orientation in the bulk fluid during shearing action.[49,52,54] This non-Newtonian behavior of ILs can be reversible or irreversible depending upon the interaction between ILs and the surface in contact and also on the alignment of IL molecules during shear thinning.[55] Moreover, the behavior became shear thickening, by adding more than 3−4 equivalents of water in ILs, due to the formation of cation−(water)−anion clusters and squeezing out of water from clusters as shown in Figure 1a.[52] In contrast, the shear thickening behavior that was observed for protic ILs of diisopropyl-ethylammonium having octanoate or heptanoate when acetonitrile or water was added, was attributed to the formation of aggregates.[56] In addition to the influence on non-Newtonian character of ILs, the incorporation of water lowered the viscosity (up to three times) of pure IL.[57]

The viscosity of ILs is usually equivalent to the oils, however, 2−4 orders of magnitude higher than the typical molecular solvents. This high viscosity of ILs can be fine-tuned by playing with the temperature or addition of cosolvent[58] but at the cost of reduction in useful properties of ILs. The viscosity of ILs can be changed up to 20% by varying the temperature within the range of 5 K.[59,60] Okoturo and VanderNoot investigated the viscosity of 23 different ILs over a temperature range from 10 to 70 °C. Arrhenius law was observed to be appropriate to fit the viscosity−temperature data of aprotic ILs, whereas the Vogel−Tamman−Fulcher relation was more suited to ILs having functionalized or a symmetric cation.[60,61] The viscosity and viscoelastic properties of ILs also decreased at the transition temperature for liquid crystalline to isotropic phase transformation.[55] Regueira et al. also reported the rheological characterization of two different ILs ($[C_2C_1im][C_6SO_4]$ and $[P_{6,6,6,14}][(C_2F_5)_3PF_3]$) and the results were compared with the reference oils used for lubrication.[62] Newtonian behavior was observed for both ILs and the viscosity values of $[C_2C_1im]$-$[C_6SO_4]$ were closer to that of polyalkylene glycol.

The functionalization of ILs can have a strong influence on the rheological fingerprint of ILs. Fluorinated ILs displayed non-Newtonian behavior (Newtonian at lower shear rates and shear thinning at higher shear rates) due to the existence of lamellar structure which was not present in pure ILs.[53,63] This lamellar structure disappeared at high temperatures and shear rate which was evident from the temperature dependent shear thinning behavior.[57] Similarly, a more pronounced shear rate dependent behavior was observed for fluorinated ILs.[50] The non-Newtonian character was also evident for the ILs functionalized with carboxyethyl, hydroxyethyl, benzyl, and cyanopropyl groups.[64] Dynamic rheological experiments revealed the liquid-like behavior of the ILs as evident from the values of storage and loss moduli ($G'' > G'$) (Figure 1b).[12] In contrast, fluorinated ILs displayed an elastic behavior as their storage modulus (G') was higher than their loss modulus (G'') over the entire studied frequency range, as shown in Figure 1c.[65]

Tao and Simon reported the rheological properties of imidazolium-based ILs having aromatic and cyclic groups.[66] Time−temperature superposition principle was employed to construct the reduced curves for dynamic shear moduli. The results demonstrated that all ILs displayed the same behavior, i.e., transition from flow to glassy behavior as a function of increasing frequency, having glassy moduli of almost 1 GPa. The higher fragility of ILs with aromatic groups (ranging from 117 to 130) as compared to the aliphatic groups was noted. A unique rheological behavior of azolium azolate based ILs was described by Pogodina et al.[67] This uniqueness resulted from the high elasticity of ILs at low frequency and the failure of time−temperature superposition principle. This peculiar behavior was attributed to the particular interactions in nitrogen rings of azolate ILs. The comparative rheological analysis of protic and aprotic ILs was performed by Sharma et al.[68] The results depicted that the viscosity of the protic ILs was higher than that of aprotic ILs whereas the polarity of protic ILs was smaller than the aprotic ones, presented in Figure 2. Moreover, the viscosity

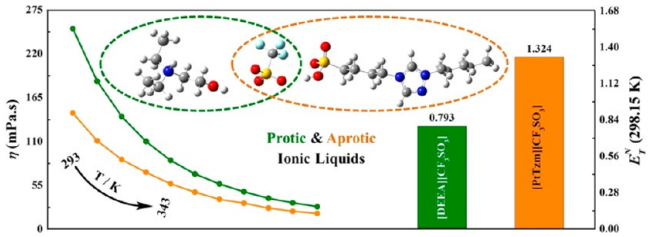

Figure 2. Temperature dependent viscosity curves and polarities of protic and aprotic ionic liquids [Reprinted with permission from ref 68. Copyright 2017. John Wiley and Sons].

decreased as a function of temperature due to the enhancement in Brownian motion of the ions in investigated ILs. The experimental conditions such as temperature, shear rate or frequency range in addition to the measuring device can have a significant effect on the rheological properties. Therefore, a summary of the rheological analysis of different IL systems along with their experimental conditions and key rheological parameters is presented in Table 1.

Blanco-Díaz et al. carried out the molecular dynamics simulations to predict the molecular interactions and rheology of ILs.[69] A Newtonian plateau regime was observed at very low shear rates followed by a shear thinning region where the viscosity values showed a decrease (Figure 3b). The calculated value of zero shear viscosity was in good agreement with the experimental values from the literature. Similarly, the stability of nanostructures in ILs under shearing conditions was investigated by Butler and Müller-Plathe using molecular dynamics simulations.[70] Nanostructures of polar and nonpolar groups (blue and red color in Figure 3c) displayed a small degree of ordering in the direction of shearing but remained intact even at the highest shear rate. This area of research is very interesting for future studies to predict the shear-thickening behaviors in ILs.

In summary, the effects of several parameters have been investigated on the steady and dynamic rheological properties, i.e., viscosity and moduli of ILs. These crucial factors include

DOI: 10.1021/acssuschemeng.9b02232
ACS Sustainable Chem. Eng. 2019, 7, 13586−13626

Table 1. Details of Rheological Analysis of Pure Ionic Liquids

ionic liquid	rheometer	characterization temperature	shear rate or angular frequency	key rheological parameters	ref
$[C_2C_1im][C_6SO_4]/[P_{6,6,6,14}][(C_2F_5)_3PF_3]$	Reologica StressTech Couette HTHP	25−80 °C	6−1000 s^{-1}	$[C_2C_1im][C_6SO_4]$ η = 31.4−737 mPa·s (10−75 MPa) $[P_{6,6,6,14}][(C_2F_5)_3PF_3]$ η = 37.9−1417 mPa·s (10−75 MPa)	62
$[P(bu)_3(CH_2)_2(CF_2)_xF][I]/[P(bu)_3CH_2)_2(CF_2)_xF]DCA]/[P(bu)_3(CH_2)_yH]Br]/[P(bu)_3CH_2)_yH][DCA]$; x = 2, 4, 6, 8, 10; y = 4, 6, 8, 10, 12	MCR 301, Anton Paar	25−100 °C	200−10,000 s^{-1}	$[P(bu)_3(CH_2)_2(CF_2)_xF][DCA]$ η_0 = 660−1580 mPa·s (x = 2−6 at 25 °C) $[P(bu)_3(CH_2)_yH][DCA]$ η_0 = 112−221 mPa·s (y = 12−6 at 25 °C)	63
$[C_2C_1pyr][C_4F_9SO_3]/[C_4C_1pyr][N(C_4F_9SO_2)_2]/[C_4C_1pyr][C_4F_9SO_3]/[C_8C_1im][C_4F_9SO_3]$	MCR 101, Anton Paar	−4−160 °C	1−900 s^{-1}, 1−900 rad/s	$[C_2C_1pyr][C_4F_9SO_3]$ η_{340K} = 16 mPa·s (10 s^{-1}) $[C_4C_1pyr][N(C_4F_9SO_2)_2]$ η_{340K} = 96 mPa·s (10 s^{-1}) $[C_4C_1pyr][C_4F_9SO_3]$ η_{340K} = 69 mPa·s (10 s^{-1}) $[C_8C_1im][C_4F_9SO_3]$ η_{340K} = 70 mPa·s (10 s^{-1})	65
[N888n-BScB]; n = 6, 8, 10 and 12	MCR 102, Anton Paar	25 °C	80−4000 s^{-1}, 1−100 rad/s	[N8886-BScB] η_0 = 257 mPa·s [N8888-BScB] η_0 = 580 mPa·s [N88810-BScB] η_0 = 350 mPa·s [N88812-BScB] η_0 = 305 mPa·s	51
[2-HEA][Ac]/[2-HDEA][Ac]/[2-HEA][Pr]/[2-HEA][L]/[2-HDEA][L]	Brookfield Viscometer (LVDV-III)	40−70 °C	0−78 s^{-1}	[2-HEA][Ac] η = 176.2−40.8 mPa·s (17 s^{-1}) [2-HDEA][Ac] η = 370.2−122.3 mPa·s (17 s^{-1}) [2-HEA][Pr] η = 294.3−109.2 mPa·s (17 s^{-1}) [2-HEA][L] η = 205.3−48.7 mPa·s (17 s^{-1}) [2-HDEA][L] η = 217.0−48.3 mPa·s (17 s^{-1})	49
$[BtTzm][CF_3SO_3]/[IpTzm][CF_3SO_3]/[HxTzm][CF_3SO_3]$	MCR, Anton Paar	20−70 °C	100−1000 s^{-1}, 1−100 rad/s	$[BtTzm][CF_3SO_3]$ η_0 = 96 mPa·s	12

DOI: 10.1021/acssuschemeng.9b02232
ACS Sustainable Chem. Eng. 2019, 7, 13586−13626

Table 1. continued

ionic liquid	rheometer	characterization temperature	shear rate or angular frequency	key rheological parameters	ref
				$[IpTzm][CF_3SO_3]$ η_0 = 139 mPa·s $[HxTzm][CF_3SO_3]$ η_0 = 119 mPa·s	
1-butyl-3-[2-[(2-methyl-1-oxo-2-propen-1-yl)oxy]ethyl]-imidazolium tetrafluoroborate (2-IL)/1-butyl-3-[3-[(2-methyl-1-oxo-2-propen-1-yl)oxy]propyl]-imidazolium tetrafluoroborate (3-IL)/1-butyl-3-[6-[(2-methyl-1-oxo-2-propen-1-yl)oxy]hexyl]-imidazolium tetrafluoroborate (6-IL)	MCR 300, Anton Paar	25 °C	10−150 s^{-1}	2-IL $\eta = 520 \times 10^6$ mPa·s (102 s^{-1}) 3-IL $\eta = 415 \times 10^6$ mPa·s (102 s^{-1}) 6-IL $\eta = 365 \times 10^6$ mPa·s (102 s^{-1})	71
$[C_4C_1Pyr][(C_2F_5)_3PF_3]/[C_4C_1Pyr][CF_3SO_3]$	Falling body viscometer, VisLPT1	30−80 °C	30−1000 s^{-1}	$[C_4C_1Pyr][(C_2F_5)_3PF_3]$ η = 24.7−3485 mPa·s (10−150 MPa) $[C_4C_1Pyr][CF_3SO_3]$ η = 22.5−737.7 mPa·s (10−150 MPa)	72
$[C_4C_1im][PF_6]/[C_4C_1im][NO_3]$	Brookfield Viscometer (LVDV-II + Pro)	10−65 °C	0.22−56 s^{-1}	$[C_4C_1im][NO_3]$ η = 156.3−48.9 mPa·s (25−50 °C; 56 s^{-1}) $[C_4C_1im][PF_6]$ η = 255.8−72.9 mPa·s (25−50 °C; 56 s^{-1})	54
$[(But)_3P(Dec)](Cl)/[(Hex)_3P(Dec)](Cl)/[(Oct)_3P(Dec)](Cl)/[(But)_3P(Dec)P(But)_3](Cl)_2/[(Hex)_3P(Dec)P(Hex)_3](Cl)_2/[(Oct)_3P(Dec)P(Oct)_3](Cl)_2/[(Hex)_3P(Dec)P(Hex)_3](PF_6)_2/[(Hex)_3P(Dec)P(Hex)_3](SbF_6)_2/[(Hex)_3P(Dec)P(Hex)_3](POA)_2/[(Hex)_3P(Dec)P(Hex)_3](NTf_2)_2/[(But)_3P(Dec)P(But)_3](OA)_2/[(But)_3P(Dec)P(But)_3](POA)_2/[(But)_3P(Dec)P(But)_3](DS)_2/[(But)_3P(Dec)P(But)_3](DOSS)_2$	AR 1000, TA Instruments	25 °C	1 Hz	$[(X)_3P(Dec)](Cl)$ η = 2.53− 5.05 × 10^3 mPa·s (X = C_4−C_8) $[(X)_3P(Dec)P(X)_3](Cl)_2$ $\eta = 2.63 \times 10^4$−3.88×10^8 mPa·s (X = C_4 − C_8) $[(Hex)_3P(Dec)P(Hex)_3]X$ $\eta = 2.01 \times 10^4$ mPa·s (X = $(PF_6)_2$) $\eta = 1.46 \times 10^4$ mPa·s (X = $(SbF_6)_2$) $\eta = 1.15 \times 10^4$ mPa·s (X = $(POA)_2$) $\eta = 2.00 \times 10^3$ mPa·s (X = $(NTf_2)_2$) $[(But)_3P(Dec)P(But)_3]X$ $\eta = 4.65 \times 10^4$ mPa·s (X = $(OA)_2$) $\eta = 1.34 \times 10^4$ mPa·s (X = $(POA)_2$) $\eta = 1.61 \times 10^4$ mPa·s (X = $(DS)_2$)	73

DOI: 10.1021/acssuschemeng.9b02232
ACS Sustainable Chem. Eng. 2019, 7, 13586−13626

Table 1. continued

ionic liquid	rheometer	characterization temperature	shear rate or angular frequency	key rheological parameters	ref
				η = 2.23 × 10^4 mPa·s (X = $(DOSS)_2$)	
$[C_nC_1im][PF_6]$; n = 2, 4, 6, 8, 10, 12/$[C_2C_1im][BF_4]$/$[C_2C_1im][Cl]$/$[C_2C_1im][DCA]$/$[C_2C_1im][Ts]$/$[C_2C_1im][Tf_2N]$/$[C_2C_1im][TFES]$/$[C_2C_1im][Br]$	MCR 501, Anton Paar	100 °C	0−1000 s^{-1}	$[C_nC_1im][PF_6]$ η = 12−48 mPa·s (n = 2−12; 1000 s^{-1}) $[C_2C_1im]X$ η = 4.11 mPa·s (X = [DCA]; 1000 s^{-1}) η = 17.8 mPa·s (X = [Br]; 1000 s^{-1}) η = 6.24 mPa·s (X = $[BF_4]$; 1000 s^{-1}) η = 22.1 mPa·s (X = [Ts]; 1000 s^{-1}) η = 11.9 mPa·s (X = $[PF_6]$; 1000 s^{-1}) η = 6.34 mPa·s (X = $[Tf_2N]$; 1000 s^{-1}) η = 9.45 mPa·s (X = [TFES]; 1000 s^{-1}) η = 14.0 mPa·s (X = [Cl]; 1000 s^{-1})	50
$[C_6C_1im][(PFBu)SO_3]$/$[NB_4][(PFBu)SO_3]$	MCR 101, Anton Paar	0−100 °C	0.5−100 s^{-1}, 1−1000 rad/s	$[C_6C_1im][(PFBu)SO_3]$ η = 144 mPa·s (40 °C; 1 s^{-1}) $[NB_4][(PFBu)SO_3]$ η = 180 mPa·s (90 °C; 1 s^{-1})	74
[EA][N]/[PA][N]/[EtA][N]/[EA][F]/[DMEA][F]	AR-G2, TA Instruments	20−50 °C	1−4000 s^{-1}	η_0 = 156.1 mPa·s ([EtA][N]; 23 °C) η_0 = 89.3 mPa·s ([PA][N]; 23 °C) η_0 = 35.9 mPa·s ([EA][N]; 23 °C) η_0 = 23.1 mPa·s ([EA][F]; 23 °C) η_0 = 9.8 mPa·s ([DMEA][F]; 23 °C)	48
$[N_{n,2,2,2}][NTf_2]$; n = 6, 7, 8, 10, 12, or 14	AR 1000, TA Instruments	20−95 °C	5820 s^{-1}, 50 rad/s	$[N_{n,2,2,2}][NTf_2]$ η = 234.5−12.78 mPa·s (n = 6) η = 253.6−12.68 mPa·s (n = 7) η = 288.4−13.60 mPa·s (n = 8) η = 358.9−15.21 mPa·s (n = 10) η = 410.0−17.24 mPa·s (n = 12)	57

DOI: 10.1021/acssuschemeng.9b02232
ACS Sustainable Chem. Eng. 2019, 7, 13586−13626

Table 1. continued

ionic liquid	rheometer	characterization temperature	shear rate or angular frequency	key rheological parameters	ref
				η = 490.3−18.99 mPa·s (n = 14)	
$[C_4C_1im][Cl]/[C_2C_1im][NTf_2]/[C_8Py][I]/[C_8Py][NTf_2]/[C_2C_1imSH][(EtO)_2PO]/[C_6C_1imSPrN][NTf_2]/[C_6C_1imSBu][PF_6]/[C_6C_1imSBu][(BuO)_2PO_2]/[btzSEt][(EtO)_2PO_2]/[(HOEt)_2NH][Ac]/[(HOEt)_2NH][CH_3SO_3]/[(HOEt)_2NH][HCO_2]/[EDA][HCO_2]/[Pyr][Ac]$	AR-G2, TA Instruments	20−90 °C	10−8000 s^{-1}	η_0 = 96 mPa·s ($[C_4C_1im][Cl]$; 75 °C) η_0 = 19 mPa·s ($[C_2C_1im][NTf_2]$; 20 °C) η_0 = 273 mPa·s ($[C_8Py][I]$; 20 °C) η_0 = 126 mPa·s ($[C_8Py][NTf_2]$; 20 °C) η_0 = 92 mPa·s ($[C_2C_1imSH][(EtO)_2PO]$; 20 °C) η_0 = 816 mPa·s ($[C_6C_1imSPrN][NTf_2]$; 20 °C) η_0 = 305 mPa·s ($[C_6C_1imSBu][PF_6]$; 20 °C) η_0 = 100 mPa·s ($[C_6C_1imSBu][(BuO)_2PO_2]$; 20 °C) η_0 = 48 mPa·s ($[btzSEt][(EtO)_2PO_2]$; 20 °C) η_0 = 5642 mPa·s ($[(HOEt)_2NH][Ac]$; 20 °C) η_0 = 1766 mPa·s ($[(HOEt)_2NH][CH_3SO_3]$; 20 °C) η_0 = 784 mPa·s ($[(HOEt)_2NH][HCO_2]$; 20 °C) η_0 = 115 mPa·s ($[EDA][HCO_2]$; 20 °C) η_0 = 38 mPa·s ($[Pyr][Ac]$; 20 °C) η_0 = 4990−100 mPa·s ($[(HOEt)_2NH][Ac]$; 20−90 °C) η_0 = 4990−100 mPa·s ($[(HOEt)_2NH][Ac]$; water content 0−30 wt %)	52
$[HOC_2C_1im][(BuO)_2PO_2]/[HOOCC_2C_1im][(BuO)_2PO_2]/[PhCH_2C_2C_1im][(BuO)_2PO_2]/[CPC_1im][(BuO)_2PO_2]/[C_4C_1im][(BuO)_2PO_2]$	RS 6000, Thermo Haake	20 °C	100−2700 s^{-1}	$[HOC_2C_1im][(BuO)_2PO_2]$ η_0 = 1800 mPa·s $[HOOCC_2C_1im][(BuO)_2PO_2]$ η_0 = 12000 mPa·s $[PhCH_2C_2C_1im][(BuO)_2PO_2]$ η_0 = 1200 mPa·s	64

DOI: 10.1021/acssuschemeng.9b02232
ACS Sustainable Chem. Eng. 2019, 7, 13586−13626

Table 1. continued

ionic liquid	rheometer	characterization temperature	shear rate or angular frequency	key rheological parameters	ref
				$[[CPC_1im][(BuO)_2PO_2]$	
				η_0 = 1300 mPa·s	
				$[C_4C_1im][(BuO)_2PO_2]$	
				η_0 = 200 mPa·s (20 °C)	
$[P(oct)_3(CH_2)_2(CF_2)_xF][NTf_2]/[P(oct)_3(CH_2)_2(CF_2)_xF][C(CN)_3]/[P(oct)_3(CH_2)_yH][NTf_2]/[P(oct)_3(CH_2)_yH][N(CN)_2]/[P(oct)_3(CH_2)_yH][C(CN)_3]$; x = 4, 6, 8; y = 6, 8, 10	MCR 301, Anton Paar	30−100 °C	100−20 000 s^{-1}	$[P(oct)_3(CH_2)_2(CF_2)_xF][NTf_2]$	53
				η_0 = 862−1368 mPa·s (x = 4−8; 25 °C)	
				$[P(oct)_3(CH_2)_2(CF_2)_xF][C(CN)_3]$	
				η_0 = 532−1367 mPa·s (x = 4−8; 25 °C)	
				$[P(oct)_3(CH_2)_yH][NTf_2]$	
				η_0 = 261−196 mPa·s (y = 6−10; 25 °C)	
				$[P(oct)_3(CH_2)_yH][N(CN)_2]$	
				η_0 = 240−290 mPa·s (y = 6−10; 25 °C)	
				$[P(oct)_3(CH_2)_yH][C(CN)_3]$	
				η_0 = 126−167 mPa·s (y = 6−10; 25 °C)	
[2-Mbua][NTf_2]/[N-*Ei*pra][NTf_2]/[Dema][NTf_2]	MCR 301, Anton Paar	25−100 °C	10−8000 s^{-1}	η_0 = 430 mPa·s ([2-Mbua][NTf_2]; 25 °C)	75
				η_0 = 95 mPa·s ([N-*Ei*pra][NTf_2]; 25 °C)	
				η_0 = 50 mPa·s ([Dema][NTf_2]; 25 °C)	
$[P_{6,6,6,14}][BMB]/[P_{6,6,6,14}][Cl]$	HR2/HR3, TA Instruments	50−200 °C		$[P_{6,6,6,14}][BMB]$	76
				η_0 = 67−11 mPa·s (100−190 °C)	
				$[P_{6,6,6,14}][Cl]$	
				η_0 = 402−9.0 mPa·s (50−190 °C)	
[DEEA][CF_3SO_3]/[DEEA][CF_3CO_2]/[PtTzm][CF_3SO_3]/[PtTzm][CF_3CO_2]	MCR 102, Anton Paar	25 °C	1−100 rad/s	η_0 = 168 mPa·s ([DEEA][CF_3SO_3])	68
				η_0 = 134 mPa·s ([DEEA][CF_3CO_2])	
				η_0 = 108 mPa·s ([PtTzm][CF_3SO_3])	
				η_0 = 30 mPa·s ([PtTzm][CF_3CO_2])	

DOI: 10.1021/acssuschemeng.9b02232
ACS Sustainable Chem. Eng. 2019, 7, 13586−13626

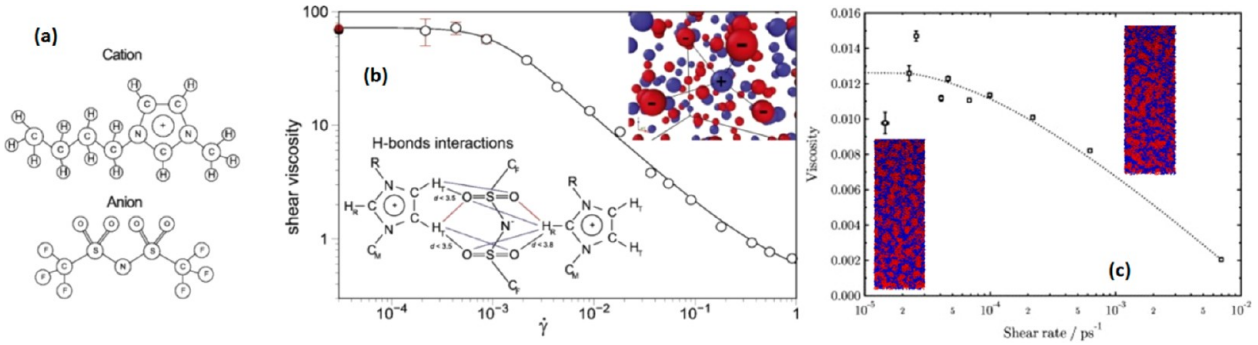

Figure 3. (a) Chemical structures of a cation and an anion. (b) Rheological flow curve of the ionic liquid. 3D network formed by the interactive ions. Schematic representation of H-bonds (colored lines) [Reprinted with permission from ref 69. Copyright 2017. Elsevier]. (c) Viscosity plotted as a function of shear rate. A trend line is drawn as an aid to the eye. Images of the visualization of IL simulation system without shear and at the highest shear rate taken at 40 ns. IL shows nanostructural organization via aggregation of polar and nonpolar regimes [Reprinted with permission from ref 70. Copyright 2014. Elsevier].

temperature, shear rate, pressure, nature of anion, structure and nature of cation, and inclusion of additives. In addition to these parameters, interionic interactions such as hydrogen bonding also significantly affect the rheological properties of ILs, unlike conventional molecular solvents. Typically, a Newtonian behavior at lower shear rates and a shear thinning character at higher shear rates are observed for ILs which are highly dependent on cation size, nature of anion, and temperature. This shear thinning behavior is linked with the existence and breakage of nanostructures in the ILs. Newtonian and shear thickening behaviors are also reported in the literature for ILs, which can be quite interesting for the applications where either viscosity change is not required or higher viscosities are needed during processing. The molecular dynamics simulations showed that the nanostructures in ILs are resistant to the shear rate after certain level and, therefore, these kind of studies are very important to predict the correct shear rate for the processing of ILs without wasting much energy. The dynamic rheological properties such as elastic and viscous modulus are also dependent on the nature of ionic counterparts of ILs and these properties are substantial to forecast the elastic recovery of the system.

RHEOLOGY OF IL BASED SOLUTIONS

The knowledge of the rheological properties of polymeric solutions in ionic liquids is essential to understand the ability of ionic liquids as processing aids particularly in film casting, fiber spinning, and spraying. These properties also assist in comprehending the thermodynamics and dynamics of polymer chains in IL. Furthermore, the hydrodynamic volume of dispersed polymer, polymer−IL interactions, chain mobility, and IL−IL interactions can be easily assessed by using viscometry and intrinsic viscosity measurements.[39,77] Most importantly, the material's response to the applied deformation (described by flow curves as a function of shear rate or shear stress) is mandatory for design and optimization of different processing techniques. Rheological analysis is also useful in understanding the self-assembly and structural transitions of surfactant molecules in ILs and the resultant properties of the systems. Therefore, the rheological analysis of IL based solutions has gained much attention from researchers in recent years.[78−81]

IL−Polymer Based Solutions. *Natural Polymer Based Solutions. IL−Polysaccharide Solutions.* Polysaccharides are the most abundant biopolymers found in nature and are available from different sources including vegetable and animal. These systems have attracted the attention of many researchers as they are renewable, biodegradable, cheap, and easy to convert into different derivatives because of their excellent reactivity with many organic molecules. Polysaccharides, therefore, cover a wide range of applications and are used as thickening agents, for encapsulation and release of active compounds, and as gelling agents for food and pharmaceutical systems.[82] The European Polysaccharide Network of Excellence (EPNOE) was established, with the help of the European Commission, consisting of 16 academic and research institutes from Europe and more than 25 industries from all over the world. The main focus of this network is to develop new products based on polysaccharides by performing fundamental and applied research.[83]

Rheological analysis is necessary to analyze the potential applications of natural or modified polysaccharides and to understand and highlight the characteristics of polysaccharides solutions in various solvents. Rheology enables monitoring and probing of the structural changes, i.e., phase separation or gelation, in polysaccharides systems particularly where other physical techniques are either difficult or impossible to apply.[41]

Even though cellulose is the biopolymer that has been the most thoroughly investigated (see next subsection), IL has also been reported as a solvent for other biopolymers like chitosan, chitin, gelatins, starch, agarose, natural gums, etc. Horinaka et al. reported the rheological analysis of concentrated solutions of three different gelatins in IL.[84] The results of dynamic viscoelasticity revealed the presence of entanglement coupling between biopolymer chains (rubbery plateau) and the master curves were also used to determine molecular weight between entanglements (M_e) as a function of gelatin concentration (c).

Likewise, the concentrated solutions of chitin/chitosan in IL were also rheologically characterized.[85] The molecular weight between entanglements (M_e), determined from the master curves of dynamic viscoelasticity, was found to be smaller for chitin as compared to chitosan which was attributed to the larger stiffness of chitin. The effect of temperature, shear rate and mixing two different polysaccharides (starch (G50) and microcrystalline cellulose (MCC)) on the rheological properties of IL based solutions was also studied.[86] The output showed a decrease in the viscosity of solutions as a function of increasing temperature whereas the solution viscosity of mixture of polysaccharides lied in between the viscosities of individual polymer solutions in the same IL. For semidilute solutions, a significant shear thinning behavior was observed at high shear

DOI: 10.1021/acssuschemeng.9b02232
ACS Sustainable Chem. Eng. 2019, 7, 13586−13626

rates due to the existence of entanglements between polymer chains (mechanism shown in Figure 4). However, a slight shear thinning behavior was also evident for dilute solutions which was linked with the alignment of the IL molecule network.

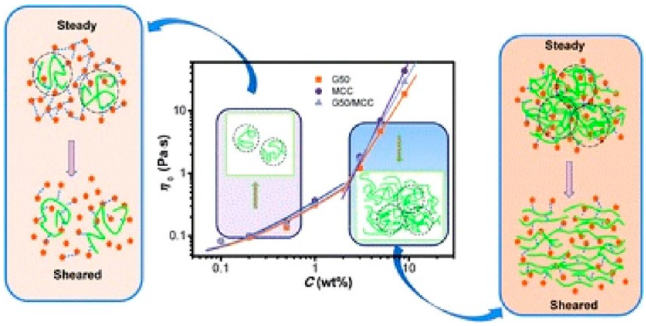

Figure 4. Concentration dependence of zero-shear-rate viscosity at 25 °C. Schematic representation of shear-thinning behavior for dilute and semidilute polymer−IL solutions [Reprinted with permission from ref 86. Copyright 2016. The Royal Society of Chemistry].

Liu and Budtova presented the comparative analysis of cellulose and starch based IL solutions on the basis of their rheological properties.[87] The Carreau−Yasuda model was selected to fit the data obtained from flow curves. A shear-thinning behavior of starch based solutions was found above 1 wt % concentration of biopolymer. Power law exponents displayed a variation from 3 to 2.5 as a function of increasing temperatures from 20 to 100 °C in the semidilute region of zero shear viscosity−starch concentration plot. Similarly, the intrinsic viscosity of starch based solutions also decreased with increasing temperature which indicated the decreasing quality of the solvent. Furthermore, this decrease in intrinsic viscosity of starch solutions was much less pronounced as compared to the cellulose based solutions.

The effect of water incorporation on the viscosity of starch−IL based solutions was determined by using rheology.[88] A higher extent of structural dissolution and disruption was found for solutions containing 7.2 mol of water, as compared to other solutions having a higher water content, at the end of the rheology test. Solutions having 0.1 mol of water showed a phase transition at higher temperature compared to solutions with 7.2 mol of water. Moreover, a moderate increase together with very small decrease in viscosity was also evident for a similar solution (0.1 mol water) at 95 °C, which was linked with the simultaneous disruption and dissolution of the structure. Horinaka et al. reported the influence of entanglement coupling between chains of agarose on the rheological properties of agarose/IL solutions.[89] Different solutions were prepared by varying the concentration of agarose from 11 to 210 kg/m^3. The master curves of storage modulus (G'), loss modulus (G''), and tan δ as a function of angular frequency (ω) displayed a flow region at lower frequencies and a rubbery regime at intermediate frequencies. The plateau modulus was used to calculate the molecular weight between entanglements (M_e) and it was found to be 2.3×10^3 for agarose melt.

Rheology was also used to examine the concentrated IL based solutions of three galactomannans: tara gum, guar gum, and locust bean gum.[90] The existence of entangled polymer chains in all three solutions was evident from the characteristic curves of storage and loss moduli as a function of angular frequency. The summary of the polysaccharides based IL systems is presented in Table 2, in terms of biopolymer content, temperature ranges, and the values of key rheological parameters.

IL−Cellulose Solutions. Cellulose is the most abundant organic polymer used in industry (1.5×10^{12} tons of total annual biomass production[91]) and covers wide range of applications such as textiles, composite materials, drug delivery systems, and personal care products. Since its discovery in 1838,[92] this biodegradable, cheap, and renewable resource has attracted a great deal of attention from researchers because of its physical and chemical properties.[93] These properties are due to the specific characteristics of cellulose and its derivatives like larger persistence length, smaller second virial coefficient, and shear-thinning behavior in semidilute and concentrated regimes, which makes possible for the cellulose chains to take semiflexible conformations in solution state.[94] Ecofriendly and economical ionic liquids have great potential, as a processing aid, in producing cellulose based fibers.[95] The different stages of cellulose processing like dissolution, handling, and spinning require extensive knowledge about the behavior of viscosity of IL based cellulose solutions. This rheological property is required to estimate the energy input for processing and the optimal design of equipment in view of upscaling.[96]

Several studies are related to the oscillatory and shear rheological measurements on cellulose/IL solutions. Gericke et al.[81] and Sescousse et al.[97] reported the shear rheological analysis of sulfite pulp, microcrystalline cellulose, and bacterial cellulose solutions in different ILs. The viscosities of $[C_2C_1im]$-$[Ac]$ based solutions were lower than the $[C_4C_1im][Cl]$ based solutions, which was attributed to the lower viscosity of the corresponding IL. Moreover, the experimental data of relative viscosity as a function of concentration converged into a single master curve for both IL solutions. Haward et al. reported a decrease in intrinsic viscosity of IL based solution as a function of increasing temperature which was linked with the decrease in radius of gyration of polymer.[98] This result indicated a decrease in thermodynamic quality of IL as a solvent for increasing temperature. The Vogel−Fulcher−Tamman (VFT) model was shown to fit the data of viscosity as a function of temperature more accurately than the Arrhenius law and provided realistic values of glass transition temperature (T_g) and pseudoactivation energies.

Oscillatory rheology can easily be used to analyze the elastic and viscous responses of IL/cellulose solutions.[99,100] Sammons et al. showed a shear thinning behavior for cellulose/IL solution at higher angular frequencies and the onset of shear thinning shifted toward higher frequencies by increasing temperature.[99] Several researchers have predicted correct spinning temperatures of cellulose/IL solutions by plotting master curves of rheological parameters over extended frequency range using the Williams−Landel−Ferry (WLF) theory. The cross viscosity model has been used predominantly in the literature to accurately fit the complex viscosity data of cellulose/IL solutions and also to find the zero shear viscosity. In order to calculate the zero shear viscosity from the fit, the Cox−Merz rule must be valid for the considered solution.[101] Haward et al.[98] reported the validity of this rule for cellulose/IL solution whereas a strong deviation from this rule, particularly at higher shear rates or cellulose content, was also showed by some authors.[79,102]

Sammons et al. reported the elongational rheology of IL/cellulose solutions using a capillary rheometer with hyperbolic dies.[103] The results revealed the shear thinning and strain hardening behaviors of the considered solution. Furthermore, an increase in viscosity with the Hencky strain was also observed

DOI: 10.1021/acssuschemeng.9b02232
ACS Sustainable Chem. Eng. 2019, 7, 13586−13626

Table 2. Some Details of Rheological Analysis of Different IL Based Solutions

ionic liquid	other component	concentration of other component (wt %)	rheometer	characterization temperature	shear rate or angular frequency	key rheological parameters	ref
$[N_{2226}][Ac]/[N_{33312}][Ac]$	cellulose, DMSO	10, 20	ARES, TA Instruments	30−90 °C	1−100 rad/s	$[N_{2226}][Ac]$/DMSO η_0 = 1.5−100 × 10^3 mPa·s (1 rad/s) $[N_{33312}][Ac]$/DMSO η_0 = 3 × 10^3−1 × 10^8 mPa·s (1 rad/s)	146
$[C_2C_1im][Ac]$	MCC, DMF	0.1−10	DHR-2, TA Instruments	25 °C		$[C_2C_1im][Ac]$ η_0 = 70−11000 mPa·s (cellulose 0.1−7 wt %) $[C_2mim][Ac]$/DMF η_0 = 3.5−6500 mPa·s	147
$[C_2C_1im][Ac]/[C_4C_1im][Ac]$	cellulose, DMSO, 1-butanol	1.3−4.8, 32−47, 32−33	Malvern Kinexus pro+	60 °C	1−1000 s^{-1}	$[C_4C_1im][Ac]$ η = 163.90−723.13 mPa·s (cellulose 2−4.8 wt %; 1000 s^{-1}) $[C_2C_1im][Ac]$ η = 87−290.70 mPa·s (cellulose 2−4.8 wt %; 1000 s^{-1}) $[C_4C_1im][Ac]$/DMSO η = 15.66−91.27 mPa·s (cellulose 1.3−3.2 wt %; 1000 s^{-1})	148
$[C_2C_1im][Cl]$	cellulose, DMSO	0.1−10, 30	AR-2000, TA Instruments	25−100 °C	0.01−1000 s^{-1}	$[C_2C_1im][Cl]$/DMSO η_0 = 150−10^6 mPa·s (cellulose 0.1−6 wt %; 25 °C) η_0 = 18−4500 mPa·s (cellulose 0.1−6 wt %; 100 °C)	149
$[C_4C_1im][Cl]/[Amim][Cl]/[C_2C_1im][Ac]$	cellulose	1−10	UDS 200, Anton Paar	20−100 °C	10 Hz	[Amim][Cl] η_0 = 800−35000 mPa·s (cellulose 0−7 wt %; 20 °C)	150
$[C_2C_1im][Ac]$	cellulose, propyl gallate	10	MCR 300, Anton Paar	60 °C	0.01−100 s^{-1}	$[C_2C_1im][Ac]$ η_0 = 537.5−281.3 × 10^3 mPa·s (storage conditions: 0−24 h; 110 °C) η_0 = 606.1−416.1 × 10^3 mPa·s (storage conditions: 0−24 h; 90 °C) η_0 = 590.8−575.1 × 10^3 mPa·s (storage conditions: 0−8 h; 60 °C) $[C_2C_1im][Ac]$/propyl gallate η_0 = 992.9−827.7 × 10^3 mPa·s (storage conditions: 0−24 h; 110 °C)	151
[DBNH][Ac]	cellulose	13−15	MCR 300, Anton Paar	70−90 °C	0.01−100 s^{-1}	η_0 = 25−36 × 10^6 mPa·s	152
$[C_2C_1im][Ac]$	cellulose, water	2−10, 0−10	CS 50, Bohlin Instruments	48 °C	0.1−100 s^{-1}	η = 16 × 10^3-72 × 10^3 mPa·s (cellulose 10 wt %; 0.1 s^{-1})	153
$[C_2C_1im][Ac]/[C_2C_1im][DEP]$	cellulose	6−10	SR 500, Rheometrics	100 °C	0.1−100 s^{-1}, 0.1−10000 rad/s	η_0 = 32.9 × 10^3−1.8 × 10^7 mPa·s	154
$[C_2C_1im][Ac]$	cellulose	10	CS 50, Bohlin Instruments	50 °C	0.01−1 s^{-1}, 0.1−100 Hz	η = 12 × 10^3−49 × 10^5 mPa·s (degree of polymerization 330−1340; 0.1 s^{-1})	155
$[C_2C_1im][Ac]$	cellulose acetate	0.1−10	Bohlin Gemini	0−80 °C	0.01−500 s^{-1}	η_0 = 1.8 × 10^2−85 × 10^3 mPa·s (20 °C)	156

DOI: 10.1021/acssuschemeng.9b02232
ACS Sustainable Chem. Eng. 2019, 7, 13586−13626

Table 2. continued

ionic liquid	other component	concentration of other component (wt %)	rheometer	characterization temperature	shear rate or angular frequency	key rheological parameters	ref
						η_0 = 3−300 × 10^3 mPa·s (cellulose 10 wt %; 10−70 °C)	
$[C_2C_1im][Ac]$	cellulose	0.1−8	AR-G2, TA Instruments	25 °C	0.1−100 s^{-1}	η_0 = 150−400 × 10^3 mPa·s	98
[Amim][Cl]	cellulose	10−25	AR-1000, TA Instruments	80−120 °C	0.1−1000 s^{-1}, 0.1−628.3 rad/s	η_0 = 2.2 × 10^6−1.2 × 10^8 mPa·s (100 °C)	102
[Amim][Cl]/$[C_4C_1im]$[Cl]	cellulose/DMSO	0.070−6, 0−50	AR-2000ex, TA Instruments	10−105 °C	0.01−500 s^{-1}	η_0 = 6.1−200 × 10^3 mPa·s (cellulose 1.5 wt %; 25 °C)	109
						η_0 = 0.8 × 10^3−3 × 10^7 mPa·s (cellulose 0.15−6 wt %; DMSO 20 wt %; 25 °C)	
$[C_2C_1im][Ac]$	cellulose	1−10	MCR 300, Anton Paar	25−100 °C	0.01−100 s^{-1}	η_0 = 0.76−2633 × 10^3 mPa·s (50 °C)	157
$[C_4C_1im][Cl]$	cellulose	5−10	MCR 301, Anton Paar	90 °C	0.01−100 s^{-1}, 0.1−100 Hz	η_0 = 3−100 × 10^3 mPa·s	158, 159
$[C_4C_1im][Cl]$/$[C_2C_1im][Cl]$/[Amim][Cl]	cellulose/cellulose acetate	12.1−15.4	MARS, Thermo Haake	85 °C	0.01−1000 rad/s	η_0 = 17.6 × 10^6 mPa·s (cellulose 12.1 wt %)	160
						η_0 = 64.7 × 10^4−23.5 × 10^6 mPa·s (cellulose acetate 12.2−14.4 wt %)	
$[C_4C_1im][Cl]$	cellulose, DMSO	1−5, 0.32	MCR 300, Anton Paar	70−120 °C	0.01 s^{-1}	η = 1−65 × 10^3 mPa·s (70 °C)	161
						η = 6−65 × 10^3 mPa·s (cellulose 5 wt %)	
[Amim][Cl]	MCC	7−19	AR-2000, TA Instruments	25 °C	0.01−100 s^{-1}, 0.1−100 rad/s	η_0 = 16.5 × 10^4−70.0 × 10^6 mPa·s	112
$[C_2C_1im][Ac]$/$[C_4C_1im][Cl]$	MCC	0−15	Bohlin Gemini, Malvern Instruments/ARES, TA Instruments	0−110 °C		η_0 = 0.15−30 × 10^3 mPa·s (cellulose 0−10 wt %; 80 °C)	97
						η_0 = 4−30 × 10^3 mPa·s (cellulose 10 wt %; 80−110 °C)	
[Amim][Cl]	MCC, water	0.25−20, 0−10	MCR 301, Anton Paar	25 °C	0.01−500 s^{-1}, 0.1−500 rad/s	η_0 = 2.5−200 × 10^3 mPa·s (water 4 wt %)	162
						η_0 = 7−90 × 10^3 mPa·s (cellulose 5 wt %)	
$[C_2C_1im][P(OCH_3)(H)O_2]$	cellulose	0.017−10	Rheometrics Dynamic Spectrometer II/Rheometrics Fluids Spectrometer II	25 °C	10^{-5}−10^3 s^{-1}	η_0 = 2.0 × 10^2−3.5 × 10^8 mPa·s	163
$[DBNH][CO_2Et]$	MCC	0−8	Bohlin Gemini, Malvern Instruments	10−60 °C	0.01−300 s^{-1}, 0.01−10 Hz	η_0 = 0.35 × 10^3−12 × 10^5 mPa·s (10 °C)	164
$[C_2C_1im][Ac]$	corn starch	0.123−10	CS 150, Bohlin Instruments	20−100 °C	0.001−500 s^{-1}	η_0 = 0.2−300 × 10^3 mPa·s (corn starch 0.2−10 wt %; 20 °C)	87
						η_0 = 0.05−0.6 × 10^3 mPa·s (corn starch 1 wt %; 20−80 °C)	
$[C_2C_1im][Ac]$	starch, water	9, 9−72	AR-G2, TA Instruments	22 °C	10^5 s^{-1}	η = 0.9−112 mPa·s (IL 0−100 wt % in starch and water mixture)	88
$[C_4C_1im][Cl]$	agarose	1−20	ARES, TA Instruments	20−120 °C	0.1−100 s^{-1}	plateau modulus = 6.0 × 10^4 Pa (agarose 20 wt %)	89
$[C_4C_1im][Cl]$	guar gum/tara gum/locust bean gum	5−20	ARES, TA Instruments	20−100 °C	0.01−100 s^{-1}	Plateau modulus = 1.6 × 10^3-3.2 × 10^4 Pa (guar gum 5−20 wt %)	90
[Amim][Cl]	silk fibroin	1−15	MCR 301, Anton Paar	0−30 °C	0.001−1000 s^{-1}, 0.0681−100 rad/s	η_0 = 1−550 × 10^3 mPa·s (30 °C)	165
$[C_2C_1im][CO_2Et]$	cellulose and chitin	0−8	MCR 301, Anton Paar	50−110 °C	0.1−150 s^{-1}	η_0 = 4−57 × 10^3 mPa·s (110 °C)	166
$[C_4C_1im][Cl]$	cellulose and silk fibroin	4	MCR 301, Anton Paar	70−100 °C	0.1−1000 s^{-1}	η_0 = 0.6−26 × 10^3 mPa·s (cellulose 0−100 wt % in silk fibroin and IL mixture; 90 °C)	167

DOI: 10.1021/acssuschemeng.9b02232
ACS Sustainable Chem. Eng. 2019, 7, 13586−13626

Table 2. continued

ionic liquid	other component	concentration of other component (wt %)	rheometer	characterization temperature	shear rate or angular frequency	key rheological parameters	ref
$[C_4C_1im][Cl]$	cellulose and silk fibroin	0.1−8	MCR 301, Anton Paar	10−50 °C	0.1−100 s^{-1}, 0.1−628 rad/s	η_0 = 7.8 × 10^3−40.4 × 10^6 mPa·s (cellulose/silk fibroin weight ratio 8/2; 20 °C)	168
$[C_2C_1im][Ac]$	β-cyclodextrin	5−25	MARS II, Thermo Haake	23−70 °C	0.002−800 s^{-1}, 0.01−20 Hz	η_0 = 0.1 × 10^3−4 × 10^6 mPa·s (23 °C)	169
[EA][N]	CTAB	2−62	ARES-G2, TA Instruments	40−130 °C	1−500 s^{-1}, 1−300 rad/s	η = 0.2−13 × 10^3 mPa·s (CTAB 52 wt %; 55−100 °C; 1 s^{-1})	142
[EA][N]/$[C_4C_1im][BF_4]$	BPS-10	80	RS 75, Thermo Haake	25 °C	0−1000 s^{-1}, 0.01−100 Hz	η_0 = 9 × 10^4−1.8 × 10^5 mPa·s (both ILs)	40
[EA][N]	DDAB	68−95	AR-G2, TA Instruments	15−120 °C	0.01−100 rad/s	G' = 2 × 10^{-3}−5 × 10^3 Pa (DDAB 85%; 45−70 °C; 1 Hz)	143
$[C_4C_1im][BF_4]$	BPS-n; n = 5, 10, 20, 30	60−90	RS 75, Thermo Haake	25 °C	0−1000 s^{-1}, 0.01−100 Hz	η_0 = 70 × 10^3−20 × 10^6 mPa·s	144
[EA][N]	$[C_mH_{2m+1}(CH_3)_2N$-$(CH_2)_2N(CH_3)_2C_nH_{2n+1}]Br_2$ $m + n = 24$, m = 16, 14, 12	75	RS 6000, Thermo Haake	40 °C	0.1−100 s^{-1}, 0.01−100 Hz	η = 2 × 10^6−2.1 × 10^7 mPa·s (0.1 s^{-1})	170
$[C_4C_1im][BF_4]$/$[C_4C_1im][PF_6]$	$Zn(OOCCH_2C_6F_{13})_2$, C_{14}DMAO	11−111 mM	CS 10, Bohlin Instruments	25 °C	0.001−10 Hz	G' = 15−50 Pa (1 Hz)	171
[dEA][N]	PEO_x-PPO_y-PEO_x	1−30	AR-G2, TA Instruments	10−60 °C	0.001−1000 s^{-1} ,0.01−628 rad/s	η = 2 × 10^3-2.5 × 10^3 mPa·s (Polymer 20−27 wt %; 30 °C; 0.1 s^{-1})	172
$[C_4C_1im][Cl]$	poly(AN-*co*-IA)	0.1−18	MCR 301, Anton Paar	20−80 °C	0.1−1000 s^{-1}, 0.1−628 rad/s	η_0 = 0.15−529.2 × 10^3 mPa·s (80 °C)	130
$[C_4C_1im][Br]$	polyacrylonitrile	2−6	Bohlin Gemini 200, Malvern Instruments	70−80 °C	0.1−30 s^{-1}	G' = 1.5−90 Pa (PAN 3−5 wt %; 1 Hz)	131
$[C_4C_1im][Br]$	polyacrylonitrile	3−6	Bohlin Gemini 200, Malvern Instruments	50−80 °C	0.1−30 s^{-1}	η_0 = 0.8−35 × 10^3 mPa·s (50 °C)	132
[2-HEA][F]/[2-HEA][Ac]/[Ch][F]/[Ch][A]	ε-poly-L-lysine	2−15	MCR 301, Anton Paar	25 °C	0.1−1000 s^{-1}	G' = 25−2100 Pa (1 Hz)	173

DOI: 10.1021/acssuschemeng.9b02232
ACS Sustainable Chem. Eng. 2019, 7, 13586−13626

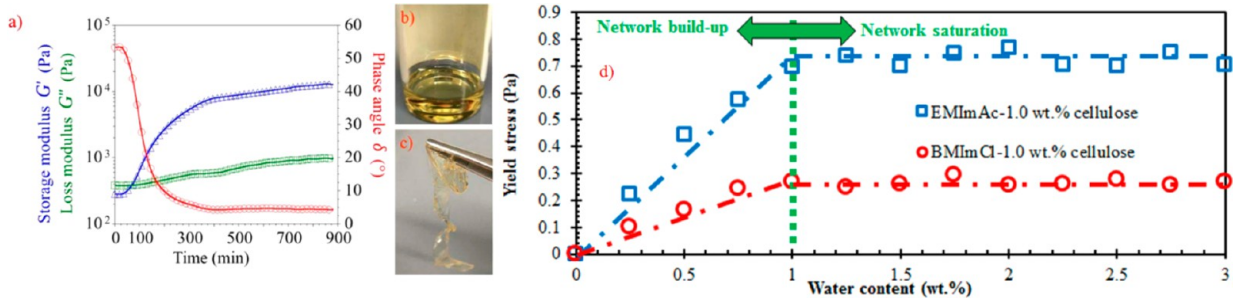

Figure 5. (a) Oscillatory time sweeps of IL solution with 5 wt % cellulose exposed to 50% RH air. (b) Solution before test and (c) material after test. (d) Yield stress of 1.0 wt % cellulose in $[C_4C_1im][Cl]$ and $[C_2C_1im][Ac]$ having different water contents [Reprinted with permission from ref 119. Copyright 2017. American Chemical Society].

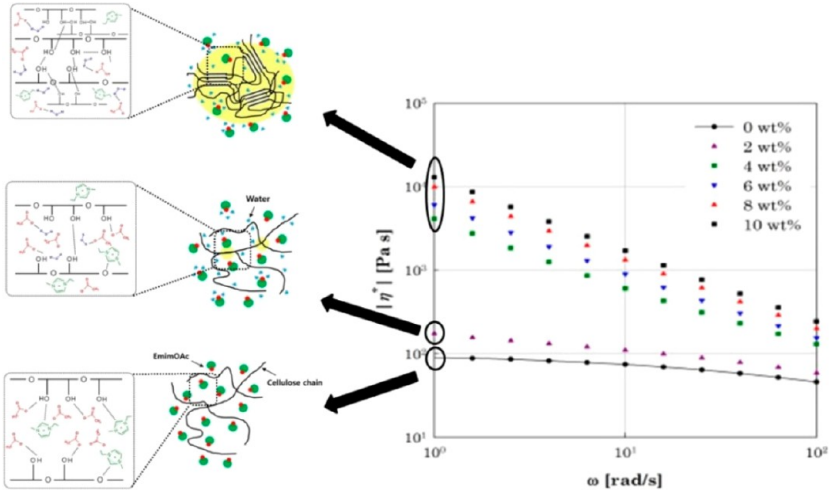

Figure 6. Influence of water content on the complex viscosity of 14 wt % MCC/$[C_2C_1im][Ac]$/water systems. Formation of self-associated LC network of cellulose in IL with no or little water [Adapted with permission from ref 120. Copyright 2016. John Wiley and Sons].

which was linked with the significant extension of biopolymer chains. Haward et al. also studied the elongational rheology of cellulose/IL system using a capillary breakup extensional rheometer (CaBER) to find the apparent extensional viscosity and extensional relaxation time.[98] In CaBER, a true unidirectional extensional flow was generated as compared to the hyperbolic dies. Equilibrium between elastic tensile stresses and capillary forces was the governing factor for the shear thinning dynamics.[104,105] Moreover, notable strain hardening behavior was only evident at higher cellulose content (implying higher viscosity). Several solvents have been proposed to reduce this high viscosity of cellulose/IL solutions like DMSO,[106] a small amount of water,[107] or 1,3-dimethyl-2-imidazolidinone.[108] In addition, the rheological analysis also revealed that the addition of DMSO has no effect on the structural arrangements (conformation) of cellulose in ILs.[109]

Cellulose[110] and its derivatives[111] usually display the formation of lytropic phases in solution state. Song et al. reported the existence of such lytropic phases for microcrystalline cellulose (MCC), a refined form of wood pulp, in different ILs using rheological measurements.[112,113] Rheological results showed the formation of lyotropic phases at a certain concentration of MCC (threshold concentration). So far, Bocell-type fibers have not been produced using ILs because of the fact that all the studied lytropic IL/cellulose solutions have a T_c lower than the processing temperature. Michels and Kosan[114] and Kosan et al.[115] reported the correlation between different rheological properties of IL/cellulose solutions and lyocell−NMMO monohydrate solutions (a solvent used in the lyocell process to produce high tenacity lyocell fibers from cellulose). Hermanutz et al. further used and developed this approach of rheology for spinnability.[116,117] Kosan and coworkers compensated for the low viscosity of IL based solutions by increasing the cellulose content, while lowering of the spinning temperature was proposed by Hermanutz and coworkers for a similar situation.

In another study, Hardelin et al. analyzed the effect of rheological properties and molecular weight on the electrospinning behavior of cellulose at several concentrations in IL with DMSO as a cosolvent.[118] The outcome of the study showed that the viscosity of the solution is a key parameter for electrospinning instead of cellulose concentration and molecular weight. In another study, the effect of water content on the solution rheology of cellulose based on ILs was also reported.[119] Initially, the solution was a viscous liquid ($G'' > G'$) (Figure 5b), but due to the moisture absorption into the solution, the elastic modulus increased (Figure 5a) and the solution became elastic solidlike ($G' > G''$) (Figure 5c). The outcome of this study also showed that a minute amount of water (0.25 wt %) was enough to change the character of solutions from viscoelastic liquids to yield stress fluids. The growth in yield stress as a function of water content was linear followed by a saturation level (Figure 5d) after which the cellulose concentration was the controlling parameter for the yield stress values of the solutions. A similar increase in zero shear viscosity of ILs based cellulose solutions by increasing water content, as shown in Figure 6, was also

DOI: 10.1021/acssuschemeng.9b02232
ACS Sustainable Chem. Eng. 2019, 7, 13586−13626

reported by Lee et al.[120] This increase in viscosity values was attributed to the formation of a self-associated liquid crystal network of cellulose chains in the presence of water molecules. There are several factors which can significantly affect the rheological fingerprint of cellulose based IL solutions particularly temperature, cellulose concentrations, and the incorporation of additives. Table 2 presents the summary of cellulose content, temperature range, and additives along with the key rheological parameters for different cellulose based systems investigated in the literature.

The rheological characterization and analysis of cellulose/IL solutions can be summarized into following four categorizes on the basis of the literature:

(1) Newtonian and shear thinning behavior: Mostly, shear thinning behavior and a shift of Newtonian plateau to lower frequencies are observed with increasing cellulose content. Some researchers also reported the existence of Newtonian plateau over wide range of shear rates which is linked with experimental problems observed at higher shear rates and also due to lower DP (degree of polymerization) of cellulose.[97] Other studies showed the existence of only a shear thinning behavior which is due to the creation of agglomerated structures in concentrated cellulose solutions.[102,113]

(2) Cox−Merz plots: Several authors have reported the results of Cox−Merz plots for IL/cellulose solutions. Cox−Merz rule is found to be valid, within the concentration range of 0.2−8 wt % and a frequency range of 0.1−100 1/s, for cellulose pulp dissolved in IL.[98] Most frequently, the Cox−Merz rule is observed to be valid for IL/cellulose solutions only in Newtonian region whereas higher values of shear viscosities are noticed, as compared to complex viscosities, in the shear thinning regime which suggested a structural transition of cellulose in this regime.[79,121,122] The typical deviation from Cox−Merz rule is also observed in cellulose/[Bmim]Cl solutions having concentrations from 6 to 14 wt %.[80]

(3) Storage and loss moduli as a function of frequency: At lower cellulose content, the loss modulus is always higher than the storage modulus and the crossover point between both moduli is not observed. This behavior is attributed to the fact that the major part of energy is dissipated by the viscous flow and, hence, the system behaves as liquidlike. With the increase in cellulose content, storage and loss moduli curves are observed to approach each other in the higher frequency regime and the slope of the lines give information about the dynamics of cellulose chains.[123] By further increasing the cellulose fraction, a crossover point is observed between the moduli at higher frequencies, which tended to move toward the lower frequencies as a function of increasing cellulose content. This response is linked with the solid or gel-like behavior of cellulose/IL system because of the formation of cellulose chain entanglements at higher content.[124] This entanglement behavior was also found for other polysaccharides (see previous section).

(4) Solvent quality: The rheological studies have also been reported to analyze the quality of mixture of different solvents like $[C_4C_1im][Cl]$, [Amim][Cl], $[C_2C_1im][Cl]$, and DMSO. The output of the studies showed that the incorporation of DMSO resulted in a reduction of ILs viscosity but the quality of IL as a solvent for cellulose was not affected. $[C_4C_1im][Cl]$/DMSO, [Amim][Cl]/DMSO, and $[C_2C_1im][Cl]$/DMSO are observed to be θ-solvents for cellulose at 25 °C.[109,125]

Synthetic Polymer Based Solutions. A huge increase in the demand for products with superior properties led to the development of synthetic polymers. These polymer products are now everywhere around us such as clothing, fiberglass, plastic bags, epoxy glue, paints, polyurethane foam, and teflon based cookware.[126] Synthetic polymers have been investigated and reported since the middle of the 19th century. The growth of the polymer industry is so rapid that it is currently surpassing the steel, copper, aluminum, and other industries.[127] Synthetic polymers can be utilized for commercial applications in various forms namely elastomers, coatings, blends, fibers, adhesives, plastics, and composites. In recent years, ionic liquid, a new generation solvent, with excellent properties like high dissolution capability, easy recycling, etc. has been recognized as a green solvent for the processing of synthetic polymers.[128,129] Shear and elongational rheology are used to explore the fundamental properties of polymer melts and solutions for their efficient processing. Studies of elongational deformation are very critical in different processes such as film blowing, melt processing, fiber spinning, and blow molding.[99]

Zhu et al. reported the rheological characterization of poly(acrylonitrile-*co*-itaconic acid) based IL solutions from dilute to concentrated regimes.[130] The Zimm model in the θ-regime and Rouse model were used to describe the linear viscoelastic behavior of dilute and semidilute polymer solutions, respectively. The different trends of the Cox−Merz plots showed the complicated behavior of polymeric solutions at higher deformation rates. The rheological behavior of polyacrylonitrile based IL solutions was investigated to analyze their suitability for electrospinning.[131] The results showed a decrease in complex viscosity of polymer solutions as a function of increasing temperature whereas both moduli (G' and G'') displayed an increasing trend with increasing polymer concentration. Furthermore, the crossover between G' and G'' was shifted toward the lower frequency by increasing the polymer concentration due to the formation of chain entanglements/cross-links.

Similarly, the rheology of polyacrylonitrile based IL solutions was also reported by Yang et al.[132] The Carreau model and the Cross model were used to get the reduced complex viscosity curves and to analyze the behavior of polymeric solutions. The outcome of this study also revealed an increase in activation energy as a function of increasing polymer content. Liu et al. compared the rheology of poly(ethylene oxide) (PEO) based IL solutions with poly(ethylene oxide) based solutions in water.[133] The rheological profiles displayed an increase in viscosity and a shear thinning behavior as a function of increasing polymer content, for both systems. IL based solutions showed a higher viscosity (by 2 orders of magnitude) as compared to water based systems for same polymer fraction. This feature was linked with the higher viscosity of IL. Similar rheological results were also reported by comparing the rheology of PEO based solutions in two ionic liquids with water based system.[134]

Phase separation kinetics and rheology of asymmetric mixtures of poly(ethylene oxide)/ionic liquid was investigated by Luo et al.[135] Different phase-separating morphologies were identified in the considered system: (i) a network structure at 10−30 wt % PEO, (ii) a cocontinuous structure at 40−50 wt %, and (iii) a droplet matrix at 60−70 wt % PEO. The gradual

DOI: 10.1021/acssuschemeng.9b02232
ACS Sustainable Chem. Eng. 2019, 7, 13586−13626

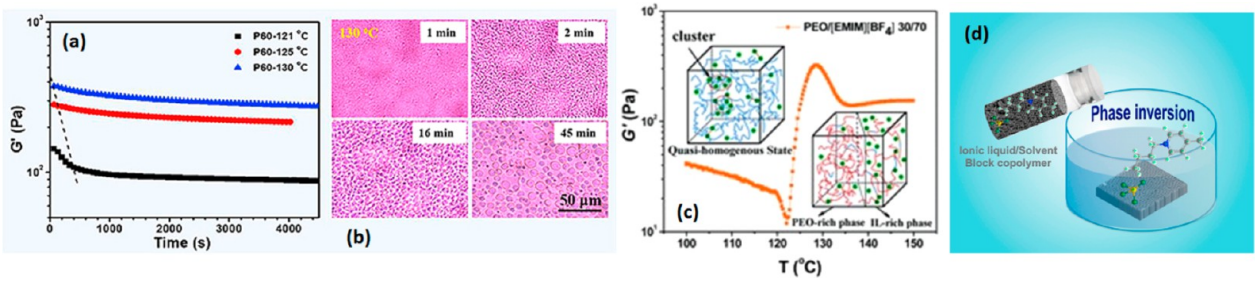

Figure 7. (a) Time dependence of storage modulus for 60 wt % PEO in $[C_2C_1im][BF_4]$ at different temperatures. (b) Optical micrographs of the phase-separating morphologies for 60 wt % PEO/$[C_2C_1im][BF_4]$ blends [Reprinted with permission from ref 135. Copyright 2017. Elsevier]. (c) Dynamic temperature ramp at a frequency of 1.0 rad/s and a heating rate of 1.0 °C/min for the mixture having 30 wt % PEO. Schematic illustration of the breaking of hydrogen-bonded clusters and IL caging upon heating [Reprinted with permission from ref 136. Copyright 2016. The Royal Society of Chemistry]. (d) Synthesis of block copolymer membranes using IL as a cosolvent [Reprinted with permission from ref 137. Copyright 2015. Elsevier].

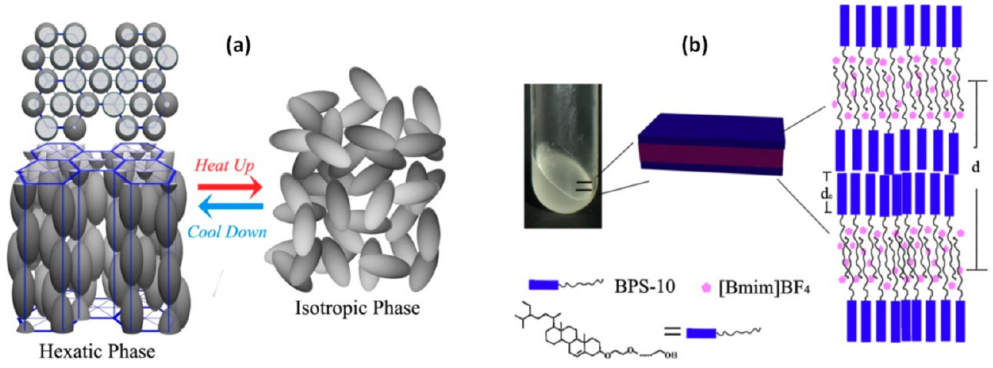

Figure 8. (a) Schematic illustration of hexatic-isotropic transition in CTAB/IL solution [Reprinted with permission from ref 142. Copyright 2012. American Chemical Society]. (b) Schematic representation of interaction between IL and surfactant [Reprinted with permission from ref 144. Copyright 2011. Elsevier].

decrease in G' as a function of time for the highest temperature was associated with the reduced interfacial area due to the droplets coalescence (Figure 7a). The IL rich droplet matrix morphology was confirmed from the optical micrographs of blends having 60 wt % PEO (Figure 7b), and the droplets became larger as a function of time followed by the coalescence phenomenon. Likewise, a novel rheological behavior of PEO/IL mixtures was also reported by Xiao et al.[136] In contrast to a typical increase in G' as a function of temperature, this study presented a unique "V-shaped" rheological response (a decrease in G' followed by an upturn) for mixtures containing less than 50 wt % of PEO, as shown in Figure 7c. The decrease in storage modulus was linked with the breaking of PEO/IL clusters whereas the upturn was attributed to the formation of an interface between the IL and PEO rich phases. Recently, Madhavan et al. also reported the use of IL as a cosolvent for the synthesis of block copolymer based membranes (Figure 7d).[137] In addition to the higher water fluxes, ILs based polymeric membranes displayed different morphological structures as a function of polarity of ILs.

IL−Surfactant Based Solutions. After the synthesis of the first room temperature ionic liquid (ethylammonium nitrate) in 1914,[138] its application as a self-assembly media was first reported by Evans et al. in the 1980s.[139] In conventional self-assembled systems, the change in system properties is bound to the modification of the surfactant. However, by varying the cation or anion in ILs, a range of suitable solvents can be prepared to obtain the desired properties of the self-assembled system. Like aqueous solutions, the self-assembly of surfactant molecules in ILs is governed by the solvophobic effect (ability of surfactant molecules to form interconnected structures by the release of solvent).[140] Greaves and Drummond has reported the detailed review on the self-assembly of surfactant molecules in aprotic and protic ILs.[141]

Rheological characterization was used to analyze the isotropic-hexatic transition (Figure 8a) in micellar solutions of hexadecyl trimethylammonium bromide (CTAB) in IL.[142] The results showed that the system behaved as a viscoelastic liquid ($G' \propto \omega^2$ and $G'' \propto \omega$) in the isotropic regime whereas a gel-like behavior ($G' \sim G'' \propto \omega^b$) was evident in the hexatic region. This difference in behavior (isotropic to hexatic transition) was also observed in steady flow analysis where viscosity was independent of shear rate (Newtonian liquid) at $T \geq 70$ °C while shear thinning behavior was witnessed at $T < 70$ °C. The self-assembly and structural transitions in the surfactant solution of didodecyldimethylammonium bromide (DDAB) and IL was similarly studied by rheology.[143] The outcome of this study showed a thermoreversible transition from sponge like structure to lamellar structure at surfactant concentration greater than 80 wt %. This was evidenced by a sudden increase in storage and loss moduli as a function of temperature.

The aggregation behavior of phytosterol ethoxylate surfactant (BPS-10) in protic and aprotic ionic liquids was studied by using rheology as an effective tool.[40] Steady shear measurements revealed the shear thinning behavior of both solutions. The higher apparent viscosity (180 000 mPa·s) of protic IL based solution as compared to aprotic IL solution, at lower shear rate, is due to the existence of strong hydrogen bonding. Dynamic analysis showed a more elastic behavior ($G' > G''$) together with higher viscosity and moduli for protic IL based solution as

DOI: 10.1021/acssuschemeng.9b02232
ACS Sustainable Chem. Eng. 2019, 7, 13586−13626

compared to aprotic IL based system. The effect of surfactant concentration on the rheology of phytosterol ethoxylates/IL based solution was also reported.[144] The output of rheological analysis indicated an increase in apparent viscosity as a function of increasing surfactant content with the highest value at 90 wt % (more than 20 000 Pa s). Dynamic rheological measurements showed a viscoelastic liquidlike behavior for the studied solutions due to the significant dependence of moduli and complex viscosity on the frequency. Moreover, at 60 wt % of surfactant, the loss modulus (G'') was higher than the storage modulus (G'). A crossover was observed at higher frequency while G' was larger than G'' at 90 wt % of surfactant which was linked with the higher elastic behavior of the solution (Figure 8b).

Mahamat Nor et al. synthesized the IL-in-oil nanoemulsions using a mixture of Tween-80 and Span-20 surfactants for drug delivery applications.[145] The ILs were stabilized inside the core of the micelles by the interfacial film between the oil and IL created by the surfactant. The drug was solubilized and captured by the core of ILs. The viscosity of these nanoemulsions displayed a sharp decrease with increasing shear rate followed by a plateau, as shown in Figure 9. Higher viscosities at lower shear

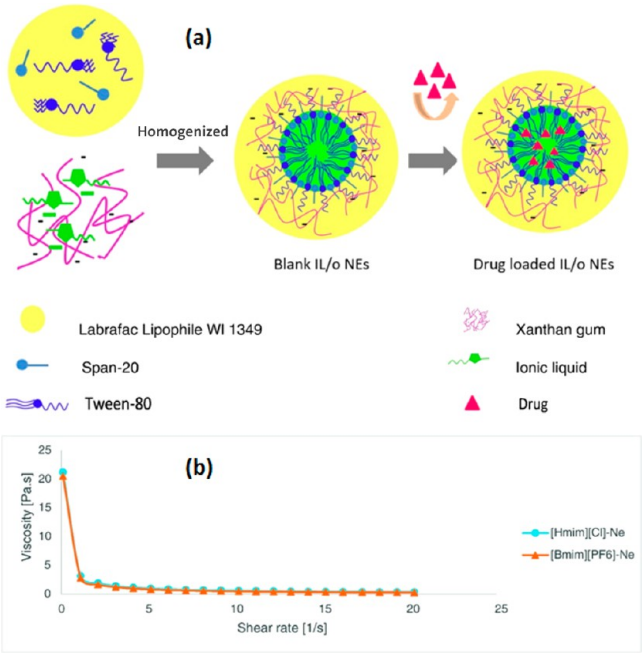

Figure 9. (a) Proposed mechanism for the formation of ILs-in-oil nanoemulsion. (b) Flow curves of prepared nanoemulsions having ratio 2:1 of surfactants [Reprinted with permission from ref 145. Copyright 2017. Elsevier].

rates were attributed to the presence of xanthan gum network around the ILs droplets. Table 2 summarizes the details of the surfactant based IL solutions including concentration of surfactant, investigated temperature ranges and the values of the key rheological parameters.

In summary, the rheological behavior of IL solutions containing polymers (polysaccharides, synthetic polymers) is qualitatively more or less similar and function of the same influencing factors i.e., temperature, polymer content, and external solvent. The results found for the extensively studied cellulose based solutions are therefore expected to be valid for other polysaccharides or synthetic polymers. Higher viscosities, more elastic character, and pronounced shear thinning behavior can be obtained in a single system with higher polymer concentration. The rheological properties of surfactant based IL solutions are different from polymer-based IL solutions because of the structural arrangements that occur within the system, due to the self-assembly properties of surfactants. Different factors have been identified as the key parameters for the rheological changes such as the nature of IL, nature and concentration of surfactants, and temperature. Tuning these parameters helps to tailor the properties of the final system to its intended use. The gel-like system with particular structural arrangements and prominent elastic character is usually observed at higher surfactant concentrations. The shear thinning behavior that is observed in these systems is highly dependent on the temperature and surfactant concentrations due to the direct link between structural breakup and these parameters. Furthermore, IL based emulsion systems have been reported in the literature by replacing the water phase with IL. The properties of such emulsions can be controlled by the amount of surfactants and viscosity modifying agent, i.e., biopolymer.

RHEOLOGY OF IL BASED GELS

Gels are semisolid formulations which are generally made of two components,[46,174−176] usually a solid component (gelator) and a liquid component (ionic liquid, in case of ionogels). Rheological characterization is useful in understanding the properties of ionogels, for example their viscosity, viscoelasticity, gelation and melting temperatures, and their mechanical strength. In gelled systems, the functionality of ionic liquids provides an enhanced solidlike character whereas maintaining the liquid mobility within the system results in retaining the useful properties of ionic liquids. As compared to traditional gel synthesis, the preparation of ionogels is cheaper, easier, and energy efficient. Ionogels can offer a range of mechanical strength from semisolid to solid with different pore shapes/sizes and interfacial interactions.[177] The mobility and structural arrangement of ionic liquids inside the pores have resulted in an improvement of charge transport,[178] activity of catalyst,[179] and electrical conductance.[180,181]

IL−Polymer Based Gels. *Natural/Biopolymer Based Ionogels.* The term biopolymer refers to the following materials: (i) naturally occurring macromolecules, (ii) polymers derived from naturally occurring macromolecules, and (iii) long chain molecules synthesized from biobased monomers.[182] Due to the renewable origin and biodegradability, biopolymers are ecofriendly and potential alternatives to petrochemical polymers.[183] Biopolymer gels have been studied from both academic and industrial points of view. Biopolymers provide the backbone structure in many solid and semisolid formulations particularly food products.[184] Zhang et al. successfully prepared and reported the rheological analysis of thermally and dimensionally stable ionic liquid gels based on guar gum and a solution of ionic liquid.[185] Their key findings were the formation of solidlike material with high elastic modulus (≈30 000 Pa) and the variation of its rheological characteristics as a function of ionic liquid weight fraction, shown in Figure 10. The formation of the structure was due to the interactions between the guar gum and the ionic liquid chains and the chain entanglements. The rheological analysis of guar gum based ionogels was also performed by Verger et al.[186] A dominant elastic character and slower relaxation dynamics of ionogels were observed at higher guar gum concentrations (>9 wt %) due to the enhanced polymer/IL interactions and polymer entanglements. At the

DOI: 10.1021/acssuschemeng.9b02232
ACS Sustainable Chem. Eng. 2019, 7, 13586−13626

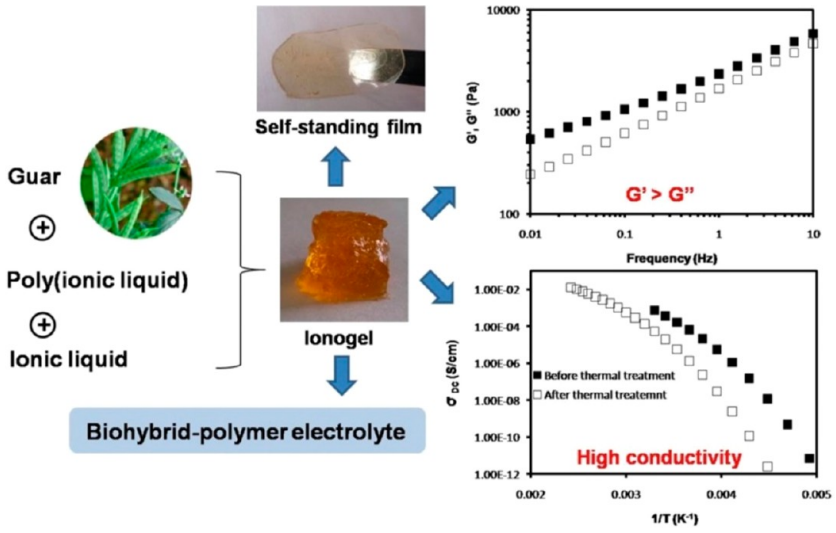

Figure 10. Preparation of ionogels having 5 wt % guar gum and 10 wt % PIL in IL. G' (filled symbols) and G'' (open symbols) as a function of frequency for 10% PIL and 5% guar gum in IL. DC conductivity as a function of inverse temperature for guar gum (5%)/PIL (10%)/IL before and after thermal treatment [Reprinted with permission from ref 185. Copyright 2017. Elsevier].

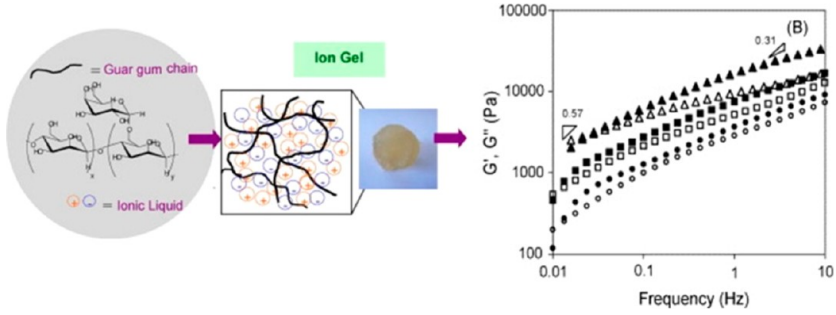

Figure 11. Storage (filled symbols) and loss (open symbols) moduli as a function of frequency for guar gum/IL solutions, with guar gum concentrations 10 wt % (○), 15 wt % (□), and 25 wt % (Δ) at 25 °C [Reprinted with permission from ref 186. Copyright 2014. Elsevier].

highest fraction of guar gum (25 wt %), moduli still showed a frequency dependence which suggested the relaxation in the system (i.e., transient character) (Figure 11).

The rheological and thermal analysis of a three component gel system comprising ionic liquid, cellulose and coagulation agent was performed by Ariño et al.[187] The results displayed that the thermal stability of $[C_4C_1im][Cl]$ based gels was higher than $[C_2C_1im][Ac]$ based gels. The stability was independent of cellulose content and coagulation agent for $[C_4C_1im][Cl]$ based gels. Furthermore, larger values of the plateau storage modulus G' were observed for ionogels having higher fraction of cellulose. The formation of cross-linked structures in the gels was confirmed by the fact that the values of G' were higher than G'' and that both moduli were independent of frequency within the studied range.

Synthetic Polymer Based Ionogels. Polymer Ionogels. Polymeric gels are structured systems in which polymer acts as a continuous phase which polymerizes/assembles to entrap the liquid phase resulting in a gelled system. This interaction between polymeric chains can either be physical or chemical.[177] Currently, there is growing demand for ILs in polymeric gels due to the retainment of useful properties of ILs within the polymeric matrix. Ziółkowski et al. reported an interesting strategy to prepare ionogels by polymerizing the *N*-isopropylacrylamide (NIPAM) monomer in five different ILs with or without adding cross-linker.[188] The results showed that the nature of the IL had a strong effect on [i] the viscosity of the polymerization medium and [ii] the polymerization speed. Rheological analysis of the prepared ionogels showed a reversible increase in modulus as a function of temperature above its lower critical solution temperature (LCST) (to give an order of magnitude, there was a 7-fold increase in modulus for $[P_{6,6,6,14}][DCA]$ based ionogel).

An interesting application of ionogels in rechargeable batteries was described by Patel et al. in which a free radical polymerization mechanism was used to polymerize acrylonitrile in an ionic liquid electrolyte (Figure 12).[189] The ionogels displayed extraordinary mechanical strength together with a greater thermal stability as compared to the ionic liquid. The viscosity of the prepared gels was also higher (by 2 orders of magnitude) than the ionic liquid whereas the ionic conductivity remained almost same ($1.1-1.7 \times 10^{-3}$ Ω^{-1} cm^{-1}). The rheological behavior of the gelled systems can be easily tuned by adjusting the gelator concentration or the temperature. The specifications of different ionogel systems, reported in the literature, are presented in Table 3 including the concentration of the gelator, temperature ranges, gelation temperature, and the values of the key rheological parameters.

Copolymer Ionogels. Another promising gel system, having self-healing or photo- and thermoreversible gelation capabilities, can be obtained from copolymeric materials as a gelator in ILs. A triblock terpolymer [poly(ethylene-*alt*-propylene)-*block*-poly-

DOI: 10.1021/acssuschemeng.9b02232
ACS Sustainable Chem. Eng. 2019, 7, 13586−13626

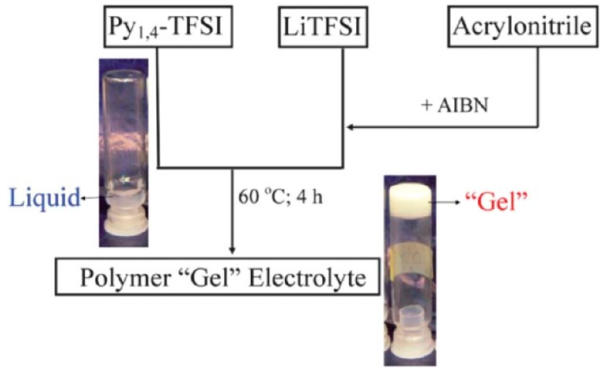

Figure 12. Synthesis of ionogels using ionic liquid electrolyte and a monomer (acrylonitrile) [Reprinted with permission from ref 189. Copyright 2011. The Royal Society of Chemistry].

(ethylene oxide)-*block*-poly(*N*-isopropylacrylamide) (PON)] and an ionic liquid based gel was studied in the literature.[190] The rheological profiles displayed the formation of a gelled structure at lower polymer concentration (1−2 wt %) and also the ability to resist high strains (up to 70%) at 10 wt % polymer content. Figure 13 depicts the schematics of ionic liquid gel formation by triblock terpolymer.

The emerging field of phototriggered reversible gelation for triblock copolymer and ionic liquid solution was reported by Ueki et al.[191] At lower polymer concentration (1 wt %), transition from unimer structure to micelles was observed whereas sol−gel transformation was witnessed for higher polymer concentration (20 wt %) in ionic liquid at bistable temperature of 50−53 °C by photostimulus. Figure 14 shows the mechanism of photoreversible gelation of ionic liquid based system.

Another novel triblock copolymer was reported by Kitazawa et al. for the gelation of ionic liquid as a function of temperature and polymer content.[192] Dynamic rheological measurements of the system containing 20 wt % polymer proved the existence of a liquid-like behavior ($G' < G''$) at lower temperature whereas at higher temperature (above the aggregation temperature of polymer) the system transformed into a gel-like material. At a particular concentration of triblock copolymer, below 10 wt %, no gelation was observed. Moreover, the system also presented the excellent ability of thermal sol−gel reversion for multiple cooling/heating cycles. Tamate et al. presented the rheological analysis of self-healing ionogels containing diblock copolymer and a hydrophobic IL which are expected to have applications in the field of flexible/wearable electronic devices.[193] The time−temperature superposition (TTS) curves displayed the existence of crossover between G' and G'' for P(DMAAm-*r*-AAc) (DA) and PS-*b*-PDMAAm (SD) based ionogels whereas no crossover was observed for PS-*b*-P(DMAAm-*r*-AAc) (SDA) based gels (Figures 15a−c). Temperature ramp tests revealed the similar and significantly higher moduli of SDA and DA based ionogels as compared to the SD based gels at lower temperatures (Figure 15d) due to the hydrogen bonding between DMAAm and AAc units. At higher temperatures, the moduli response of SDA and DA based ionogels became considerably different (i.e., $G'' \gg G'$ for DA ionogels) which was attributed to the dissociation of hydrogen bonding in DA gels. The strain sweep tests showed a decrease in critical strain, required to deviate from linearity, by increasing temperature of SDA ionogels, presented in Figure 15f, which was linked with the reduction in hydrogen bonding strengths at elevated temperatures.

Polyelectrolyte Ionogels. Apart from conventional ionogels, another ionic liquid gelled system was reported by Nagasawa et al. based on polyelectrolytes having different polyethylene spacer length (m = 2, 4, and 10).[194] The output of this study showed that the gelation temperature (T_{gel}) and the critical gelation concentration of the polymer increased with the decrease in spacer length whereas no effect of spacer length was found on the elastic modulus and ion conductivity of ionogels. The resulting ionogels also displayed better strength and ion conductivity as compared to the conventional ionogels. Nagasawa et al. studied the gelation of different ionic liquids by using modified polymeric electrolytes.[195] The critical gelation concentration for the reported modified gelators was very low (0.9−10 g/L) and also the prepared ionogels, based on bis(fluorosulfonyl)-amide (FSA) and trifluoromethanesulfonate (TfO) anions containing ionic liquids, exhibited the higher temperatures (>100 °C) for gel−sol transformation.

The gelation of ionic liquid was also reported by Ishioka et al. using self-assembly of supramolecular gelators.[196] The observations revealed that the storage modulus was approximately 20 times higher than the loss modulus within the investigated frequency range which testified the gel-like behavior of the system. The time sweep analysis confirmed the rapid formation (within a few minutes) of gel structure at 30 °C, as evidenced by a rapid increase in G' and G'' for few initial minutes followed by a steady state value.

IL−Surfactant Based Gels. Surfactants are interesting systems because of their ability to self-assemble and phase-separate into a diverse range of microstructures. Research on the viscoelasticity of surfactant solutions started back in 1970s[197] and has continuously gained the attention of researchers due to several potential applications. These interesting applications include oil fields, heat transfer fluids, and personal care products.[198] Surfactants can form rodlike, spherical, and inverted vesicles, micelles, and bilayers. They can also form lyotropic phases at high concentration of surfactants.[199] The microstructure of surfactants, which is dependent on their concentration, has a significant effect on the rheological properties of the system. Usually, dilute surfactant solutions display low viscosity because of the development of spherical micelles. However, self-assembly of surfactants can also provide viscoelastic and gel-like properties to the solution either in the presence of additives or under certain conditions.

A gelled system based on ionic liquid and a surfactant was prepared by Zhou et al. in the presence of a binary solvent mixture, i.e., water and ethylammonium nitrate [EA][N].[200] The observations proved the ability of the surfactant ($[C_4MP][C_{12}H_{25}SO_4]$) to act as a gelator. This resulted in the formation of a gel structure in addition to the development of lytropic, hexagonal, and lamellar crystal phases. The outcomes of this study also showed a decreasing effect of the viscoelasticity of the system as a function of increasing EAN fraction/decreasing ionic liquid content. Wang et al. investigated the gelation of two ionic liquids $[C_6C_1im][BF_4]$ and $[C_6C_1im][NTF_2]$ by using sugar surfactant as a gelator.[201] There was a structural transition of the surfactant from a ribbon structure (melt state) at high temperature to a lamellar structure (gel state) at room temperature, shown in Figure 16. $[C_6C_1im][NTF_2]$ based gels displayed higher thixotropy and lower wear resistance than the $[C_6C_1im][BF_4]$ based gels which might be linked with the viscoelasticity of gels.

Nanocomposite Ionogels. Nanocomposite gels (nanoparticles entrapped within gel matrix) offer materials with

DOI: 10.1021/acssuschemeng.9b02232
ACS Sustainable Chem. Eng. 2019, 7, 13586−13626

Table 3. Some Details of Rheological Analysis of Ionic Liquid Based Gels

ionic liquid	polymer	concentration of gelator (wt %)	rheometer	characterization temperature	shear rate or angular frequency	gelation temperature	key rheological parameters	ref
$[C_4C_1im][Cl]$	guar gum, PAEMIBr	5, 5−20	DHR-2, TA Instruments	25 °C	0.01−10 Hz		G' = 800−27000 Pa (1 Hz)	185
$[C_2C_1im][TFSA]$	PON	1−10	AR-G2, TA Instruments	−10−70 °C	0.1−100 rad/s	16−27 °C	G_x = 60−8850 Pa (0 °C)	190
$[C_6C_1im][BF_4]/[C_6C_1im][NTf_2]$	sugar surfactant (HLG)	2−4	RS 6000, Thermo Haake	25 °C	0.01−1000 s^{-1}, 0.01−10 Hz	113.4−122.8 °C	G' = 10^4−10^5 Pa (1 Hz)	201
$[C_2C_1im][TFSA]/[C_2C_1im][FSA]$	CDBA*m*●X; *m* = 2, 4, 6, 10; X = TFSA, FSA	5−70 g/L	ARES, TA Instruments		0.01−16 Hz		G' = 10^2−10^5 Pa (0.1 Hz)	194
$[C_4C_1im][Cl]$	agarose (AG), chitosan (CH)	5	RS 1, Thermo Haake	25−100 °C	0−22 Hz	56 °C	G' (10 Hz; 25 °C) CH = 190 Pa AG = 50 Pa AG-CH = 32 Pa Nps-AG-CH = 17 Pa	203
$[C_2C_1im][CF_3SO_3]$	1,3,5-benzenetriarboxamides, substituted with amino acids and amino acid methyl esters	1	MCR 301, Anton Paar	30 °C	0.1−100 rad/s	90−160 °C	G' = 2.8 × 10^4 Pa (1 Hz)	196
$[C_4C_1im][Cl]/[C_2C_1im][Ac]$	MCC, ethanol, water	5−10	SR 200, Rheometrics	25−180 °C	0.01−10 Hz	160−185 °C	G' = 64−429 Pa (70 °C; 1 Hz)	187
$[C_4C_1im][Cl]$	guar gum (GG), MWCNTs	10, 0.2	RS 1, Thermo Haake		0−1000 s^{-1}		G' (1 Hz) GG/IL = 62 Pa GG/IL/MWCNTs = 16 Pa	204
$[C_2C_1im][Ac]$	MCC, nanosilica	5−18, 0.05−2.5	AR-2000ex, TA Instruments	30−140 °C	0.01−100 rad/s	60−125 °C	G' = 0.6−10^5 Pa (MCC 9 wt %; silica 0−1.11 wt %; 30 °C; 1 Hz)	205
$[C_2C_1im][NTf_2]$	BMB	10−20	MCR 301, AntonPaar	0−140 °C	0.1−100 rad/s	100 °C	G' = 0.15−7 Pa (25 °C; 1 Hz)	192
$[C_4C_1im][Cl]$	cellulose, silk fibroin	6	MCR 301, AntonPaar	0−70 °C	0.01−10 s^{-1}, 0.1−100 rad/s	14.5 ± 3.1−18.2 ± 2.3 °C	G' = 300−2500 Pa (cellulose/silk ratio 4/6; 40−10 °C; 1 Hz)	208
$[C_2C_1im][Ac]$	MCC	5−18	AR-2000, TA Instruments	25−120 °C	0.01−100 rad/s	59.2−107.1 °C	G' = 0.3−10^5 Pa (25 °C; 1 Hz)	113
$[C_4C_1im][PF_6]/[C_4C_1im][BF_4]/[C_4C_1im][SCN]/[C_4C_1pyr][NTf_2]/[C_4C_1im][NTf_2]$	Dicarboxylate diimidazolium salts	1−9	AR-G2, TA Instruments	25 °C	0.1−100 rad/s	21−72 °C	G' = 1.2 × 10^3−1.7 × 10^4 Pa	209
$[C_8C_1im][Cl]$	DNA	0.1−1 w/v%	AR-500, TA Instruments	20−80 °C	1−100 rad/s	52−72 °C	G' = 10−40 Pa (DNA 0.3−1 wt %; 20 °C; 1 Hz)	210
$[C_4C_1im][BF_4]/[C_4C_1im][PF_6]/[C_4C_1im][SbF_6]/[C_4C_1im][NTf_2]/[C_4C_1pyr][NTf_2]/[C_4Et_3N][NTf_2]/[Bzmim][NTf_2]$	$[C_{12}C_{12}im]_n$[1,4-BDC], $[C_{12}C_{12}im]_n$[2,6-NDC], $[C_{12}C_{12}im]_n$[Trim], $[C_{12}C_{12}im]_n$[Cit]	5	AR-G2, TA Instruments	25 °C	1 rad/s	16−39 °C	G' = 1.5 × 10^3−1.5 × 10^4 Pa (1 Hz)	211
$[N_{2224}][NTf_2]/[N_{1444}][NTf_2]/[C_1C_4pip][NTf_2]/[C_1C_4pyr][NTf_2]$	$[P_{66614}][Glu]$, $[P_{4444}][Glu]$, $[N_{4444}][Glu]$	6.5		25 °C	1 Hz	13.7−30.1 °C	yield strain (%) = 0.37−25.28 (1 Hz)	212
$[C_2C_1im][NTf_2]$	PVDF, PVDF-*co*-HFP, $[Co(b\text{-}py)_3]^{2+/3+}[NTf_2^-]_{2/3}$	2.5−18	DHR-3, TA Instruments	25−70 °C	0.1−20 Hz		G' = 200−350 Pa (gelator = 2.5 wt %; 25 °C; 1 Hz)	213
$[Amim][Cl]/[C_4C_1im][Cl]/[C_4C_1im][MP]$	guar gum	5−25	AR-1000, TA Instruments	25 °C	0.01−10 Hz		G' = 500−25000 Pa (1 Hz)	186
$[C_2C_1im][NTf_2]$	PS-*b*-P(DMAAm-r-AAc), PS-*b*-PDMAAm, P(DMAAm-r-AAc)	30	MCR 301, AntonPaar	20−120 °C	0.1−100 rad/s		yield strain (%) = 10−100 (100−30 °C; 1 rad/s)	193

DOI: 10.1021/acssuschemeng.9b02232
ACS Sustainable Chem. Eng. 2019, 7, 13586−13626

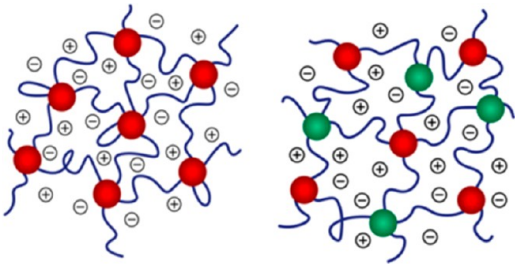

Figure 13. Schematic representation of ionogel formation by triblock terpolymer [Reprinted with permission from ref 190. Copyright 2016. American Chemical Society]

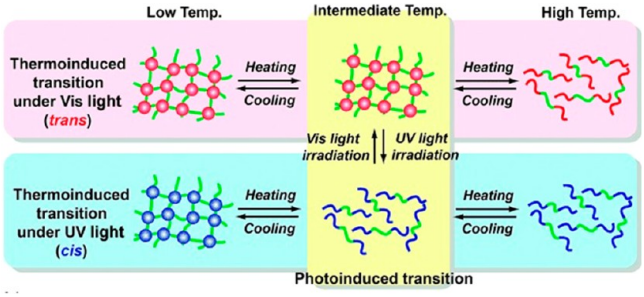

Figure 14. Schematic representation of photoreversible gelation of ionic liquid based system [Reprinted with permission from ref 191. Copyright 2015. John Wiley and Sons].

tunable properties due to the functionality of nanoparticles together with the synergistic interaction between polymeric matrix and nanoparticles.[202] Recently, ionic liquids have been found to contribute to this nanomaterial field. Trivedi et al. investigated a nanocomposite ionogel system based on biopolymers (agarose (AG) and chitosan (CH)), silver oxide nanoparticles (AgNps), and IL.[203] In contrast to conventional ionogels, nanocomposite ionogels displayed an increase in

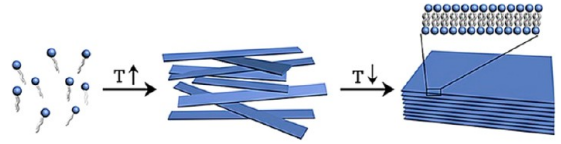

Figure 16. Illustration of structural transition of surfactant in ionic liquid as a function of temperature [Reprinted with permission from ref 201. Copyright 2016. John Wiley and Sons].

storage modulus as a function of frequency whereas the loss modulus remains approximately constant. The rheological analysis confirmed the viscous behavior of system ($G'' > G'$) at low frequency, crossover between both moduli at ~5 Hz, and gelled systems ($G' > G''$) at higher frequency. The melting temperature of the prepared gel was found to be ~80 °C by thermorheological analysis.

Solvent healing characteristics of conventional ionogels, based on guar gum/ionic liquid and nanocomposite ionogels, prepared by incorporating multiwalled carbon nanotubes (MWCNTs) within the conventional ionogels, (Figure 17a) were investigated by Sharma et al.[204] Figure 17b shows the schematics of the healing mechanism in conventional and composite ionogels. The rheological findings revealed a higher shear viscosity, a more predominant storage modulus over loss modulus, a higher yield stress (183 Pa), and a higher recovered storage modulus (20% higher) for the nanocomposite ionogels as compared to conventional ionogels. This indicated a stronger gel network and healing nature of the composite systems.

Likewise, a novel utilization of hydrophilic nanosilica particles to alter the gelation characteristics of ionic liquid/cellulose based gels was studied by Song et al.[205] The rheological analysis highlighted two important parameters, cellulose content and nanoparticles fraction, for manipulating the sol−gel transition temperature and storage modulus (G') of the nanocomposite gels. The salient feature of the prepared nanocomposite ionogels was their high tensile strength without significant loss of ionic

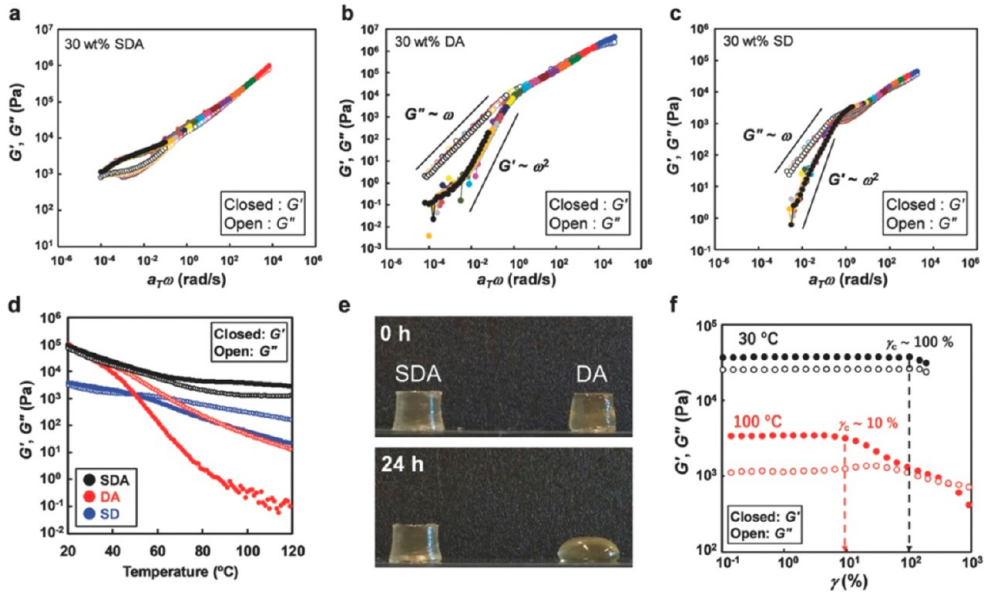

Figure 15. (a−c) TTS moduli curves for 30 wt % (a) SDA, (b) DA, and (c) SD ionogels at a reference temperature of 40 °C. (d) Moduli as a function of temperature for 30 wt % SDA, DA, and SD ionogels cooled at 1 °C/min within the LVE regime. (e) Shape changes in cylindrical SDA (left) and DA (right) ionogels at room temperature. (f) Strain sweeps for SDA ionogel at a frequency of 1 rad/s at 30 and 100 °C [Reprinted with permission from ref 193. Copyright 2018. John Wiley and Sons].

DOI: 10.1021/acssuschemeng.9b02232
ACS Sustainable Chem. Eng. 2019, 7, 13586−13626

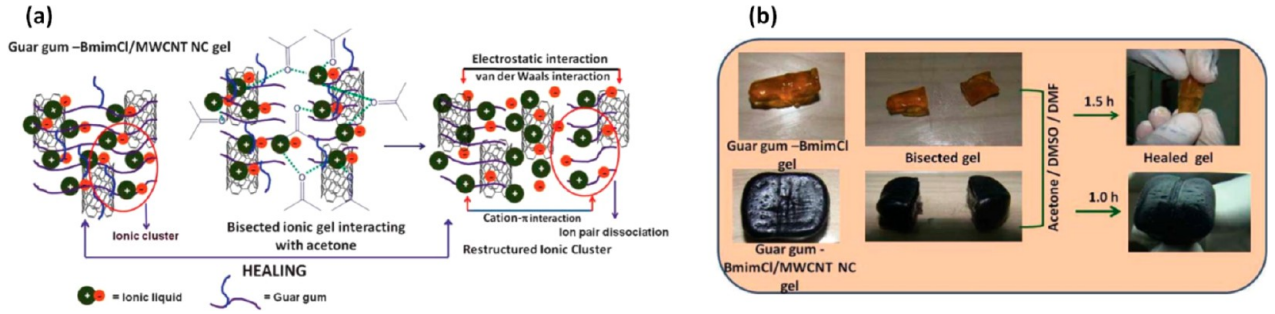

Figure 17. (a) Schematic representation of formation and restructuring of ionic cluster in conventional and composite ionogels. (b) Healing of conventional and nanocomposite ionogels in the presence of acetone [Reprinted with permission from ref 204. Copyright 2013. The Royal Society of Chemistry].

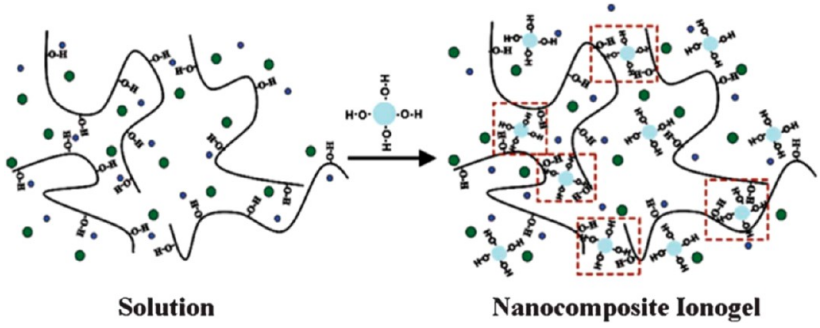

Figure 18. Schematic representation for the formation of nanocomposite ionogels by gelation of cellulose/ionic liquid solutions with the help of nanosilica particles [Reprinted with permission from ref 205. Copyright 2013. The Royal Society of Chemistry].

conductivity. Figure 18 shows the schematic representation of ionogels formation with the help of nanosilica particles.

Ramesh and Liew performed the rheological characterization of polymeric gel electrolyte and nanocomposite gel electrolyte (containing silica nanoparticles) based on ionic liquids.[206] Rheological profiles depicted the higher values of storage modulus (G') than the loss modulus (G'') which was linked with the elastic behavior of the samples. The linear viscoelastic (LVE) regime increased with the increasing fraction of silica nanoparticles and ionic liquid whereas the latter had also a significant effect on the long-term stability of the structure. The elastic character of the samples was also affirmed by frequency sweep tests. A reduction in zero shear viscosities was observed as a function of increasing ionic liquid and nanoparticles content. This was also attributed to the increasing shear rate. Ponyrko et al. synthesized a high performance epoxy/silica/IL nanocomposites displaying shape memory effects.[207] The nanocomposites displayed a dual shape-memory effect, where some part of the shape were regained at 60 °C while the complete shape was recovered at 100 °C (Figure 19). Several parameters related to shape memory phenomenon, such as efficiency of elastic energy and stress recovery, and completeness of shape fixity and recovery, were enhanced by incorporating a very small amount of IL (0.2 wt %).

In summary, IL based gels have highly tunable rheological properties that meets the industry requirements. These properties can be adjusted by changing the nature of the IL and the nature and concentration of the gelator (which can be a (bio)polymer, surfactant, or copolymer). The elastic character and thermal stability of ionogels are primarily governed by the gelator content. For example, a thermally resistant solidlike system can be obtained with higher concentrations of gelator due to the interactions between gelator and IL and also because

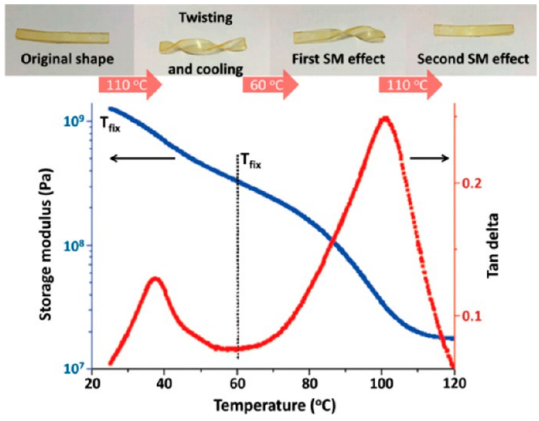

Figure 19. Snapshots from epoxy/silica/IL nanocomposites showing its initial shape, twisting after heating up to 110 °C, and subsequent cooling down and first and second stages of the shape memory effect. The storage modulus and tan δ are plotted as a function of temperature, displaying the transitions related to the dual shape memory phenomenon [Reprinted with permission from ref 207. Copyright 2016. The Royal Society of Chemistry].

of gelator chain entanglements. Copolymers and polyelectrolytes are found to have the ability to jellify the ILs at small concentrations resulting in better rheological and self-healing properties of ionogels. IL based nanocomposite gels have better mechanical and rheological properties as compared to the conventional ionogels (i.e., without nanomaterials) due to the inclusion of nanomaterials. The thermal transition (i.e., sol–gel), elasticity, stimuli responsiveness, and structural recovery of such systems depend extremely on the fractions of IL and nanomaterials.

DOI: 10.1021/acssuschemeng.9b02232
ACS Sustainable Chem. Eng. 2019, 7, 13586–13626

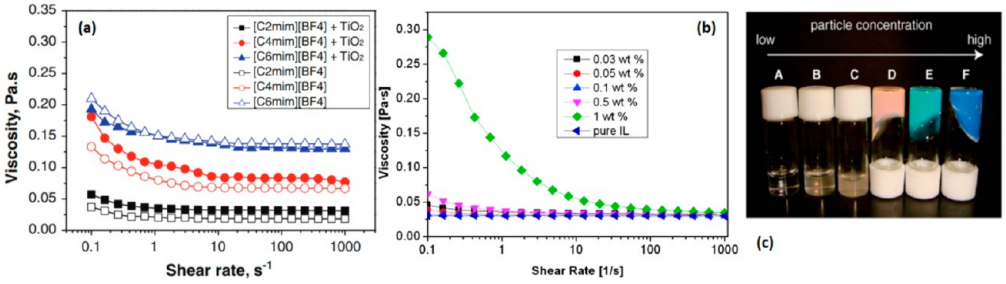

Figure 20. (a) Effect of alkyl chain length on the dispersibility of 26.4 nm nanoparticles with 0.5 wt % [Reprinted with permission from ref 224. Copyright 2013. Springer Nature]. (b) Effect of nanoparticle fraction on the rheology of dispersions in the hydrophobic ionic liquid prepared with 1 h ultrasonic treatment [Reprinted with permission from ref 217. Copyright 2012. American Chemical Society]. (c) Picture of dispersions of polymer-grafted nanoparticles in IL having different particle fraction (A) 0, (B) 1, (C) 3, (D) 14.2, (E) 25, and (F) 33.3 wt % [Reprinted with permission from ref 226. Copyright 2010. American Chemical Society].

RHEOLOGY OF IL BASED DISPERSIONS

Dispersion can be defined as a system having immiscible phases from which one is continuous and at-least one phase is dispersed within the continuous matrix.[214] Conventionally, dispersions are usually produced by using polyethylene glycol (PEG), ethylene glycol (EG), or water as the continuous phase.[215] Recently, the combination of ILs and nanophases has evolved as a new field of nanostructured dispersions, with exciting engineering applications.[216] The specific properties of ILs like higher thermal stability, low vapor pressure, less toxicity, enhanced colloidal stability, and inertness toward water and air make them useful candidates to replace classical solvents in dispersions.[217,218] These physical and chemical properties of ionic liquids give rise to their application in solidified electrolytes,[219] nanoparticle synthesis,[220] and magnetorheological fluids.[221] The rheological analysis of such systems will enable us to characterize their viscoelastic properties together with the existence of colloidal interactions. Several factors can influence the rheological behavior of dispersions like the polarity of ionic liquid, surface polarity and concentration of nanophases together with the temperature.[42]

Nanoparticle Based Dispersions. In recent years, interest in nanomaterials has progressively increased. Nanoparticle based dispersions have potential applications because of their enhanced thermal performance and thermophysical properties.[215] Recently, the use of ionic liquids for the preparation of nanoparticle based dispersions has gained interest because of the useful properties of ionic liquids.

Gao et al. studied the rheology of modified silica nanoparticles dispersions in IL as a function of temperature.[222] The results revealed the stronger shear thickening behavior of dispersions due to the formation of thinner solvation layers (approximately 3 nm) originating by the hydrogen bonding between hydrocarbon coating and the anion of IL. The reduction in solvation layer thickness on the nanoparticle and the corresponding weakening of hydrogen bonding were confirmed by the gelation of the system at temperatures above 30 °C. The stability and settling of silica particles (weight fraction of 10 wt %) in different protic ionic liquids through oscillatory rheology was reported by Smith et al.[223] The rheological analysis affirmed the viscoelastic nature of propylammonium nitrate (PAN) and [DMEA][F] based suspensions due to the existence of long-range and persistent structure in the samples which in turn slowed down the settling of particles.

In addition to bulk rheology, the local rheology of two different ionic liquids ($[C_4C_1im][BF_4]$ and $[P_{6,6,6,14}][NTf_2]$) using magnetic resonance (MR) velocity imaging was first investigated by Novak and Britton, with the addition of silica nanoparticles.[218] At lower shear rates (<10 s^{-1}), a Newtonian behavior was observed whereas shear-thickening characteristics were evident at higher shear rates (>10 s^{-1}) for 15 wt % silica dispersions in $[C_4C_1im][BF_4]$. A more complex behavior, shear-thinning together with shear-banding, was found by both rheological analysis for a 5 wt % dispersion of silica particles in $[P_{6,6,6,14}][NTf_2]$.

Rheological analysis was also used to study the influence of nanoparticle content and temperature on the stability of silica nanoparticles based dispersions in ILs.[42] A destabilization (i.e., phase separation) phenomenon was observed for all the prepared systems as a function of increasing nanoparticles fraction and temperature. The suspension of unmodified nanoparticles in hydrophilic ionic liquid was very stable whereas an unstable system (or stable at very small nanoparticles content or temperature) was obtained by dispersing the unmodified nanoparticles in a hydrophobic ionic liquid system. The surface functionalization of silica nanoparticles with hydrophobic groups resulted in the enhancement of their stabilization in hydrophobic ionic liquid for larger nanoparticles concentration and sometimes higher temperatures.

Wittmar et al. investigated the effect of the cation alkyl chain length of IL, titanium dioxide (TiO_2) nanoparticle size, and concentration on its suspension stability using advanced rheology.[224] The increasing length of the alkyl chain resulted in an enhanced viscosity and a non-Newtonian behavior together with a decrease in Brownian motion of the nanoparticles. The outcome of the rheological analysis is shown in Figure 20a. This figure shows that a homogeneous dispersion of nanoparticles in the IL with the longest chain has a similar rheological profile as the IL without the addition of TiO_2. At smaller nanoparticle content, the interaction between IL molecules controls the suspension stability whereas at higher nanoparticles content, the internanoparticle interaction starts to play a role because of the smaller average distance between particles. It was also observed that large particles were more homogeneously dispersed in all ILs as compared to the small particles, which tend to agglomerate, particularly at higher content (resulting in larger viscosities at lower shear rates).

The influence of the polarity (hydrophilic or hydrophobic) of the IL, period of ultrasound treatment, and nanoparticle concentration on the dispersibility of TiO_2 nanopowders in ILs was investigated using rheological analysis.[217] A non-Newtonian behavior was observed, irrespective of the period of ultrasound treatment, for the dispersion of nanoparticles in a hydrophobic IL. In the case of hydrophilic IL, Newtonian

DOI: 10.1021/acssuschemeng.9b02232
ACS Sustainable Chem. Eng. 2019, 7, 13586−13626

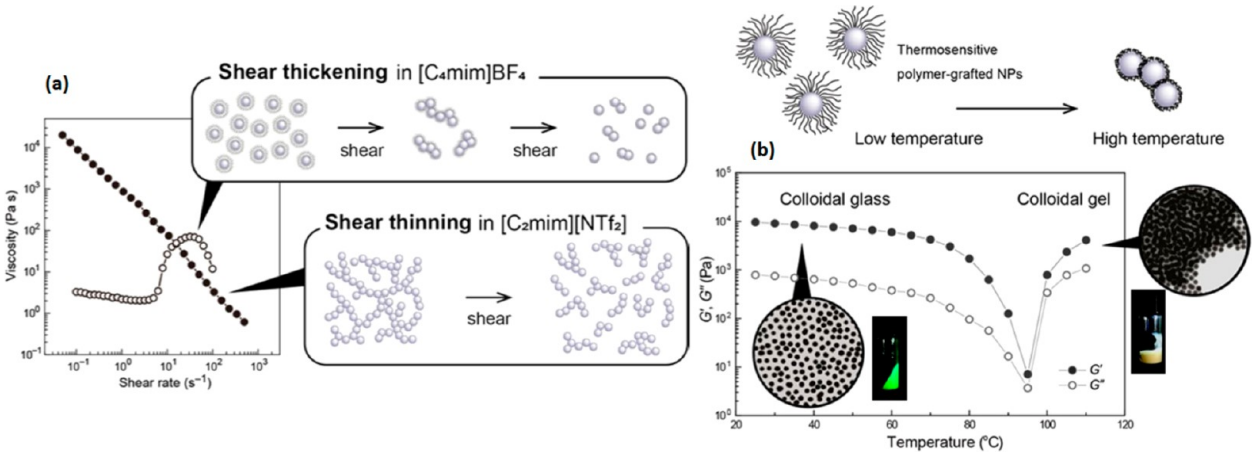

Figure 21. (a) Viscosity as a function of shear rate for a colloidal gel of 5 wt % silica NPs in NTf_2 based IL (closed circle) and a stable suspension of 15 wt % silica NPs in BF_4 based IL (open circle) and schematic representation of the changes in the microstructures by shearing action. (b) Schematic representation for thermosensitive polymer grafted NPs. Storage (closed circles) and loss (open circles) moduli as a function of temperature for colloidal glass with 25.0 wt % polymer grafted NPs in NTf_2 based ILs and the TEM images [Reprinted with permission from ref 229. Copyright 2018. Springer Nature].

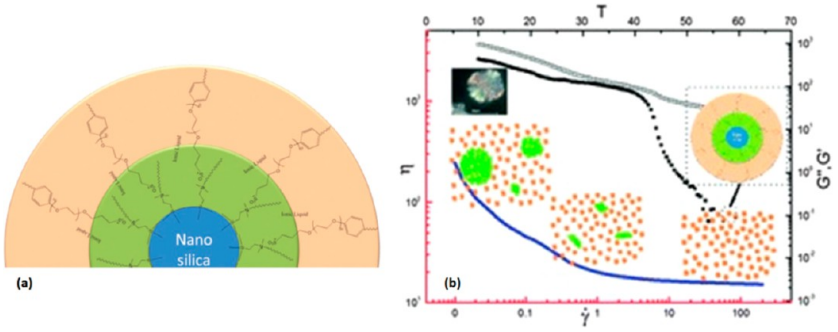

Figure 22. (a) Schematic illustration of the structure of NILs with a nanosilica core. (b) Storage (filled symbols) and loss (empty symbols) moduli as a function of temperature during a heating run at 1 °C/min and flow curves of NILs [Reprinted with permission from ref 230. Copyright 2015. The Royal Society of Chemistry].

behavior was evident for short ultrasonic treatment periods whereas an extended treatment resulted in non-Newtonian systems due to the reorganization of particles. At small concentrations (less than 0.5 wt %), Newtonian behavior was evident for the hydrophobic IL whereas a change to non-Newtonian was observed above concentrations of 0.5 wt % (Figure 20b).

An application of nanoparticle based ionic liquid dispersions (NEILs) for concentrating solar power was proposed by Paul et al. by dispersing different volume fractions of aluminum oxide (Al_2O_3) nanoparticles in ILs.[215] The prepared dispersions displayed shear thinning behavior at all studied temperatures and this pseudoplasticity of dispersions enhanced with increasing temperature. An increase in the shear viscosity of dispersions was observed as a function of increasing nanoparticle content. Conventional viscosity model was suitable for predicting the shear viscosity of the dispersions up to 0.18 vol %, whereas at larger fractions, the convention model underestimated the experimental shear viscosity values. A different approach to study the rheology of magnetite nanoparticles dispersion in an IL is to use a magnetic field which was done by Rodríguez-Arco et al.[225] A magneto-viscous (MV) effect (enhancement of shear stress and viscosity as a function of magnetic field intensity for same shear rate) was observed, particularly for the unstable dispersions, due to the creation of chainlike agglomerates. The intensity of this MV effect was linked with the size and concentration of larger particles within the dispersion.

Ueno et al. reported a system prepared by dispersing polymer-grafted silica nanoparticles in an IL.[226] At smaller nanoparticles fraction, dispersions displayed liquidlike (Newtonian) behavior without the presence of particles agglomerates whereas a solidlike (shear thinning) behavior and different colors were observed after the additions of specific amount of silica nanoparticles (Figure 20c). Rheological analysis revealed the dependence of the zero shear viscosity (η_0) on the effective volume fraction of nanoparticles (φ_{eff}), which was higher than the volume fraction ($\varphi \sim 0.64$) for close packing of hard spheres due to the deformability and interpenetrability of the grafted polymeric layer. For smaller values of φ_{eff} (less than or equal to 0.62), the dispersions showed a liquidlike behavior (the loss modulus was higher than the storage modulus) over the studied frequency range. An intermediate behavior (storage and loss moduli were close to each other together with dependency on frequency having exponent of 0.5) was observed for the systems having value of φ_{eff} around 0.74. At very large φ_{eff} values (4.96), the system displayed solidlike behavior by having its storage modulus (G') higher than its loss modulus (G'') and its moduli being independent of frequency over entire considered frequency range.

DOI: 10.1021/acssuschemeng.9b02232
ACS Sustainable Chem. Eng. 2019, 7, 13586−13626

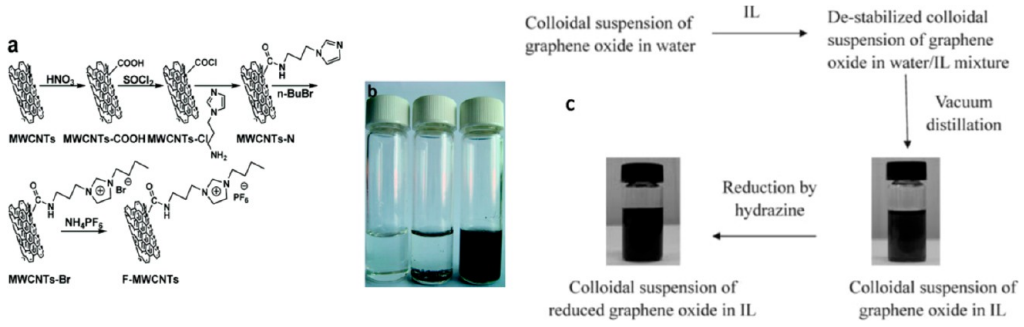

Figure 23. (a) Synthesis of F-MWCNTs and (b) photos of pure IL, IL based suspensions having pristine MWCNTs, and F-MWCNTs (from left to right) [Reprinted with permission from ref 235. Copyright 2010. American Chemical Society]. (c) Procedure used to synthesize stable reduced graphene oxide dispersions in ionic liquid [Reprinted with permission from ref 237. Copyright 2010. The Royal Society of Chemistry]

Ueno et al. reported another study on hydrophobic and hydrophilic silica based dispersions in ILs.[227] The colloidal gel of 5 wt % silica in NTf_2 based ILs showed a reversible shear thinning behavior. Instead of a colloidal gel, a stable suspension was obtained with the same nanoparticles of 15 wt % concentration in BF_4 based ILs due to the solvation forces of IL. These stable suspensions displayed a shear thickening character, shown in Figure 21a, which was linked with the destruction of the solvation structure at the surface of ions at intermediate shear rates. This resulted in the aggregation of nanoparticles. A thermosensitive colloidal glass/gel based on polymer grafted silica nanoparticles and IL was also prepared by Ueno et al.[228] The colloidal glass of polymer grafted nanoparticles (NPs) in ILs showed a transition from a glass to a gel system when the temperature was increased. This was attributed to the desolvation of PBnMA shell around the NPs surface leading to the NPs aggregation. This transition was also evident in the V-shaped moduli response as a function of temperature (Figure 21b) due to the decrease in particle volume fraction and development of interconnected networks of grafted NPs at higher temperatures.

A novel nanoparticle ionic liquid (NIL) system was developed by using long-chain ILs grafted silica NPs (Figure 22a).[230] The flow curve analysis revealed the shear thinning behavior of NILs (viscosity decreased below the shear rate of 1 s^{-1} followed by a Newtonian regime at higher shear rates). In dynamic temperature ramp tests, NILs displayed a liquid-like behavior within the temperature range of 10−55 °C, shown in Figure 22b, and a five times higher moduli than the ILs at 10 °C due to the enhanced crystallinity of PEG segments. A rapid decrease in storage modulus (more than 3 orders of magnitude) was also observed for NILs at temperatures higher than 40 °C.

Nanotube Based Dispersions. Nanotubes are an emerging field of interest, particularly carbon nanotubes (CNTs) which are tubular structures having diameters in the nanometer range together with high L/D ratios. High tensile strength and Young's modulus of CNTs are linked with their one-dimensional structure and arrangement of carbon atoms. This makes them suitable for applications where enhanced mechanical properties are desired.[231] ILs are promising alternate for classical solvents to prepare CNTs based dispersions because of the homogeneity and stability of the resultant dispersions, which gives rise to a new class of nanomaterials with improved properties and wide range of technical applications.[232]

The rheological analysis of IL systems having single-walled carbon nanotubes (SWCNTs) has been reported in the literature. Fukushima et al. reported the synthesis of gelled and oriented crystalline material by grinding and centrifuging the suspension of SWCNTs in room-temperature ILs of imidazolium ions.[233] The frequency sweep results showed the existence of a permanent and elastic network structure at smaller strains which diminished at higher level of strain (1.0) and no plateau was observed for moduli. This strong dependence of moduli on strain amplitude was attributed to the molecular ordering of ILs which resulted from the weak physical interactions between the SWCNTS.

Rheological characterization was also reported to study the influence of temperature, types and concentration of multiwalled carbon nanotubes (MWCNTs) on the viscosity of resultant dispersions in IL.[232] The incorporation of small amount of MWCNTs resulted in lower viscosity of dispersions at high shear rate as compared to pure IL whereas in the case of concentrated dispersions, the viscosity values were always (for all studied shear rates) higher than the pure IL. As far as the effect of MWCNTs types is concerned, the viscosity of dispersions is greatly affected when MWCNTs are aligned as compared to the case they are not. At room temperature, all the prepared dispersions displayed liquidlike behavior (G'' was higher than G' and no crossover was observed between them) while a sol−gel transition was evident at higher temperatures for pure ILs and concentrated systems with a more pronounced effect in the case of aligned MWCNTs.

The effect of temperature on the rheological properties of MWCNT based ionic liquid dispersions was reported by Ferreira et al.[234] The dispersions exhibited a shear thinning behavior which shifted toward lower shear rates by increasing temperature due to the reduction in size/cohesiveness of aggregates. The dispersions also showed a decrease in viscosity as compared to pure IL, i.e., by adding 0.05 v/v% of MWCNTs the viscosity decrease was 82%. Wang et al. reported the fabrication of nanofluids containing IL and functionalized multiwalled carbon nanotubes (F-MWCNTs) (Figure 23a−b).[235] The rheological analysis of these nanofluids revealed the shear thinning behavior of the considered system at low nanotube concentration. This was linked with the flexibility of the functionalized carbon nanotubes, higher specific ratio, and network formation due to nanotube−nanotube and nanotube−ionic liquid interactions. Nanofluids also displayed a lower shear viscosity as compared to pure ILs, particularly at higher shear rates, due to the self-lubrication effect of the functionalized carbon nanotubes.

The utilization of ionic liquid in composite fiber synthesis by dispersing microcrystalline cellulose (MCC) and halloysite nanotubes (HNTs) in IL was also reported.[236] The dynamic

DOI: 10.1021/acssuschemeng.9b02232
ACS Sustainable Chem. Eng. 2019, 7, 13586−13626

Table 4. Some Details of Rheological Analysis of Ionic Liquid Based Dispersions

ionic liquid	other component	concentration of dispersed medium (wt%)	rheometer	characterization temperature	shear rate or angular frequency	key rheological parameters	ref
$[C_4C_1im][BF_4]$	silica nanoparticles	0.1−0.5 vol %	DHR, TA Instruments	10−80 °C	0.1−350 s^{-1}, 0.1−100 rad/s	η_0 = 0.8−7 × 10^3 mPa·s (silica 0.4%)	222
$[C_6C_1im][Cl]/[C_4C_1im][C_8SO_4]/[C_4C_1im][Br]$	bentonite, water	2, 100 mL	DHR, TA Instruments	20 °C	20 s^{-1}, 0.01−0.5 Hz	η = 110−210 mPa·s (untreated and treated bentonite; 20 s^{-1})	238
$[C_4C_1im][NTf_2]$	Al_2O_3 nanoparticles	0.18−0.9 vol %	Brookfield viscometer (LVDV-II + pro)	20−90 °C	0−35 s^{-1}	η_0 = 40−400 mPa·s (25 °C)	215
[Amim][Cl]	MCC, Halloysite nanotubes (HNTs)	9, 0−0.80	AR-2000ex, TA Instruments	30 °C	0.01−100 s^{-1}, 0.1−100 rad/s	η_0 = 85−200 × 10^3 mPa·s	236
[EA][N]/[EtA][N]/[PA][N]/[DMEA][F]	silica particles	10	AR-G2, TA Instruments	20−50 °C	1−4000 s^{-1}	η_0 = 10−160 mPa·s (20 °C)	223
$[C_2C_1im][BF_4]/[C_4C_1im][BF_4]/[C_6C_1im][BF_4]$	TiO_2 nanopowders	0.05−1	MCR 301, Anton Paar		0.1−1000 s^{-1}	η_0 = 50−280 mPa·s (TiO_2 0.5 wt %; different ILs)	224
$[P_{6,6,6,14}][NTf_2]/[C_4C_1im][BF_4]$	hydrophilic silica nanoparticles	0−15	AR-G2, TA Instruments	25 °C	0.05−1000 s^{-1}	η_0 = 0.7−850 × 10^3 mPa·s (silica 5−15 wt %)	218
$[(C_6)_3PC_{14}][Phosph]/[(C_6)_3PC_{14}][NTf_2]$	MWCNTs	0.05−0.2 vol %	RS 1, Thermo Haake	25−60 °C	0−30 s^{-1}	η = 500−550 mPa·s (MWCNTs 0.05−0.1 vol %; 25 °C; 3.6 s^{-1})	234
[Amim][Cl]	MCC, Nano-SiO_2	5−9, 0.2−12	AR-2000ex, TA Instruments	30 °C	0.01−100 s^{-1}, 0.1−100 rad/s	η_0 = 85−300 × 10^3 mPa·s (MCC 7 wt %; SiO_2 0−12 wt %)	239
$[C_6C_1im][NTf_2]/[C_6C_1im][BF_4]$	SiO_2 nanopowder	0.1−2	MCR 301, Anton Paar	25−200 °C	0.1−1000 s^{-1}, 0.1−100 rad/s	η_0 = 8−6000 mPa·s (both ILs; 100 °C)	42
$[C_2C_1im][NTf_2]/[C_2C_1im][BF_4]$	TiO_2 nanoparticles	0.03−1	MCR 301, Anton Paar		0.1−1000 s^{-1}	η_0 = 25−285 mPa·s	217
$[C_2C_1im][EtSO_4]$	magnetite nanoparticles	5−9.5 vol %	MCR 300, Anton Paar		0−75 s^{-1}	dynamic yield stress = 0−3 Pa (0−56 kA/m magnetic field strength)	225
$[C_2C_1im][NTf_2]$	PMMA-g-NPs	0−40	MCR 301, Anton Paar	25 °C	0.0001−1000 s^{-1}, 0.1−100 rad/s	η_0 = 3 × 10^2−8 × 10^8 mPa·s (PMMA-g-NPs 10−18 wt %)	226
$[C_4C_1im][PF_6]$	F-MWCNTs	0−0.1	RS 6000, Thermo Haake	25−45 °C	0.05−1000 s^{-1}, 0.01−10 rad/s	η_0 = 238−314 mPa·s (25 °C)	235
$[C_2C_1im][DCA]/[C_2C_1im][TFSA]$	graphene	0.5−1	AR-G2, TA Instruments	25−125 °C	10^{-3}−500 s^{-1}	η_0 = 4 (0−7) × 10^5 mPa·s (graphene 0−1 wt %; 25 °C)	240
$[b((MeO)_3Sip)im][NTf_2]$	SnO_2 nanoparticles	0.5−2	Bohlin Gemini 2, Malvern Instruments	25 °C	0.1−100 Hz, 0.1−1000 s^{-1}	η_0 = 30−50 × 10^3 mPa·s	241
$[C_2C_1im][NTf_2]$	iron oxide nanoparticles	20−40	Kinexus Pro, Malvern Instruments	25 °C	0−200 s^{-1}	η_0 = 2−175 × 10^3 mPa·s (γ-Fe_2O_3 35 wt %; 0−3.5 kG magnetic field)	242
[EA][N]	graphene oxide liquid crystals	9 mg/mL	AR-1500ex, TA Instruments	25 °C	0.01−1000 s^{-1}	yield stress = 1−5 Pa (0−250 rad/s)	243
$[C_2C_1im][EtSO_4]$	a-Fe_2O_3 nanoparticles	20−40	UDS 200, Anton Paar	25−80 °C	0.1−1800 s^{-1}	η_0 = 1−10 × 10^3 mPa·s (40 °C)	244
$[C_2C_1im][DCA]$	SWCNTs, MWCNTs	1	AR-G2, TA Instruments	25−100 °C	0.01−500 s^{-1}, 0.5−500 rad/s	η_0 = 0.08−200 × 10^3 mPa·s (25 °C)	245

DOI: 10.1021/acssuschemeng.9b02232
ACS Sustainable Chem. Eng. 2019, 7, 13586−13626

rheological analysis showed that the system behaved as liquidlike in the absence of nanotubes whereas at 0.27 wt % of nanotubes, a crossover was observed between storage (G') and loss moduli (G'') (solid-like behavior) which shifted toward the smaller frequency. The outcome of the rheological study also displayed an increase in the complex viscosity with increasing nanotubes content from 0.27 to 0.63 wt %. However, a decrease in viscosity together with the disappearance of crossover was found for the nanotubes content of 0.80 wt %. This unique behavior was due to the transition of the isotropic phase to a liquid crystal phase which resulted in the reduced chain entanglements of cellulose. Steady rheological measurements also displayed similar results as a function of nanotubes content.

Zhang et al. synthesized stable dispersions of reduced graphene oxide in different ILs using higher concentrations of graphene oxide without adding any stabilizers (Figure 23c).[237] The effective dispersion of graphene oxide in ILs was confirmed by the rheological results. The output of this study also revealed that the critical gelation concentration for the considered system was in the range of 0.21−0.53 mg/mL after which the system became a gel by having storage modulus (G') higher than the loss modulus (G''). The systems having lower content of graphene oxide (0.21 mg/mL) displayed a liquidlike behavior (G'' was always higher than G'). The concentration of the dispersed medium is very critical for the rheological properties of the IL based suspensions. Table 4 summarizes the rheological analysis of IL based dispersions reported in the literature which are particularly dependent on the concentration of the dispersed medium.

In summary, the stability and flow behavior of nanoparticles based IL dispersions are strong functions of temperature, type of IL, size and amount of nanoparticles, and surface functionalization of the particles. Typically a non-Newtonian shear thinning behavior is observed for nanoparticle based IL dispersions which become pronounced at higher nanoparticles concentrations. An interesting shear thickening response is observed for the dispersions having polymer grafted nanoparticles due to the depletion of the surface layer either at higher temperatures or shear rates which results in a colloidal gel system. The stability of nanoparticle based IL dispersions is found to be best at lower temperatures, when they are composed of large nanoparticles and in the presence of long alkyl chain ILs. A unique nanoparticle ionic liquid system (NIL) has also been reported in the literature which can be an interesting alternative to conventional nanoparticle based IL dispersions. The rheological fingerprint of nanotube based IL dispersions can be tuned by varying the temperature, nature, and content of nanotubes together with the surface morphology of the nanotubes. It has in particular been shown that MWCNTs based IL dispersions have a lower viscosity at higher shear rates as compared to pure ILs due to the self-lubrication phenomenon of carbon nanotubes. The sol−gel transition and shear thinning behavior of nanotube based dispersions become more pronounced at higher nanotube contents and higher temperatures.

RHEOLOGY OF SYSTEMS HAVING AN IL AS A PLASTICIZER

The conventional method for polymer processing involves the use of large amounts of toxic solvents as plasticizers like acetone, phthalates, phosphates, triethyl citrate, and glycerol derivatives.[246,247] These solvents pose some serious problems like altering the structure of parent polymer, toxicity, or leakage issues during processing.[248] The glass transition temperature (T_g) of a (bio)polymer is an important parameter for the preparation of polymeric blends, composites and dispersions by melt-mixing procedure. However, attainment of this glass transition temperature for polymeric materials is critical due to the problem of thermal degradation at higher temperature.[249]

The structure of ILs is similar to the conventional plasticizers as they have an aromatic core and pendant alkyl groups. ILs may therefore be used as plasticizers due to their excellent advantages like high thermal stability and their adjustable polarity and acidity. They are environmental friendly and have small evaporation losses[31] and good compatibility with polymers; they broaden the processing window (i.e., by lowering T_g) and enhance the elasticity range.[250] Recently, ionic liquids (ILs) have been shown to be indeed effective plasticizers by the use of various thermomechanical processing techniques such as melt-mixing, shear processing, extrusion, etc. Study of the rheological properties of IL based polymeric melts, blends, and composites can help to analyze the plasticization efficiency and the final properties of the composite system.

Li et al. reported the use of IL ($[C_4C_1im][BF_4]$) as a plasticizer for the melt processing of cellulose diacetate (CDA) as a function of different IL concentrations and melt spinning temperatures.[251] The rheological results showed that increasing IL content (from 15 to 35 wt %) had a decreasing effect on the zero shear viscosity (from 1.69×10^6 to 5.46×10^4 Pa·s) but an increasing effect on the power law index (from 0.20 to 0.43). The temperature effect on the viscosity demonstrated a decreasing trend in viscosity as function of temperature which suggested that the optimum temperature for melt spinning of CDA was about 190 °C.

The melt rheology of cellulose acetate was reported in the presence of $[C_4C_1im][Cl]$ as a plasticizer.[252] The melt spinning temperature was found to be 150 °C for the considered polymeric material. The results revealed that the incorporation of IL resulted in weaker interactions between the molecular chains of cellulose acetate. The effect of temperature and concentration of ionic liquid on the rheological behaviors of polyacrylonitrile (PAN) melt was also reported.[253] The rheological results showed the increase in modulus and zero-shear viscosity with decreasing temperature while an opposite trend was found as function of ionic liquid content. Moreover, the crossover between G' and G'' shifted toward the higher frequencies as function of increasing temperature/decreasing ionic liquid content. The optimum melt spinning temperature for this polymer was observed to be 180 °C.

The partial replacement (15−30 wt %) of conventional plasticizers with ionic liquids [(trihexyl(tetradecyl) phosphonium dicyanamide and trihexyl(tetradecyl) phosphonium bis(trifluoromethylsulfonyl)imide)] has been reported for the processing of emulsion grade PVC.[254] The findings of this study showed a decrease in the viscosity of the system by adding ILs and a change in rheological behavior from shear thinning (pseudoplastic) to almost Newtonian. The melt mixing of PVDF-co-HFP and polyaniline doped with dodecylbenzene sulfonic acid (PAni.DBSA) in the presence of ionic liquid (tributyl(tetradecyl) phosphonium dodecylbenzenesulfonate) has been reported.[255] The observations revealed a decrease in viscosity and an improved aid in processing by the addition of IL, which further enhanced the dispersion of one polymer into the other polymer matrix, resulting in better electrical properties. Likewise, the rheological analysis of IL based poly(butylene succinate) (PBS)/starch blends displayed an increase in complex viscosity (≈2700 to 4700 Pa·s) and a shear thinning

DOI: 10.1021/acssuschemeng.9b02232
ACS Sustainable Chem. Eng. 2019, 7, 13586−13626

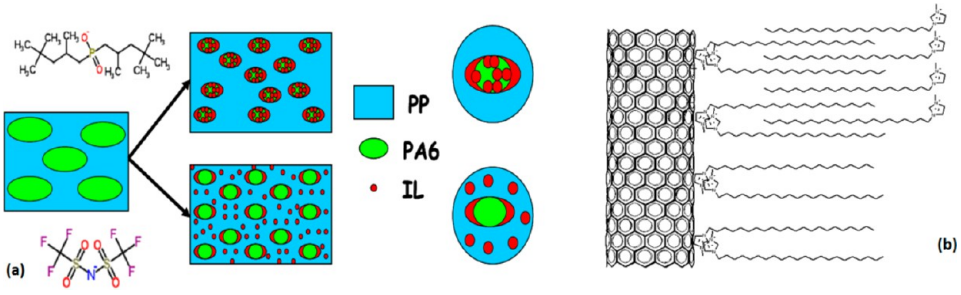

Figure 24. (a) Schematic representation of effect of IL on the structural distribution of polymer phases within the blend [Reprinted with permission from ref 257. Copyright 2014. Elsevier]. (b) Schematic representation of the $\pi-\pi$ interactions between IL modified CNF and the cation of the ionic liquid [Reprinted with permission from ref 259. Copyright 2014. Elsevier].

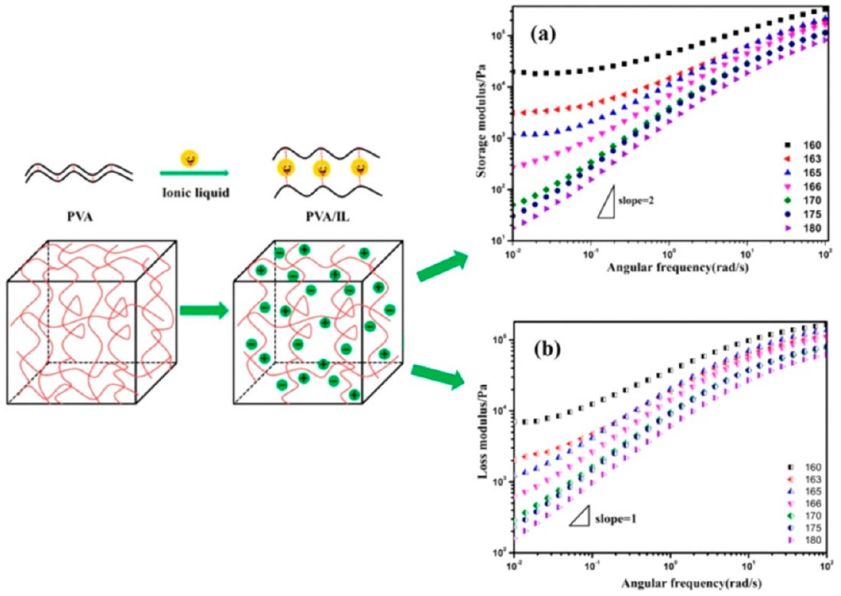

Figure 25. Schematic illustration of the hydrogen bonding between PVA and IL. (a) Storage and (b) loss moduli of 35% PVA/IL as a function of angular frequency at various temperatures [Adapted with permission from ref 38. Copyright 2018. American Chemical Society].

behavior with the increase in IL ($[C_4C_1im][Cl]$) content (20–40 wt %). This resulted in the effective dispersion of starch within the PBS matrix.[256] The results showed the elastic nature of IL based blends, which was linked with the higher viscosity of the melt and also with the formation of aggregated networks of filler (starch). The rheological data also showed that the properties of IL based blends have higher storage modulus than loss modulus.

The effect of two different ILs, $[P_{6,6,6,14}][NTf_2]$ and $[P_{6,6,6,14}][TMP]$ on the rheological properties of polypropylene (PP)/polyamide 6 (PA6) blends has been reported.[257] Both ionic liquids based polymeric blends displayed higher complex viscosity at smaller frequencies as compared to the blends without IL. At higher frequencies, IL-NTf_2 based polymeric blends displayed lower complex viscosities which indicated that there was a small effect on the short-range motions of polymeric chains. The ILs based blends also displayed a more elastic character than the unfilled polymeric blends due to the compatibilization effect. Furthermore, IL-NTf_2 based blends having 10 wt % of IL exhibited larger cross-links relaxation time (10 s) than IL-TMP based blends (1.5 s). This effect was linked with the formation of stronger surfactant cross-links at this particular concentration of ionic liquid. The schematic representation of effect of ILs on the structural distribution of polymer phases within the blend is shown in Figure 24a.

Silva et al. reported the dispersions of MWCNTs within a polystyrene (PS) matrix in the presence of trihexyl(tetradecyl)-phosphonium bistriflamide (IL) prepared by melt processing.[258] The cross over between G' and G'' at lower frequencies indicated the formation of a 3-D network of these IL based dispersions. In the same way, Ma et al. also reported the preparation of nanocomposite film by blending IL modified carbon nanofibers (CNFs) and ultrahigh molecular weight polyethylene (UHMWPE).[259] There was an increase in the complex viscosity of these molten composites and of their storage modulus with the ionic liquid concentration at lower frequency range (less than 0.05 s^{-1}). An opposite behavior was observed for higher frequencies. Figure 24b shows the interaction between IL modified CNF and the cation of the ionic liquid through $\pi-\pi$ interactions.

An application of IL in the emerging field of wood–plastic composites was reported by Ou et al. The effect of IL incorporation on the rheological behavior of wood flour/high density polyethylene (WF/HDPE) blends was investigated.[260] An increase in storage modulus, loss modulus, complex viscosity, and shear viscosity as a function of increasing [Hemim][Cl] content was observed. The addition of IL also broadened the processing window of blends by maintaining a high melt viscosity at low shear rates while an opposite behavior was found

DOI: 10.1021/acssuschemeng.9b02232
ACS Sustainable Chem. Eng. 2019, 7, 13586–13626

Table 5. Details of the Rheological Characterization of Ionic Liquid Based Composite Systems Prepared by Melt Processing

ionic liquid	polymer	concentration of dispersed phase/ionic liquid (wt %)	rheometer	characterization temperature	shear rate or angular frequency	key rheological parameters	ref
$[P_{6,6,6,14}][NTf_2]$	PS, MWCNTs	0−5, 0−1	MCR 302, Anton Paar	200 °C	0.1−100 Hz	$G' = 1-2 \times 10^4$ Pa (1 Hz)	258
$[C_4C_1im][BF_4]$	cellulose diacetate	15−35	AR-G1, TA Instruments	170−200 °C	0.01−100 s^{-1}	$\eta_0 = 5.64 \times 10^7-1.69 \times 10^9$ mPa·s (190 °C)	251
$[P_{4,4,4,14}][DBS]$	PVDF-co-HFP, PAni.DBSA	0−5	MRC 302, Anton Paar	200 °C	0.1−100 Hz	$\eta^* = 8 \times 10^6-2.5 \times 10^8$ mPa·s (1 Hz)	255
$[C_4C_1im][Cl]$	PBS, starch	3.4−5.8	MCR 301, Anton Paar	140 °C	0.01−100 Hz	$G' = 700-8000$ Pa (1 Hz)	256
$[C_4C_1im][Cl]$	cellulose acetate	20−40	ARES, TA Instruments	170 °C		plateau modulus = 40100−250000 Pa	252
$[P_{6,6,6,14}][DCA]/[P_{14,6,6,6}][NTf_2]$	PVC, DINP, CITROFOL AHII	0−30	RS 1, Thermo Haake	23 °C	0.5−30 s^{-1}	$\eta = 0.6-1.9 \times 10^3$ mPa·s (15 s^{-1})	254
[Hemim][Cl]	wood flour, HDPE	0−5	CTW5, 600p, Thermo Scientific/Acer 2000, Rheometric Scientific/HR-2, TA Instruments	175 °C	20−2000 s^{-1}, 0.1−500 rad/s	$G' = 2 \times 10^5-1 \times 10^6$ Pa (1 Hz)	260
$[P_{14,6,6,6}][NTf_2]/[3C_6C_{14}P][(C_8H_{17})_2PO_2]$	PP, PA6	0−10	ARES, TA Instruments	240 °C	0.1−100 rad/s	$G' = 500-4000$ Pa (1 Hz)	257
$[C_4C_1im][PF_6]$	PVDF, CNTs	1−5	DHR-1, TA Instruments	190 °C	0.01−100 Hz	$G' = 1-2 \times 10^4$ Pa (1 Hz)	261
[Hemim][Cl]	PVA	30	capillary rheometer Rosand RH7D, Malvern Instruments	170−200 °C	0.01−100 s^{-1}	$\eta_0 = 6.6. \times 10^6-2.5 \times 10^7$ mPa·s	262
$[P_{6,6,6,14}][NTf_2]$	PS, EVA, MWCNTs	70, 30, 0.25−1	DHR-1, TA Instruments	200 °C	0.1−100 Hz	$G' = 4 \times 10^4$ Pa (1 Hz; IL-CNT 1 wt %)	263

DOI: 10.1021/acssuschemeng.9b02232
ACS Sustainable Chem. Eng. 2019, 7, 13586−13626

for higher shear rates. This enabled definition of this particular IL as a stable and effective plasticizer.

Chen et al. reported the use of IL as a novel plasticizer for poly(vinyl alcohol) (PVA) to improve its thermal processing.[38] The outcome of the rheological study demonstrated the existence of hydrogen bonds between the hydroxyl and chloride groups of the ILs and the hydroxyl groups of PVA. The storage and loss moduli of the PVA/IL system displayed a decrease with the increase in temperature, with a clear and visible rubbery plateau at lower frequencies below 166 °C (Figure 25). The variation in the rubbery plateau of PVA/IL system within the temperature range of 160−170 °C was linked with the dynamic changes in the hydrogen bonding between IL and PVA. Table 5 summarizes the details of the rheological characterization of IL based composite systems prepared by melt processing.

In summary, the plasticization efficiency of IL in polymeric melts is strongly dependent on the concentration of ILs. The processing temperature, elasticity, and viscosity of the polymeric melts are reduced by increasing the content of IL in the polymer melts. This reduction in viscosity and shear thinning phenomenon due to the incorporation of ILs facilitate the dispersion of one polymer into another. Thus, a polymeric blend or a composite is produced which possesses better mechanical and rheological properties. The shear viscosity, elastic modulus, and complex viscosity of polymeric blends can be increased by increasing the amount of ILs. The main reason for these enhanced properties is due to the fact that the presence of ILs in blends leads to a homogeneous dispersion of the polymers within the blend. The dynamic rheological properties of polymeric melts with ILs also become affected due to the interaction between IL and polymeric chains.

CONCLUSION AND FUTURE PERSPECTIVE

This review presents the literature regarding the rheology of pure ionic liquids and of different systems based on ILs like solutions, gels, dispersions, composites, and melts. Ionic liquids (ILs) possess an interesting set of properties that includes good chemical and thermal stability, low vapor pressures, good solvation interaction with a wide range of organic, inorganic, and polymeric compounds, excellent ionic conductivity, and tunable viscosity. They offer a broad processing window for polymers by lowering down their glass transition temperature (T_g) and also enhance their elasticity range. ILs are easily recyclable, promote an enhanced colloidal stability, and help to prevent aggregate formation. They are inert toward water and air and have structural similarity with conventional solvents. In particular, they are environmentally friendly which makes them good alternatives for more toxic conventional solvents (i.e., NMMO, DMAc, DMSO, etc.) for industrial applications.

The rheological analysis of ILs and their different systems provides critical information about several parameters like viscosity, viscoelasticity (viscous and elastic behavior), solid−liquid transition, colloidal stability, plasticization efficiency, and also the effect of IL structure and concentration on the above-mentioned parameters. As far as structural changes are concerned, rheology enables the study of the thermodynamics and dynamics of polymer chains in ILs. The hydrodynamic volume of the dispersed polymers can be evaluated, and the polymer−IL or IL−IL interactions and the chain motilities can be probed by varying either concentration or temperature. More practically for industry, rheology also helps to optimize processing techniques, plasticization efficiency, and tune the composition of composite systems to achieve the desired rheological optimum (elasticity or viscosity).

The unusual deviation of ILs/cellulose solutions from the Cox−Merz rule needs to be further investigated. There are limited studies on ILs based emulsions, which nonetheless are interesting systems as they are thought to be relevant for drug delivery applications. Nanoparticle IL systems (NILs) are found to be dispersions with improved properties above ILs. Future research should be directed toward this novel system particularly to optimize their rheological properties. Apart from experimental studies, few molecular simulation studies have also been reported in literature for ILs. However, further research should be performed in this area of research in order to understand the interactions between ILs and external components and also to predict the rheological properties for particular processing conditions.

AUTHOR INFORMATION

Corresponding Author

*Mailing address: Department of Hydraulic Engineering, Faculty of Civil Engineering and Geosciences, Delft University of Technology, Stevinweg 1, 2628 CN Delft, The Netherlands. Email: a.shakeel@tudelft.nl. Tel.: +31(0)613091407.

ORCID

Ahmad Shakeel: 0000-0002-0627-7540

Zahoor Ullah: 0000-0001-5355-1314

Notes

The authors declare no competing financial interest.

Biographies

Ahmad Shakeel received his Bachelor's degree in Chemical (Polymer) Engineering from the University of Engineering & Technology Lahore, Pakistan, in 2013. He obtained his Master's degree in Erasmus Mundus Engineering Rheology from KU Leuven Belgium, University of Minho Portugal, and the University of Calabria Italy in 2015. From 2015 to 2018, he served as a lecturer in the Department of Chemical, Polymer & Composite Materials Engineering, University of Engineering & Technology Lahore. During this period, he worked on the synthesis and rheological characterization of bigels (mixture of organogel and hydrogel). He also worked on the nanoindentation analysis of polymeric surfaces with and without surface treatment. He is now a Ph.D. candidate at the Faculty of Civil Engineering & Geosciences, Delft University of Technology, The Netherlands. His research topic focuses on the rheological analysis of natural and artificial suspensions under the supervision of Professor Julie Pietrzak and Dr. Claire Chassagne.

DOI: 10.1021/acssuschemeng.9b02232
ACS Sustainable Chem. Eng. 2019, 7, 13586−13626

Hamayoun Mahmood received his B.Sc. (2007) and M.Sc. (2011) in Chemical Engineering from the University of Engineering & Technology (UET), Lahore, Pakistan. He served as a faculty member in the Department of Chemical Engineering, University of Gujrat, Pakistan, and King Khalid University, Saudi Arabia. He then moved to Malaysia where he got his Ph.D. (2017) under supervision of Dr. Muhammad Moniruzzaman from Universiti Teknologi PETRONAS. Currently, H. Mahmood is serving as an assistant professor in the Department of Chemical, Polymer & Composite Materials Engineering, UET, Lahore, Pakistan. During his PhD work, he explored the use of ionic liquids for pretreatment of lignocellulosic biomass to fabricate green composite materials. He is currently interested in the optimization, comparison, and environmental impact assessment for use of ionic liquids in the biorefinery applications.

Ujala Farooq received her Bachelor's degree in Polymer Engineering from University of Engineering & Technology Lahore, Pakistan, in 2015. She obtained her Master's degree in Erasmus Mundus Membrane Engineering from Université Montpellier, Université Paul Sabatier, Institute of Chemical Technology Prague, and University of Zaragoza in 2017. From 2017 to 2019, she served as a lecturer in the Department of Chemical, Polymer & Composite Materials Engineering, University of Engineering & Technology Lahore. During this period, she worked on the synthesis and rheological characterization of bigels (mixture of organogel and hydrogel). She is now a Ph.D. candidate at the Faculty of Aerospace Engineering, Delft University of Technology, The Netherlands. Her research topic focuses on the polymeric composites under the supervision of Professor Clemens Dransfeld and Dr. Julie Teuwen.

Dr. Zahoor Ullah received his Ph.D. degree in 2016 in Chemical Engineering from the Universiti Teknologi Petronas Malaysia. Since June 2017, he is working as an Assistant Professor in Chemistry Department, Balochistan University of Information Technology, Engineering and Management Sciences (BUITEMS). His research interests are biofuel, biomass, and natural products using ionic liquids.

Dr. Saima is serving as an Associate Professor at the Chemical, Polymer & Composite Materials Engineering Department, University of Engineering & Technology, KSK Campus, Lahore. She worked extensively on adsorption of polymers/dispersants used for making stable dispersions of graphitic carbon black. She possesses vast experience of rheological measurements using cylindrical rheometers. The rheological measurements performed during this study involve both steady state (viscosity) tests and viscoelastic tests (storage and loss modulus).

Dr. Iqbal is serving as an Associate Professor at the Chemical, Polymer & Composite Materials Engineering Department, University of Engineering & Technology, KSK Campus, Lahore. His principal area of research is the surface mechanical characterization and tribological

DOI: 10.1021/acssuschemeng.9b02232
ACS Sustainable Chem. Eng. 2019, 7, 13586−13626

studies of polymers and their composites at the micro- as well as the nanoscales. In particular, he has worked on the surface mechanical properties based on the indentation and the scratching response of amorphous and semicrystalline polymeric surfaces and their composites. Surface deformation mechanisms and hardness determine product life and usage and hence play a vital role in material selection and design.

Dr. Claire Chassagne is an assistant professor at the Delft University of Technology (The Netherlands). With a background in physics and mathematics, she specialized in colloid science. Her current work focuses on the characterization of colloidal suspensions using electrokinetic techniques (electrophoresis, impedance spectroscopy, electroacoustics). The surface properties of the colloidal particles thus assessed are then related to the suspensions' bulk properties by complementary techniques such as light scattering, rheology, or consolidation tests. The experiments enable her to derive new models or improve existing ones. These models aim to couple physical and chemical processes at different scales.

Muhammad Moniruzzaman received his B.Sc. in Chemical Engineering from the Bangladesh University of Engineering and Technology (BUET), Bangladesh. He then moved to Japan where he got his M.Sc. (2004) and Ph.D. (2007) in biochemical engineering from Kanazawa University. In 2007, he moved to Kyushu University as a JSPS (Japan Society for the Promotion of Science) Postdoctoral fellow. Currently, M. Moniruzzaman serves as an Associate Professor in the Department of Chemical Engineering at the Universiti Teknologi PETRONAS, Malaysia. His current research interests focus on the application of ionic liquids as alternative "green" solvents for the design of bioconversion processes and novel drug delivery systems.

■ ABBREVIATIONS

$[C_2C_1im][C_6SO_4]$: 1-ethyl-3-methylimidazolium hexylsulfate

$[P_{6,6,6,14}][(C_2F_5)_3PF_3]$: trihexyl(tetradecyl)phosphonium tris(pentafluoroethyl)trifluorophosphate

$[P(bu)_3(CH_2)_2(CF_2)_xF][I]$: tributyl(1*H*,1*H*,2*H*,2*H*-perfluoroalkyl)phosphonium iodide

$[P(bu)_3(CH_2)_2(CF_2)_xF][DCA]$: tributyl(1*H*,1*H*,2*H*,2*H*-perfluoroalkyl)phosphonium dicyanamide

$[P(bu)_3(CH_2)_yH][Br]$: tributyl-alkyl-phosphonium bromide

$[P(bu)_3(CH_2)_yH][DCA]$: tributyl-alkyl-phosphonium dicyanamide

$[C_2C_1pyr][C_4F_9SO_3]$: 1-ethyl-1-methypyrrolidinium perfluorobutanesulfonate

$[C_4C_1pyr][N(C_4F_9SO_2)_2]$: 1-butyl-1-methypyrrolidinium bis(nonafluorobutanesulfonyl)imide

$[C_4C_1pyr][C_4F_9SO_3]$: 1-butyl-1-methypyrrolidinium perfluorobutanesulfonate

$[C_6C_1im][C_4F_9SO_3]$: 1-hexyl-3-methylimidazolium perfluorobutanesulfonate

$[C_8C_1im][C_4F_9SO_3]$: 1-octyl-3-methylimidazolium perfluorobutanesulfonate

[N8886][BScB]: trioctylhexylammonium bis(salicylato)-borate

[N8888][BScB]: tetraoctylammonium bis(salicylato)borate

[N88810][BScB]: trioctyldecylammonium bis(salicylato)-borate

[N88812][BScB]: trioctyldodecylammonium bis-(salicylato)borate

[2-HEA][Ac]: 2-(hydroxy)ethylammonium acetate

[2-HDEA][Ac]: 2-hydroxydiethanolamine acetate

$[2\text{-HEA}][F]$ or $[2\text{-HEA}][HCO_2]$: 2-(hydroxy)-ethylammonium formate

[2-HEA][Pr]: 2-hydroxyethylammonium propionate

[2-HEA][L]: 2-hydroxy ethylammonium lactate

[2-HDEA][L]: 2-hydroxy diethylammonium lactate

$[BtTzm][CF_3SO_3]$: 1-butyl-4-(4-sulfobutyl)-1*H*-1,2,4-triazol-4-ium trifluoro-methanesulfonate

$[IpTzm][CF_3SO_3]$: 1-isopentyl-4-(4-sulfobutyl)-1*H*-1,2,4-triazol-4-ium trifluoromethanesulfonate

$[HxTzm][CF_3SO_3]$: 1-hexyl-4-(4-sulfobutyl)-1*H*-1,2,4-triazol-4-ium trifluoromethanesulfonate

$[EMcBim][BF_4]$: 1-butyl-3-[2-[(2-methyl-1-oxo-2-propen-1-yl)oxy]ethyl]-imidazolium tetrafluoroborate

$[PMcBim][BF_4]$: 1-butyl-3-[3-[(2-methyl-1-oxo-2-propen-1-yl)oxy]propyl]-imidazolium tetrafluoroborate

$[HMcBim][BF_4]$: 1-butyl-3-[6-[(2-methyl-1-oxo-2-propen-1-yl)oxy]hexyl]-imidazolium tetrafluoroborate

$[C_4C_1Pyr][(C_2F_5)_3PF_3]$: 1-butyl-1-methypyrrolidinium tris-(pentafluoroethyl)trifluorophosphate

$[C_4C_1Pyr][CF_3SO_3]$: 1-butyl-1-methypyrrolidinium trifluoromethanesulfonate

$[C_4C_1im][PF_6]$: 1-butyl-3-methylimidazolium hexafluorophosphate

$[C_4C_1im][NO_3]$: 1-butyl-3-methylimidazolium *nitrate*

$[(But)_3P(Dec)](Cl)$: Tributylphosphoniumdecane chloride

$[(Hex)_3P(Dec)](Cl)$: trihexylphosphoniumdecane chloride

$[(Oct)_3P(Dec)](Cl)$: trioctylphosphoniumdecane chloride

$[(But)_3P(Dec)P(But)_3](Cl)_2$: di(tributylphosphonium)-decane dichloride

$[(Hex)_3P(Dec)P(Hex)_3](Cl)_2$: di(trihexylphosphonium)-decane dichloride

$[(Oct)_3P(Dec)P(Oct)_3](Cl)_2$: di(trioctylphosphonium)-decane dichloride

$[(Hex)_3P(Dec)P(Hex)_3](PF_6)_2$: di(trihexylphosphonium)-decane dihexafluorophosphate

DOI: 10.1021/acssuschemeng.9b02232
ACS Sustainable Chem. Eng. 2019, 7, 13586−13626

[$(Hex)_3P(Dec)P(Hex)_3](SbF_6)_2$: di(trihexylphosphonium)-decane dihexafluoroantimonate
[$(Hex)_3P(Dec)P(Hex)_3](POA)_2$: di(trihexylphosphonium)decane diperfluorooctanoate
[$(Hex)_3P(Dec)P(Hex)_3](NTf_2)_2$: di(trihexylphosphonium)decane di[bis(trifluoromethylsulfonyl)imide
[$(But)_3P(Dec)P(But)_3](OA)_2$: di(trihexylphosphonium)-decane dioctanoate
[$(But)_3P(Dec)P(But)_3](POA)_2$: di(trihexylphosphonium)-decane diperfluorooctanoate
[$(But)_3P(Dec)P(But)_3](DS)_2$: di(trihexylphosphonium)-decane didodecyl sulfate
[$(But)_3P(Dec)P(But)_3](DOSS)_2$: di(trihexylphosphonium)decane bis(dioctyl sulfosuccinate)
[$C_nC_1im][PF_6$]: 1-alkyl-3-methylimidazolium hexafluorophosphate
[$C_2C_1im][BF_4$]: 1-ethyl-3-methylimidazolium tetrafluoroborate
[C_2C_1im][Cl]: 1-ethyl-3-methyl-imidazolium chloride
[C_2C_1im][DCA]: 1-ethyl-3-methylimidazolium dicyanamide
[C_2C_1im][Ts]: 1-ethyl-3-methylmidazolium *p*-toluenesulfonate
[$C_2C_1im][NTf_2$]: 1-ethyl-3-methylimidazolium bis-(trifluoromethylsulfonyl)imide
[C_2C_1im][TFES]: 1-ethyl-3-methylmidazolium 1,1,2,2-tetrafluoroethanesulfonate
[C_2C_1im][Br]: 1-ethyl-3-methyl-imidazolium bromide
[C_4C_1im][Br]: 1-butyl-3-methyl-imidazolium bromide
[$C_6C_1im][(PFBu)SO_3$]: 1-hexyl-3-methylimidazolium perfluorobutanesulfonate
[$NB_4][(PFBu)SO_3$]: tetrabutylammonium perfluorobutanesulfonate
[EA][NO_3] or [EA][N]: ethylammonium nitrate or ethylamine nitrate
[PA][N]: propylammonium nitrate
[EtA][NO_3] or [EtA][N]: ethanolammonium nitrate
[dEA][N]: deuterated ethylammonium nitrate
[EA][HCO_2] or [EA][F]: ethylammonium formate
[DMEA][HCO_2] or [DMEA][F]: dimethylethylammonium formate
[$N_{n,2,2,2}][NTf_2$]: *N*-alkyl-triethylammonium bis-(trifluoromethylsulfonyl)imide
[$C_4C_1im][BF_4$]: 1-butyl-3-methylimidazolium tetrafluoroborate
[C_4C_1im][4Ni-Im]: 1-butyl-3-methylimidazolium 4-nitroimidazolate
[C_4C_1im][5AT]: 1-butyl-3-methylimidazolium 5-ami-notetrazolate
[TMP][Tos]: Triisobutylmethylphosphonium tosylate
[$C_2C_1im][EtSO_4$]: 1-ethyl-3-methylimidazolium ethylsulfate
[C_2C_1im][[Ac]: 1-ethyl-3-methylimidazolium acetate
[C_4C_1im][Cl]: 1-butyl-3-methylimidazolium chloride
[C_6C_1im][Cl]: 1-hexyl-3-methylimidazolium chloride
[$C_2C_1im][NTf_2$]: 1-ethyl-3-methylimidazolium bis(trifluoromethylsulfonyl)imide
[$C_4C_1im][NTf_2$]: 1-butyl-3-methylimidazolium bis-(trifluoromethylsulfonyl)imide
[C_8Py][I]: 1-octylpyridinium iodide
[$C_8Py][NTf_2$]: 1-octylpyridinium bis-(trifluoromethanesulfonyl)imide
[$C_2C_1imSH][(EtO)_2PO$] and [$C_6C_1imSPrN][NTf_2$]: 3-ethyl-1-methylmethimidazolium diethylphosphate
[$C_6C_1imSBu][PF_6$]: *S*-butyl-3-methylmethimidazolium hexafluorophosphate
[$C_6C_1imSBu][(BuO)_2PO_2$]: *S*-butyl-3-methylmethimidazolium dibutylphosphate
[btzSEt][$(EtO)_2PO_2$]: 1-butyl-2-ethyl thiotetrazolium diethylphosphate
[$(HOEt)_2NH$][Ac]: diethanolamine acetate
[$(HOEt)_2NH][CH_3SO_3$]: diethanolamine methanesulfonate
[$(HOEt)_2NH][HCO_2$]: diethanolammonium formate
[EDA][HCO_2]: ethylenediamine formate
[Pyr][Ac]: pyrrolidinium acetate
[$HOC_2C_1im][(BuO)_2PO_2$]: 1-hydroxyethyl-3-methylimidazolium dibutylphosphate
[$HOOCC_2C_1im][(BuO)_2PO_2$]: 1-(2-carboxyethyl)-3-methylimidazolium dibutylphosphate
[$PhCH_2C_2C_1im][(BuO)_2PO_2$]: 1-benzyl-3-methylimidazolium dibutylphosphate
[$CPC_1im][(BuO)_2PO_2$]: 1-(3-cyanopropyl)-3-methylimidazolium dibutylphosphate
[$C_4C_1im][(BuO)_2PO_2$]: 1-butyl-3-methylimidazolium dibutylphosphate
[$P(oct)_3(CH_2)_2(CF_2)_xF][I$]: perfluoroalkyltrioctylphosphonium iodide
[$P(oct)_3(CH_2)_2(CF_2)_xF][NTf_2$]: perfluoroalkyltrioctylphosphonium bis(trifluoromethanesulfonyl)imide
[$P(Oct)_3(CH_2)_2(CF_2)_xF][N(CN)_2$]: perfluoroalkyltrioctylphosphonium dicyanamide
[$P(Oct)_3(CH_2)_2(CF_2)_xF][C(CN)_3$]: perfluoroalkyltrioctylphosphonium tricyanomethanide
[$P(Oct)_3(CH_2)_yH][NTf_2$]: alkylated trioctylphosphonium bis(trifluoromethanesulfonyl)imide
[$P(Oct)_3(CH_2)_yH][N(CN)_2$]: alkylated trioctylphosphonium dicyanamide
[$P(Oct)_3(CH_2)_yH][C(CN)_3$]: alkylated trioctylphosphonium tricyanomethanide
[DDA][NTf_2]: didecyldimethylammonium bis-(trifluoromethylsulfonyl)imide
[2-Mbua][NTf_2]: 2-methylbutylammonium bis-(trifluoromethanesulfonyl)amide
[N-E*i*pra][NTf_2]: *N*-ethylisopropylammonium bis-(trifluoromethanesulfonyl)amide
[Dema][NTf_2]: diethylmethylammonium bis-(trifluoromethanesulfonyl)amide
[$P_{6,6,6,14}$][BMB]: trihexyl(tetradecyl)phosphonium bis-(mandelato)borate
[$P_{6,6,6,14}$][Cl]: trihexyl(tetradecyl)phosphonium chloride
[$P_{6,6,6,14}][NTf_2$]: trihexyl(tetradecyl)phosphonium bis-(trifluoromethylsulfonyl) imide
[DEEA][CF_3SO_3]: 1,1-diethylethanolamine trifluoromethanesulfonate
[DEEA][CF_3CO_2]: 1,1-diethylethanolamine trifluoroacetate
[PtTzm][CF_3SO_3]: 1-pentyl-4-(4-sulfobutyl)-1*H*-1,2,4-triazol-4-ium trifluoromethanesulfonate
[PtTzm][CF_3CO_2]: 1-pentyl-4-(4-sulfobutyl)-1*H*-1,2,4-triazol-4-ium trifluoroacetate
[Amim][Cl]: 1-allyl-3-methylimidazolium chloride
[Hemim][Cl]: 1-(2-hydroxyethyl)-3-methylimidazolium chloride
[$P_{6,6,6,14}$][TMP]: trihexyltetradecylphosphonium bis-2,4,4-(trimethylpentyl) phosphinate
[N_{2226}][Ac]: triethylhexylammonium acetate
[N_{33312}][Ac]: tripropyldodecylammonium acetate

DOI: 10.1021/acssuschemeng.9b02232
ACS Sustainable Chem. Eng. 2019, 7, 13586−13626

[DIPEA][C_7COO]: diisopropyl-ethylammonium octanoate
[DIPEA][C_6COO]: diisopropyl-ethylammonium heptanoate
[N_{4444}][$C_4F_9SO_3$]: tetrabutylammonium perfluorobutanesulfonate
[DBNH][Ac]: 1,5-diazabicyclo[4.3.0]non-5-ene-1-ium acetate
[C_2C_1im][DEP]: 1-ethyl-3-methylimidazolium diethyl phosphate
[C_2C_1im][P(OCH_3)(H)O_2]: 1-ethyl-3-methylimidazolium methylphosphonate
[DBNH][CO_2Et]: 1,5-diazabicyclo[4.3.0]non-5-enium propionate
[C_2C_1im][CO_2Et]: 1-ethyl-3-methylimidazolium propionate
[Ch][F]: choline formate
[Ch][Ac]: choline acetate
[$P_{6,6,6,14}$][DCA]: trihexyl(tetradecyl)phosphonium dicyanamide
[C_2C_1im][TFSA]: 1-ethyl-3-methylimidazolium bis(trifluoromethylsulfonyl)amide
[C_6C_1im][BF_4]: 1-hexyl-3-methylimidazolium tetrafluoroborate
[C_6C_1im][NTf_2]: 1-hexyl-3-methylimidazolium bis(trifluoromethylsulfonyl) amide
[C_2C_1im][FSA]: 1-ethyl-3-methylimidazolium bis(fluoromethylsulfonyl) amide
[C_2C_1im][CF_3SO_3]: 1-ethyl-3-methylimidazolium trifluoromethanesulfonate
[C_4C_1im][SCN]: 1-butyl-3-methyl-imidazolium thiocyanate
[C_4C_1pyr][NTf_2]: 1-butyl-1-methylpyrrolidinium bis(trifluoromethylsulfonyl)imide
[C_8C_1im][Cl]: 1-octyl-3-methyl-imidazolium chloride
[C_4C_1im][SbF_6]: 1-butyl-3-methylimidazolium hexafluoroantimonate
[C_4Et_3N][NTf_2]: butyl-triethylammonium bis(trifluoromethylsulfonyl) amide
[Bzmim][NTf_2]: 1-benzyl-3-methylimidazolium bis(fluoromethylsulfonyl) amide
[N_{2224}][NTf_2]: triethylbutylammonium bis(fluoromethylsulfonyl) amide
[N_{1444}][NTf_2]: tributylmethylammonium bis(fluoromethylsulfonyl) amide
[C_1C_4pip][NTf_2]: 1-methyl-1-butylpiperidinium bis(fluoromethylsulfonyl) amide
[C_4C_1im][MP]: 1-butyl-3-methyl-imidazolium methylphosphonate
[C_4C_1im][C_8SO_4]: 1-butyl-3-methyl-imidazolium octylsulfate
[(C_6)$_3$PC_{14}][Phosph]: trihexyltetradecylphosphonium phosphinate
[(C_6)$_3$PC_{14}][NTf_2]: trihexyltetradecylphosphonium bis(trifluoromethylsulfonyl) amide
[b((MeO)$_3$Sip)im][NTf_2]: butyl-3-(3-trimethoxysilylpropyl)-imidazolium bis(trifluoromethanesulfonyl) amide
[$P_{4,4,4,14}$][DBS]: tributyl-tetradecylphosphonium dodecylbenzenesulfonate
[$P_{14,6,6,6}$][NTf_2]: tris(P-hexyl) tetradecylphosphonium trifluorotris(pentafluoroethyl)phosphate
[3C_6C_{14}P][(C_8H_{17})$_2PO_2$]: trihexyltetradecylphosphonium bis(2,4,4-trimethylpentyl) phosphinate
[C_4Mpyr][$C_{12}H_{25}SO_4$]: *N*-butyl-*N*-methylpyrrolidinium dodecyl sulfate
NMMO: *N*-methylmorpholine-*N*-oxide
DMAc: *N*,*N*-dimethylacetamide
DMSO: dimethyl sulfoxide
DMF: dimethylformamide
Zn($OOCCH_2C_6F_{13}$)$_2$: zinc 2,2-dihydroperfluoroctanoate
C_{14}DMAO: tetradecyldimethylamine oxide
PEO_x-PPO_y-PEO_x: pluronic block copolymer
poly(AN-co-IA): poly(acrylonitrile-co-itaconic acid)
PAEMIBr: poly-(1-[2-acryloylethyl]-3-methylimidazolium bromide)
BMB: poly(benzyl methacrylate-*b*-methyl methacrylate-*b*-benzyl methacrylate)
[$C_{12}C_{12}$im]$_n$[1,4-BDC]: 1,3-didodecylimidazolium-1,4-benzenedicarboxylate
[$C_{12}C_{12}$im]$_n$[2,6-NDC]: 1,3-didodecylimidazolium-2,6-naphthalenedicarboxylate
[$C_{12}C_{12}$im]$_n$[Trim]: 1,3-didodecylimidazolium trimesate
[$C_{12}C_{12}$im]$_n$[Cit]: 1,3-didodecylimidazolium citrate
[P_{66614}][Glu]: trihexyltetradecylphosphonium gluconate
[P_{4444}][Glu]: tetrabutylphosphonium gluconate
[N_{4444}][Glu]: tetrabutylammonium gluconate
PVDF: polyvinylidene fluoride
PVDF-co-HFP: poly(vinylidene fluoride-co-hexafluoropropylene)
PMMA-g-NPs: poly(methyl methacrylate)-grafted-nanoparticles
SnO_2: tin(IV) oxide
PS: polystyrene
PVC: polyvinyl chloride
DINP: diisononyl phthalate
CITROFOL AHII: tris(2-ethylhexyl) *O*-acetylcitrate
EVA: ethylene-vinyl acetate

REFERENCES

(1) Wasserscheid, P.; Welton, T. *Ionic liquids in synthesis*; John Wiley & Sons: 2008.
(2) Crowhurst, L.; Mawdsley, P. R.; Perez-Arlandis, J. M.; Salter, P. A.; Welton, T. Solvent−solute interactions in ionic liquids. *Phys. Chem. Chem. Phys.* **2003**, *5* (13), 2790−2794.
(3) Earle, M. J.; Esperança, J. M.; Gilea, M. A.; Lopes, J. N. C.; Rebelo, L. P.; Magee, J. W.; Seddon, K. R.; Widegren, J. A. The distillation and volatility of ionic liquids. *Nature* **2006**, *439* (7078), 831−834.
(4) Aschenbrenner, O.; Supasitmongkol, S.; Taylor, M.; Styring, P. Measurement of vapour pressures of ionic liquids and other low vapour pressure solvents. *Green Chem.* **2009**, *11* (8), 1217−1221.
(5) Kosmulski, M.; Gustafsson, J.; Rosenholm, J. B. Thermal stability of low temperature ionic liquids revisited. *Thermochim. Acta* **2004**, *412* (1−2), 47−53.
(6) Anderson, J. L.; Ding, J.; Welton, T.; Armstrong, D. W. Characterizing ionic liquids on the basis of multiple solvation interactions. *J. Am. Chem. Soc.* **2002**, *124* (47), 14247−14254.
(7) Welton, T. Ionic liquids in green chemistry. *Green Chem.* **2011**, *13* (2), 225−225.
(8) Verdía, P.; Brandt, A.; Hallett, J. P.; Ray, M. J.; Welton, T. Fractionation of lignocellulosic biomass with the ionic liquid 1-butylimidazolium hydrogen sulfate. *Green Chem.* **2014**, *16* (3), 1617−1627.
(9) Lu, B.; Xu, A.; Wang, J. Cation does matter: how cationic structure affects the dissolution of cellulose in ionic liquids. *Green Chem.* **2014**, *16* (3), 1326−1335.
(10) Skarmoutsos, I.; Dellis, D.; Matthews, R. P.; Welton, T.; Hunt, P. A. Hydrogen bonding in 1-butyl-and 1-ethyl-3-methylimidazolium chloride ionic liquids. *J. Phys. Chem. B* **2012**, *116* (16), 4921−4933.
(11) Passos, H.; Freire, M. G.; Coutinho, J. A. Ionic liquid solutions as extractive solvents for value-added compounds from biomass. *Green Chem.* **2014**, *16* (12), 4786−4815.

DOI: 10.1021/acssuschemeng.9b02232
ACS Sustainable Chem. Eng. 2019, 7, 13586−13626

(12) Singh, D.; Gardas, R. L. Influence of Cation Size on the Ionicity, Fluidity, and Physiochemical Properties of 1, 2, 4-Triazolium Based Ionic Liquids. *J. Phys. Chem. B* **2016**, *120* (21), 4834−4842.
(13) Hayes, R.; Imberti, S.; Warr, G. G.; Atkin, R. Effect of Cation Alkyl Chain Length and Anion Type on Protic Ionic Liquid Nanostructure. *J. Phys. Chem. C* **2014**, *118* (25), 13998−14008.
(14) Maia, A. Room Temperature Ionic Liquids: a "Green" Alternative to Conventional Organic Solvents? *Mini-Rev. Org. Chem.* **2011**, *8* (2), 178−185.
(15) Welton, T. Room-temperature ionic liquids. Solvents for synthesis and catalysis. *Chem. Rev.* **1999**, *99* (8), 2071−2084.
(16) Zhou, Y. Recent advances in ionic liquids for synthesis of inorganic nanomaterials. *Curr. Nanosci.* **2005**, *1* (1), 35−42.
(17) Xu, P.; Zheng, G.-W.; Du, P.-X.; Zong, M.-H.; Lou, W.-Y. Whole-Cell Biocatalytic Processes with Ionic Liquids. *ACS Sustainable Chem. Eng.* **2016**, *4* (2), 371−386.
(18) Chatel, G.; Rogers, R. D. Review: Oxidation of Lignin Using Ionic Liquids—An Innovative Strategy To Produce Renewable Chemicals. *ACS Sustainable Chem. Eng.* **2014**, *2* (3), 322−339.
(19) Visser, A. E.; Swatloski, R. P.; Griffin, S. T.; Hartman, D. H.; Rogers, R. D. Liquid/liquid extraction of metal ions in room temperature ionic liquids. *Sep. Sci. Technol.* **2001**, *36* (5−6), 785−804.
(20) Rajabi, M. S.; Moniruzzaman, M.; Mahmood, H.; Sivapragasam, M.; Bustam, M. A. Extraction of β-carotene from organic phase using ammonium based ionic liquids aqueous solution. *J. Mol. Liq.* **2017**, *227*, 15−20.
(21) Berthod, A.; Ruiz-Ángel, M. J.; Carda-Broch, S. Recent advances on ionic liquid uses in separation techniques. *Journal of Chromatography A* **2018**, *1559*, 2−16.
(22) Antonietti, M.; Kuang, D.; Smarsly, B.; Zhou, Y. Ionic liquids for the convenient synthesis of functional nanoparticles and other inorganic nanostructures. *Angew. Chem., Int. Ed.* **2004**, *43* (38), 4988−4992.
(23) Minea, A. A.; Murshed, S. M. S. A review on development of ionic liquid based nanofluids and their heat transfer behavior. *Renewable Sustainable Energy Rev.* **2018**, *91*, 584−599.
(24) Yao, C.; Zhao, Y.; Chen, G. Multiphase processes with ionic liquids in microreactors: hydrodynamics, mass transfer and applications. *Chem. Eng. Sci.* **2018**, *189*, 340−359.
(25) Avilés, M.-D.; Saurín, N.; Sanes, J.; Carrión, F.-J.; Bermúdez, M.-D. Ionanocarbon lubricants. The combination of ionic liquids and carbon nanophases in tribology. *Lubricants* **2017**, *5* (2), 14−22.
(26) Figoli, A.; Marino, T.; Simone, S.; Di Nicolo, E.; Li, X.-M.; He, T.; Tornaghi, S.; Drioli, E. Towards non-toxic solvents for membrane preparation: a review. *Green Chem.* **2014**, *16* (9), 4034−4059.
(27) Khan, A.; Gunawan, C. A.; Zhao, C. Oxygen Reduction Reaction in Ionic Liquids: Fundamentals and Applications in Energy and Sensors. *ACS Sustainable Chem. Eng.* **2017**, *5* (5), 3698−3715.
(28) Yoshida, Y.; Kitagawa, H. Ionic Conduction in Metal−Organic Frameworks with Incorporated Ionic Liquids. *ACS Sustainable Chem. Eng.* **2019**, *7* (1), 70−81.
(29) Toledo Hijo, A. A. C.; Maximo, G. J.; Costa, M. C.; Batista, E. A. C.; Meirelles, A. J. A. Applications of Ionic Liquids in the Food and Bioproducts Industries. *ACS Sustainable Chem. Eng.* **2016**, *4* (10), 5347−5369.
(30) Moniruzzaman, M.; Goto, M. Ionic liquids: future solvents and reagents for pharmaceuticals. *J. Chem. Eng. Jpn.* **2011**, *44* (6), 370−381.
(31) Wang, H.; Gurau, G.; Rogers, R. D. Ionic liquid processing of cellulose. *Chem. Soc. Rev.* **2012**, *41* (4), 1519−1537.
(32) Lee, S. H.; Doherty, T. V.; Linhardt, R. J.; Dordick, J. S. Ionic liquid-mediated selective extraction of lignin from wood leading to enhanced enzymatic cellulose hydrolysis. *Biotechnol. Bioeng.* **2009**, *102* (5), 1368−1376.
(33) Mahmood, H.; Moniruzzaman, M.; Yusup, S.; Akil, H. M. Ionic liquid pretreatment at high solids loading: A clean approach for fabrication of renewable resource based particulate composites. *Polym. Compos.* **2018**, *39* (6), 1994−2003.
(34) Barnes, H. A.; Hutton, J. F.; Walters, K. *An introduction to rheology*; Elsevier: 1989.
(35) Malkin, A. Y.; Isayev, A. I. Applications of Rheology. In *Rheology Concepts, Methods, and Applications*, Second ed.; Oxford: Elsevier, 2012; pp 365−420.
(36) Pogodina, N.; Nowak, M.; Läuger, J.; Klein, C.; Wilhelm, M.; Friedrich, C. Molecular dynamics of ionic liquids as probed by rheology. *J. Rheol.* **2011**, *55* (2), 241−256.
(37) Amarasekara, A. S. Acidic ionic liquids. *Chem. Rev.* **2016**, *116* (10), 6133−6183.
(38) Chen, G.; Chen, N.; Li, L.; Wang, Q.; Duan, W. Ionic Liquid Modified Poly(vinyl alcohol) with Improved Thermal Processability and Excellent Electrical Conductivity. *Ind. Eng. Chem. Res.* **2018**, *57* (15), 5472−5481.
(39) Graessley, W. W. *Polymeric Liquids and Networks: Structure and Properties*; Garland Science: New York, 2004; p 801.
(40) Yue, X.; Chen, X.; Li, Q. Comparison of aggregation behaviors of a phytosterol ethoxylate surfactant in protic and aprotic ionic liquids. *J. Phys. Chem. B* **2012**, *116* (31), 9439−9444.
(41) Lefebvre, J.; Doublier, J.-L. Rheological behavior of polysaccharides aqueous systems. In *Polysaccharides: Structural diversity and functional versatility*; Marcel Dekker: New York, 2005; pp 357−394.
(42) Wittmar, A.; Ruiz-Abad, D.; Ulbricht, M. Dispersions of silica nanoparticles in ionic liquids investigated with advanced rheology. *J. Nanopart. Res.* **2012**, *14* (2), 651−660.
(43) Sheldon, R. A. The E factor 25 years on: the rise of green chemistry and sustainability. *Green Chem.* **2017**, *19* (1), 18−43.
(44) Kümmerer, K. Sustainable Chemistry: A Future Guiding Principle. *Angew. Chem., Int. Ed.* **2017**, *56* (52), 16420−16421.
(45) Vanda, H.; Dai, Y.; Wilson, E. G.; Verpoorte, R.; Choi, Y. H. Green solvents from ionic liquids and deep eutectic solvents to natural deep eutectic solvents. *C. R. Chim.* **2018**, *21* (6), 628−638.
(46) Shakeel, A.; Farooq, U.; Iqbal, T.; Yasin, S.; Lupi, F. R.; Gabriele, D. Key characteristics and modelling of bigels systems: A review. *Mater. Sci. Eng., C* **2019**, *97*, 932−953.
(47) Cecchini, M. M.; Charnay, C.; De Angelis, F.; Lamaty, F.; Martinez, J.; Colacino, E. Poly (ethylene glycol)-Based Ionic Liquids: Properties and Uses as Alternative Solvents in Organic Synthesis and Catalysis. *ChemSusChem* **2014**, *7* (1), 45−65.
(48) Smith, J.; Webber, G. B.; Warr, G. G.; Atkin, R. Rheology of protic ionic liquids and their mixtures. *J. Phys. Chem. B* **2013**, *117* (44), 13930−13935.
(49) Camargo, D.; Andrade, R. S.; Ferreira, G. A.; Mazzer, H.; Cardozo-Filho, L.; Iglesias, M. Investigation of the rheological properties of protic ionic liquids. *J. Phys. Org. Chem.* **2016**, *29* (11), 604−612.
(50) Dold, C.; Amann, T.; Kailer, A. Influence of structural variations on imidazolium-based ionic liquids. *Lubr. Sci.* **2013**, *25* (4), 251−268.
(51) Gusain, R.; Bakshi, P. S.; Panda, S.; Sharma, O. P.; Gardas, R.; Khatri, O. P. Physicochemical and tribophysical properties of trioctylalkylammonium bis (salicylato) borate (N888 n-BScB) ionic liquids: effect of alkyl chain length. *Phys. Chem. Chem. Phys.* **2017**, *19* (9), 6433−6442.
(52) Burrell, G. L.; Dunlop, N. F.; Separovic, F. Non-Newtonian viscous shear thinning in ionic liquids. *Soft Matter* **2010**, *6* (9), 2080−2086.
(53) Rauber, D.; Heib, F.; Schmitt, M.; Hempelmann, R. Trioctylphosphonium room temperature ionic liquids with perfluorinated groups−Physical properties and surface behavior in comparison with the nonfluorinated analogues. *Colloids Surf., A* **2018**, *537*, 116−125.
(54) Moosavi, M.; Daneshvar, A. Investigation of the rheological properties of two imidazolium-based ionic liquids. *J. Mol. Liq.* **2014**, *190*, 59−67.
(55) Amann, T.; Dold, C.; Kailer, A. Rheological characterization of ionic liquids and ionic liquid crystals with promising tribological performance. *Soft Matter* **2012**, *8* (38), 9840−9846.
(56) Jacquemin, J.; Anouti, M. r. m.; Lemordant, D. Physico-chemical properties of non-Newtonian shear thickening diisopropyl-ethyl-ammonium-based protic ionic liquids and their mixtures with water and acetonitrile. *J. Chem. Eng. Data* **2011**, *56* (3), 556−564.

DOI: 10.1021/acssuschemeng.9b02232
ACS Sustainable Chem. Eng. 2019, 7, 13586−13626

(57) Machanová, K.; Boisset, A. l.; Sedláková, Z.; Anouti, M. r. m.; Bendová, M.; Jacquemin, J. Thermophysical properties of ammonium-based bis {(trifluoromethyl) sulfonyl} imide ionic liquids: volumetric and transport properties. *J. Chem. Eng. Data* **2012**, *57* (8), 2227−2235.
(58) Wang, J.; Tian, Y.; Zhao, Y.; Zhuo, K. A volumetric and viscosity study for the mixtures of 1-n-butyl-3-methylimidazolium tetrafluoroborate ionic liquid with acetonitrile, dichloromethane, 2-butanone and N, N − dimethylformamide. *Green Chem.* **2003**, *5* (5), 618−622.
(59) McEwen, A. B.; Ngo, H. L.; LeCompte, K.; Goldman, J. L. Electrochemical properties of imidazolium salt electrolytes for electrochemical capacitor applications. *J. Electrochem. Soc.* **1999**, *146* (5), 1687−1695.
(60) Okoturo, O.; VanderNoot, T. Temperature dependence of viscosity for room temperature ionic liquids. *J. Electroanal. Chem.* **2004**, *568*, 167−181.
(61) Fulcher, G. S. Analysis of recent measurements of the viscosity of glasses. *J. Am. Ceram. Soc.* **1925**, *8* (6), 339−355.
(62) Regueira, T.; Lugo, L.; Comuñas, M. J.; Fernández, J. High Pressure Rheological Behavior of 1-Ethyl-3-methylimidazolium n-Hexylsulfate and Trihexyl (tetradecyl) phosphonium Tris (pentafluoroethyl) trifluorophosphate. *J. Chem. Eng. Data* **2017**, *62* (9), 2927−2936.
(63) Rauber, D.; Zhang, P.; Huch, V.; Kraus, T.; Hempelmann, R. Lamellar structures in fluorinated phosphonium ionic liquids: the roles of fluorination and chain length. *Phys. Chem. Chem. Phys.* **2017**, *19* (40), 27251−27258.
(64) Han, Y.; Qiao, D.; Sun, L.; Feng, D. Functional alkylimidazolium ionic liquids as lubricants for steel/aluminum contact: Influence of the functional groups on tribological performance. *Tribol. Int.* **2018**, *119*, 766−774.
(65) Ferreira, M. L.; Pastoriza-Gallego, M. J.; Araújo, J. o. M.; Canongia Lopes, J. N.; Rebelo, L. P. N.; M. Piñeiro, M.; Shimizu, K.; Pereiro, A. B. Influence of Nanosegregation on the Phase Behavior of Fluorinated Ionic Liquids. *J. Phys. Chem. C* **2017**, *121* (9), 5415−5427.
(66) Tao, R.; Simon, S. L. Rheology of imidazolium-based ionic liquids with aromatic functionality. *J. Phys. Chem. B* **2015**, *119* (35), 11953−11959.
(67) Pogodina, N.; Metwalli, E.; Müller-Buschbaum, P.; Wendler, K.; Lungwitz, R.; Spange, S.; Shamshina, J.; Rogers, R.; Friedrich, C. Peculiar Behavior of Azolium Azolate Energetic Ionic Liquids. *J. Phys. Chem. Lett.* **2011**, *2* (20), 2571−2576.
(68) Sharma, G.; Singh, D.; Gardas, R. L. Effect of Fluorinated Anion on the Physicochemical, Rheological and Solvatochromic Properties of Protic and Aprotic Ionic Liquids: Experimental and Computational Study. *ChemistrySelect* **2017**, *2* (35), 11653−11658.
(69) Blanco-Díaz, E. G.; Castrejón-González, E. O.; Alvarado, J. F. J.; Estrada-Baltazar, A.; Castillo-Borja, F. Rheological behavior of ionic liquids: Analysis of the H-bond formation by molecular dynamics. *J. Mol. Liq.* **2017**, *242*, 265−271.
(70) Butler, S. N.; Müller-Plathe, F. Nanostructures of ionic liquids do not break up under shear: A molecular dynamics study. *J. Mol. Liq.* **2014**, *192*, 114−117.
(71) Dworak, C.; Ligon, S. C.; Tiefenthaller, R.; Lagref, J. J.; Frantz, R.; Cherkaoui, Z. M.; Liska, R. Imidazole-based ionic liquids for free radical photopolymerization. *Des. Monomers Polym.* **2015**, *18* (3), 262−270.
(72) Gaciño, F. M.; Comuñas, M. J.; Regueira, T.; Segovia, J. J.; Fernández, J. On the viscosity of two 1-butyl-1-methylpyrrolidinium ionic liquids: Effect of the temperature and pressure. *J. Chem. Thermodyn.* **2015**, *87*, 43−51.
(73) Yonekura, R.; Grinstaff, M. W. The effects of counterion composition on the rheological and conductive properties of mono-and diphosphonium ionic liquids. *Phys. Chem. Chem. Phys.* **2014**, *16* (38), 20608−20617.
(74) Pereiro, A. B.; Pastoriza-Gallego, M.; Shimizu, K.; Marrucho, I. M.; Lopes, J. N. C.; Piñeiro, M. M.; Rebelo, L. P. N. On the Formation of a Third, Nanostructured Domain in Ionic Liquids. *J. Phys. Chem. B* **2013**, *117* (37), 10826−10833.
(75) Hoque, M.; Thomas, M. L.; Miran, M. S.; Akiyama, M.; Marium, M.; Ueno, K.; Dokko, K.; Watanabe, M. Protic ionic liquids with primary alkylamine-derived cations: the dominance of hydrogen bonding on observed physicochemical properties. *RSC Adv.* **2018**, *8* (18), 9790−9794.
(76) Sarman, S.; Wang, Y.-L.; Rohlmann, P.; Glavatskih, S.; Laaksonen, A. Rheology of phosphonium ionic liquids: a molecular dynamics and experimental study. *Phys. Chem. Chem. Phys.* **2018**, *20* (15), 10193−10203.
(77) Larson, R. G. *The Structure and Rheology of Complex Fluids*, 1st ed.; Oxford University Press: 1998; p 688.
(78) Horinaka, J. i.; Yasuda, R.; Takigawa, T. Entanglement properties of cellulose and amylose in an ionic liquid. *J. Polym. Sci., Part B: Polym. Phys.* **2011**, *49* (13), 961−965.
(79) Chen, X.; Zhang, Y.; Wang, H.; Wang, S.-W.; Liang, S.; Colby, R. H. Solution rheology of cellulose in 1-butyl-3-methyl imidazolium chloride. *J. Rheol.* **2011**, *55* (3), 485−494.
(80) Chen, X.; Zhang, Y.; Cheng, L.; Wang, H. Rheology of concentrated cellulose solutions in 1-butyl-3-methylimidazolium chloride. *J. Polym. Environ.* **2009**, *17* (4), 273−279.
(81) Gericke, M.; Schlufter, K.; Liebert, T.; Heinze, T.; Budtova, T. Rheological properties of cellulose/ionic liquid solutions: from dilute to concentrated states. *Biomacromolecules* **2009**, *10* (5), 1188−1194.
(82) Renaud, M.; Belgacem, M. N.; Rinaudo, M. Rheological behaviour of polysaccharide aqueous solutions. *Polymer* **2005**, *46* (26), 12348−12358.
(83) Persin, Z.; Stana-Kleinschek, K.; Foster, T. J.; Van Dam, J. E.; Boeriu, C. G.; Navard, P. Challenges and opportunities in polysaccharides research and technology: The EPNOE views for the next decade in the areas of materials, food and health care. *Carbohydr. Polym.* **2011**, *84* (1), 22−32.
(84) Horinaka, J.-i.; Okamoto, A.; Takigawa, T. Rheological properties of concentrated solutions of gelatin in an ionic liquid 1-ethyl-3-methylimidazolium dimethyl phosphate. *Int. J. Biol. Macromol.* **2016**, *91*, 789−793.
(85) Horinaka, J. i.; Urabayashi, Y.; Takigawa, T.; Ohmae, M. Entanglement network of chitin and chitosan in ionic liquid solutions. *J. Appl. Polym. Sci.* **2013**, *130* (4), 2439−2443.
(86) Tan, X.; Li, X.; Chen, L.; Xie, F. Solubility of starch and microcrystalline cellulose in 1-ethyl-3-methylimidazolium acetate ionic liquid and solution rheological properties. *Phys. Chem. Chem. Phys.* **2016**, *18* (39), 27584−27593.
(87) Liu, W.; Budtova, T. Dissolution of unmodified waxy starch in ionic liquid and solution rheological properties. *Carbohydr. Polym.* **2013**, *93* (1), 199−206.
(88) Mateyawa, S.; Xie, D. F.; Truss, R. W.; Halley, P. J.; Nicholson, T. M.; Shamshina, J. L.; Rogers, R. D.; Boehm, M. W.; McNally, T. Effect of the ionic liquid 1-ethyl-3-methylimidazolium acetate on the phase transition of starch: Dissolution or gelatinization? *Carbohydr. Polym.* **2013**, *94* (1), 520−530.
(89) Horinaka, J. i.; Yasuda, R.; Takigawa, T. Rheological properties of concentrated solutions of agarose in ionic liquid. *J. Appl. Polym. Sci.* **2012**, *123* (5), 3023−3027.
(90) Horinaka, J.-i.; Yasuda, R.; Takigawa, T. Rheological properties of concentrated solutions of galactomannans in an ionic liquid. *Carbohydr. Polym.* **2012**, *89* (4), 1018−1021.
(91) Klemm, D.; Heublein, B.; Fink, H. P.; Bohn, A. Cellulose: fascinating biopolymer and sustainable raw material. *Angew. Chem., Int. Ed.* **2005**, *44* (22), 3358−3393.
(92) Krassig, H. A. *Cellulose: Structure Accessibility and Reactivity*; Gordon and Breach Science Publishers, 1993.
(93) Roy, D.; Semsarilar, M.; Guthrie, J. T.; Perrier, S. Cellulose modification by polymer grafting: a review. *Chem. Soc. Rev.* **2009**, *38* (7), 2046−2064.
(94) Kamide, K. *Cellulose and cellulose derivatives*; Elsevier: 2005.
(95) Hina, S.; Zhang, Y.; Wang, H. Role of ionic liquids in dissolution and regeneration of cellulose. *Rev. Adv. Mater. Sci.* **2015**, *40* (3), 215−226.
(96) Gericke, M.; Fardim, P.; Heinze, T. Ionic liquids—promising but challenging solvents for homogeneous derivatization of cellulose. *Molecules* **2012**, *17* (6), 7458−7502.

DOI: 10.1021/acssuschemeng.9b02232
ACS Sustainable Chem. Eng. 2019, 7, 13586−13626

(97) Sescousse, R.; Le, K. A.; Ries, M. E.; Budtova, T. Viscosity of cellulose− imidazolium-based ionic liquid solutions. *J. Phys. Chem. B* **2010**, *114* (21), 7222−7228.
(98) Haward, S. J.; Sharma, V.; Butts, C. P.; McKinley, G. H.; Rahatekar, S. S. Shear and extensional rheology of cellulose/ionic liquid solutions. *Biomacromolecules* **2012**, *13* (5), 1688−1699.
(99) Sammons, R.; Collier, J.; Rials, T.; Petrovan, S. Rheology of 1-butyl-3-methylimidazolium chloride cellulose solutions. I. Shear rheology. *J. Appl. Polym. Sci.* **2008**, *110* (2), 1175−1181.
(100) Collier, J.; Watson, J.; Collier, B.; Petrovan, S. Rheology of 1-butyl-3-methylimidazolium chloride cellulose solutions. II. Solution character and preparation. *J. Appl. Polym. Sci.* **2008**, *111* (2), 1019−1027.
(101) Cox, W.; Merz, E. Correlation of dynamic and steady flow viscosities. *J. Polym. Sci.* **1958**, *28* (118), 619−622.
(102) Lu, F.; Cheng, B.; Song, J.; Liang, Y. Rheological characterization of concentrated cellulose solutions in 1-allyl-3-methylimidazolium chloride. *J. Appl. Polym. Sci.* **2012**, *124* (4), 3419−3425.
(103) Sammons, R. J.; Collier, J. R.; Rials, T. G.; Petrovan, S. Rheology of 1-butyl-3-methylimidazolium chloride cellulose solutions. III. Elongational rheology. *J. Appl. Polym. Sci.* **2008**, *110* (5), 3203−3208.
(104) Anna, S. L.; McKinley, G. H. Elasto-capillary thinning and breakup of model elastic liquids. *J. Rheol.* **2001**, *45* (1), 115−138.
(105) Stelter, M.; Brenn, G.; Yarin, A.; Singh, R.; Durst, F. Investigation of the elongational behavior of polymer solutions by means of an elongational rheometer. *J. Rheol.* **2002**, *46* (2), 507−527.
(106) Ma, B.; Qin, A.; Li, X.; He, C. Preparation of cellulose hollow fiber membrane from bamboo pulp/1-butyl-3-methylimidazolium chloride/dimethylsulfoxide system. *Ind. Eng. Chem. Res.* **2013**, *52* (27), 9417−9421.
(107) Le, K. A.; Sescousse, R.; Budtova, T. Influence of water on cellulose-EMIMAc solution properties: a viscometric study. *Cellulose* **2012**, *19* (1), 45−54.
(108) Rinaldi, R. Instantaneous dissolution of cellulose in organic electrolyte solutions. *Chem. Commun.* **2011**, *47* (1), 511−513.
(109) Lv, Y.; Wu, J.; Zhang, J.; Niu, Y.; Liu, C.-Y.; He, J.; Zhang, J. Rheological properties of cellulose/ionic liquid/dimethylsulfoxide (DMSO) solutions. *Polymer* **2012**, *53* (12), 2524−2531.
(110) Boerstoel, H.; Maatman, H.; Westerink, J.; Koenders, B. Liquid crystalline solutions of cellulose in phosphoric acid. *Polymer* **2001**, *42* (17), 7371−7379.
(111) Onofrei, M.-D.; Dobos, A. M.; Stoica, I.; Olaru, N.; Olaru, L.; Ioan, S. Lyotropic liquid crystal phases in cellulose acetate phthalate/hydroxypropyl cellulose blends. *J. Polym. Environ.* **2014**, *22* (1), 99−111.
(112) Song, H.; Zhang, J.; Niu, Y.; Wang, Z. Phase transition and rheological behaviors of concentrated cellulose/ionic liquid solutions. *J. Phys. Chem. B* **2010**, *114* (18), 6006−6013.
(113) Song, H.; Niu, Y.; Wang, Z.; Zhang, J. Liquid Crystalline Phase and Gel− Sol Transitions for Concentrated Microcrystalline Cellulose (MCC)/1-Ethyl-3-methylimidazolium Acetate (EMIMAc) Solutions. *Biomacromolecules* **2011**, *12* (4), 1087−1096.
(114) Michels, C.; Kosan, B. Structure of lyocell fibers, spun from aqueous amino oxides and/or ionic liquids. *Lenzinger Ber.* **2006**, *86*, 144−153.
(115) Kosan, B.; Michels, C.; Meister, F. Dissolution and forming of cellulose with ionic liquids. *Cellulose* **2008**, *15* (1), 59−66.
(116) Hermanutz, F.; Meister, F.; Uerdingen, E. New developments in the manufacture of cellulose fibers with ionic liquids. *Chem. Fibers Int.* **2006**, *56* (6), 342−344.
(117) Hermanutz, F.; Gähr, F.; Uerdingen, E.; Meister, F.; Kosan, B. In *New developments in dissolving and processing of cellulose in ionic liquids*; Macromolecular symposia, Wiley Online Library: 2008; pp 23−27.
(118) Härdelin, L.; Perzon, E.; Hagström, B.; Walkenström, P.; Gatenholm, P. Influence of molecular weight and rheological behavior on electrospinning cellulose nanofibers from ionic liquids. *J. Appl. Polym. Sci.* **2013**, *130* (4), 2303−2310.
(119) Nazari, B.; Utomo, N. W.; Colby, R. H. The Effect of Water on Rheology of Native Cellulose/Ionic Liquids Solutions. *Biomacromolecules* **2017**, *18* (9), 2849−2857.
(120) Lee, Y. J.; Kwon, M. K.; Lee, S. J.; Jeong, S. W.; Kim, H. C.; Oh, T. H.; Lee, S. G. Influence of water on phase transition and rheological behavior of cellulose/ionic liquid/water ternary systems. *J. Appl. Polym. Sci.* **2017**, *134* (22), 44658.
(121) Kuang, Q.-L.; Zhao, J.-C.; Niu, Y.-H.; Zhang, J.; Wang, Z.-G. Celluloses in an ionic liquid: the rheological properties of the solutions spanning the dilute and semidilute regimes. *J. Phys. Chem. B* **2008**, *112* (33), 10234−10240.
(122) Lu, F.; Song, J.; Cheng, B.-W.; Ji, X.-J.; Wang, L.-J. Viscoelasticity and rheology in the regimes from dilute to concentrated in cellulose 1-ethyl-3-methylimidazolium acetate solutions. *Cellulose* **2013**, *20* (3), 1343−1352.
(123) Rubinstein, M.; Colby, R. H. *Polymer physics*; Oxford University Press New York, 2003; Vol. *23*.
(124) Ferry, J. D.; Ferry, J. D. *Viscoelastic properties of polymers*; John Wiley & Sons: 1980.
(125) Wang, L.; Gao, L.; Cheng, B.; Ji, X.; Song, J.; Lu, F. Rheological behaviors of cellulose in 1-ethyl-3-methylimidazolium chloride/dimethylsulfoxide. *Carbohydr. Polym.* **2014**, *110*, 292−297.
(126) Namazi, H. Polymers in our daily life. *BioImpacts* **2017**, *7* (2), 73−74.
(127) Karak, N. *Fundamentals of polymers: raw materials to finish products*; PHI Learning Pvt. Ltd.: 2009.
(128) Seddon, K. R. Ionic liquids for clean technology. *J. Chem. Technol. Biotechnol.* **1997**, *68* (4), 351−356.
(129) Ranke, J.; Stolte, S.; Störmann, R.; Arning, J.; Jastorff, B. Design of sustainable chemical products the example of ionic liquids. *Chem. Rev.* **2007**, *107* (6), 2183−2206.
(130) Zhu, X.; Chen, X.; Saba, H.; Zhang, Y.; Wang, H. Linear viscoelasticity of poly (acrylonitrile-co-itaconic acid)/1-butyl-3-methylimidazolium chloride extended from dilute to concentrated solutions. *Eur. Polym. J.* **2012**, *48* (3), 597−603.
(131) Yang, T.; Yao, Y.; Lin, Y.; Wang, B.; Xiang, R.; Wu, Y.; Wu, D. Electrospinning of polyacrylonitrile fibers from ionic liquid solution. *Appl. Phys. A: Mater. Sci. Process.* **2010**, *98* (3), 517−523.
(132) Yang, T.; Yao, Y.; Lin, Y.; Wang, B.; Niu, A.; Wu, D. Rheological behaviour of polyacrylonitrile in an ionic liquid solution. *Iran. Polym. J.* **2010**, *19* (11), 843−852.
(133) Liu, F.; Lv, Y.; Liu, J.; Yan, Z.-C.; Zhang, B.; Zhang, J.; He, J.; Liu, C.-Y. Crystallization and rheology of poly (ethylene oxide) in imidazolium ionic liquids. *Macromolecules* **2016**, *49* (16), 6106−6115.
(134) Smith, J.; Webber, G.; Warr, G.; Zimmer, A.; Atkin, R.; Werzer, O. Shear dependent viscosity of poly (ethylene oxide) in two protic ionic liquids. *J. Colloid Interface Sci.* **2014**, *430*, 56−60.
(135) Luo, H.; Xiao, Z.; Chen, Y.; Niu, Y.; Li, G. Phase separation kinetics and rheological behavior of Poly(ethylene oxide)/ionic liquid mixtures with large dynamic asymmetry. *Polymer* **2017**, *123*, 290−300.
(136) Xiao, Z.; Larson, R. G.; Chen, Y.; Zhou, C.; Niu, Y.; Li, G. Unusual phase separation and rheological behavior of poly(ethylene oxide)/ionic liquid mixtures with specific interactions. *Soft Matter* **2016**, *12* (36), 7613−7623.
(137) Madhavan, P.; Sougrat, R.; Behzad, A. R.; Peinemann, K.-V.; Nunes, S. P. Ionic liquids as self-assembly guide for the formation of nanostructured block copolymer membranes. *J. Membr. Sci.* **2015**, *492*, 568−577.
(138) Walden, P. Molecular weights and electrical conductivity of several fused salts. *Bull. Acad. Imper. Sci. (St. Petersburg)* **1914**, *1800* (85).405422
(139) Evans, D. F.; Yamauchi, A.; Roman, R.; Casassa, E. Z. Micelle formation in ethylammonium nitrate, a low-melting fused salt. *J. Colloid Interface Sci.* **1982**, *88* (1), 89−96.
(140) Morse, D. C. Topological instabilities and phase behavior of fluid membranes. *Phys. Rev. E: Stat. Phys., Plasmas, Fluids, Relat. Interdiscip. Top.* **1994**, *50* (4), R2423−R2426.
(141) Greaves, T. L.; Drummond, C. J. Ionic liquids as amphiphile self-assembly media. *Chem. Soc. Rev.* **2008**, *37* (8), 1709−1726.

DOI: 10.1021/acssuschemeng.9b02232
ACS Sustainable Chem. Eng. 2019, 7, 13586−13626

(142) López-Barrón, C. R.; Wagner, N. J. Structural transitions of CTAB micelles in a protic ionic liquid. *Langmuir* **2012**, *28* (35), 12722−12730.
(143) López-Barrón, C. R.; Basavaraj, M. G.; DeRita, L.; Wagner, N. J. Sponge-to-lamellar transition in a double-tail cationic surfactant/protic ionic liquid system: structural and rheological analysis. *J. Phys. Chem. B* **2012**, *116* (2), 813−822.
(144) Yue, X.; Chen, X.; Wang, X.; Li, Z. Lyotropic liquid crystalline phases formed by phyosterol ethoxylates in room-temperature ionic liquids. *Colloids Surf., A* **2011**, *392* (1), 225−232.
(145) Mahamat Nor, S. B.; Woi, P. M.; Ng, S. H. Characterisation of ionic liquids nanoemulsion loaded with piroxicam for drug delivery system. *J. Mol. Liq.* **2017**, *234*, 30−39.
(146) Meng, X.; Devemy, J.; Verney, V.; Gautier, A.; Husson, P.; Andanson, J. M. Improving Cellulose Dissolution in Ionic Liquids by Tuning the Size of the Ions: Impact of the Length of the Alkyl Chains in Tetraalkylammonium Carboxylate. *ChemSusChem* **2017**, *10* (8), 1749−1760.
(147) Napso, S.; Rein, D. M.; Khalfin, R.; Cohen, Y. Semidilute solution structure of cellulose in an ionic liquid and its mixture with a polar organic co-solvent studied by small-angle X-ray scattering. *J. Polym. Sci., Part B: Polym. Phys.* **2017**, *55* (11), 888−894.
(148) Gunasekera, D. H.; Kuek, S.; Hasanaj, D.; He, Y.; Tuck, C.; Croft, A. K.; Wildman, R. D. Three dimensional ink-jet printing of biomaterials using ionic liquids and co-solvents. *Faraday Discuss.* **2016**, *190*, 509−523.
(149) Lu, F.; Wang, L.; Zhang, C.; Cheng, B.; Liu, R.; Huang, Y. Influence of temperature on the solution rheology of cellulose in 1-ethyl-3-methylimidazolium chloride/dimethyl sulfoxide. *Cellulose* **2015**, *22* (5), 3077−3087.
(150) Kathirgamanathan, K.; Grigsby, W. J.; Al-Hakkak, J.; Edmonds, N. R. Two-dimensional FTIR as a tool to study the chemical interactions within cellulose-ionic liquid solutions. *Int. J. Polym. Sci.* **2015**, *2015*, 958653.
(151) Michud, A.; Hummel, M.; Haward, S.; Sixta, H. Monitoring of cellulose depolymerization in 1-ethyl-3-methylimidazolium acetate by shear and elongational rheology. *Carbohydr. Polym.* **2015**, *117*, 355−363.
(152) Michud, A.; Hummel, M.; Sixta, H. Influence of molar mass distribution on the final properties of fibers regenerated from cellulose dissolved in ionic liquid by dry-jet wet spinning. *Polymer* **2015**, *75*, 1−9.
(153) Olsson, C.; Idström, A.; Nordstierna, L.; Westman, G. Influence of water on swelling and dissolution of cellulose in 1-ethyl-3-methylimidazolium acetate. *Carbohydr. Polym.* **2014**, *99*, 438−446.
(154) Ingildeev, D.; Effenberger, F.; Bredereck, K.; Hermanutz, F. Comparison of direct solvents for regenerated cellulosic fibers via the lyocell process and by means of ionic liquids. *J. Appl. Polym. Sci.* **2013**, *128* (6), 4141−4150.
(155) Olsson, C.; Westman, G. Wet spinning of cellulose from ionic liquid solutions−viscometry and mechanical performance. *J. Appl. Polym. Sci.* **2013**, *127* (6), 4542−4548.
(156) Rudaz, C.; Budtova, T. Rheological and hydrodynamic properties of cellulose acetate/ionic liquid solutions. *Carbohydr. Polym.* **2013**, *92* (2), 1966−1971.
(157) Hummel, M.; Michud, A.; Sixta, H. Extensional rheology of cellulose-ionic liquid solutions. *Nordic Rheology Conference*, Helsinki, Finland, 2011.
(158) Liu, Z.; Wang, H.; Li, Z.; Lu, X.; Zhang, X.; Zhang, S.; Zhou, K. Characterization of the regenerated cellulose films in ionic liquids and rheological properties of the solutions. *Mater. Chem. Phys.* **2011**, *128* (1−2), 220−227.
(159) Liu, Z.; Wang, H.; Li, Z.; Lu, X.; Zhang, X.; Zhang, S.; Zhou, K. Rheological properties of cotton pulp cellulose dissolved in 1-butyl-3-methylimidazolium chloride solutions. *Polym. Eng. Sci.* **2011**, *51* (12), 2381−2386.
(160) Kosan, B.; Dorn, S.; Meister, F.; Heinze, T. Preparation and subsequent shaping of cellulose acetates using ionic liquids. *Macromol. Mater. Eng.* **2010**, *295* (7), 676−681.
(161) Quan, S.-L.; Kang, S.-G.; Chin, I.-J. Characterization of cellulose fibers electrospun using ionic liquid. *Cellulose* **2010**, *17* (2), 223−230.
(162) Rajeev, A.; Deshpande, A. P.; Basavaraj, M. G. Rheology and microstructure of concentrated microcrystalline cellulose (MCC)/1-allyl-3-methylimidazolium chloride (AmimCl)/water mixtures. *Soft Matter* **2018**, *14* (37), 7615−7624.
(163) Chen, X.; Liang, S.; Wang, S.-W.; Colby, R. H. Linear viscoelastic response and steady shear viscosity of native cellulose in 1-ethyl-3-methylimidazolium methylphosphonate. *J. Rheol.* **2018**, *62* (1), 81−87.
(164) Druel, L.; Niemeyer, P.; Milow, B.; Budtova, T. Rheology of cellulose-[DBNH][CO 2 Et] solutions and shaping into aerogel beads. *Green Chem.* **2018**, *20* (17), 3993−4002.
(165) Wang, Q.; Yang, Y.; Chen, X.; Shao, Z. Investigation of rheological properties and conformation of silk fibroin in the solution of AmimCl. *Biomacromolecules* **2012**, *13* (6), 1875−1881.
(166) Mundsinger, K.; Müller, A.; Beyer, R.; Hermanutz, F.; Buchmeiser, M. R. Multifilament cellulose/chitin blend yarn spun from ionic liquids. *Carbohydr. Polym.* **2015**, *131*, 34−40.
(167) Yao, Y.; Mukuze, K. S.; Zhang, Y.; Wang, H. Rheological behavior of cellulose/silk fibroin blend solutions with ionic liquid as solvent. *Cellulose* **2014**, *21* (1), 675−684.
(168) Yao, Y.; Yan, Z.; Li, Z.; Zhang, Y.; Wang, H. Viscoelastic behavior and sol-gel transition of cellulose/silk fibroin/1-butyl-3-methylimidazolium chloride extended from dilute to concentrated solutions. *Polym. Eng. Sci.* **2018**, *58* (11), 1931−1936.
(169) Gonsior, N.; Hetzer, M.; Kulicke, W.-M.; Ritter, H. First studies on the influence of methylated β-cyclodextrin on the rheological behavior of 1-ethyl-3-methyl imidazolium acetate. *J. Phys. Chem. B* **2010**, *114* (39), 12468−12472.
(170) Wang, X.; Li, Q.; Chen, X.; Li, Z. Effects of Structure Dissymmetry on Aggregation Behaviors of Quaternary Ammonium Gemini Surfactants in a Protic Ionic Liquid EAN. *Langmuir* **2012**, *28* (48), 16547−16554.
(171) Hao, J.; Song, A.; Wang, J.; Chen, X.; Zhuang, W.; Shi, F.; Zhou, F.; Liu, W. Self-Assembled Structure in Room-Temperature Ionic Liquids. *Chem. - Eur. J.* **2005**, *11* (13), 3936−3940.
(172) López-Barrón, C. R.; Li, D.; Wagner, N. J.; Caplan, J. L. Triblock copolymer self-assembly in ionic liquids: effect of PEO block length on the self-assembly of PEO−PPO−PEO in ethylammonium nitrate. *Macromolecules* **2014**, *47* (21), 7484−7495.
(173) Sequeira, R. A.; Singh, N.; Pereira, M. M.; Chudasama, N. A.; Bhattacharya, S.; Sharma, M.; Mondal, D.; Prasad, K. High concentration solubility and stability of ϵ-poly-l-lysine in an ammonium-based ionic liquid: A suitable media for polypeptide packaging and biomaterial preparation. *Int. J. Biol. Macromol.* **2018**, *120*, 378−384.
(174) Lupi, F. R.; Shakeel, A.; Greco, V.; Oliviero Rossi, C.; Baldino, N.; Gabriele, D. A rheological and microstructural characterisation of bigels for cosmetic and pharmaceutical uses. *Mater. Sci. Eng., C* **2016**, *69*, 358−365.
(175) Shakeel, A.; Lupi, F. R.; Gabriele, D.; Baldino, N.; De Cindio, B. Bigels: A unique class of materials for drug delivery applications. *Soft Mater.* **2018**, *16* (2), 77−93.
(176) Lupi, F. R.; Shakeel, A.; Greco, V.; Baldino, N.; Calabrò, V.; Gabriele, D. Organogelation of extra virgin olive oil with fatty alcohols, glyceryl stearate and their mixture. *LWT* **2017**, *77*, 422−429.
(177) Marr, P. C.; Marr, A. C. Ionic liquid gel materials: applications in green and sustainable chemistry. *Green Chem.* **2016**, *18* (1), 105−128.
(178) Iacob, C.; Sangoro, J.; Kipnusu, W.; Valiullin, R.; Kärger, J.; Kremer, F. Enhanced charge transport in nano-confined ionic liquids. *Soft Matter* **2012**, *8* (2), 289−293.
(179) Craythorne, S. J.; Anderson, K.; Lorenzini, F.; McCausland, C.; Smith, E. F.; Licence, P.; Marr, A. C.; Marr, P. C. The Co-Entrapment of a Homogeneous Catalyst and an Ionic Liquid by a Sol−gel Method: Recyclable Ionogel Hydrogenation Catalysts. *Chem. - Eur. J.* **2009**, *15* (29), 7094−7100.

DOI: 10.1021/acssuschemeng.9b02232
ACS Sustainable Chem. Eng. 2019, 7, 13586−13626

(180) Atkin, R.; Warr, G. G. Structure in confined room-temperature ionic liquids. *J. Phys. Chem. C* **2007**, *111* (13), 5162−5168.
(181) Perkin, S. Ionic liquids in confined geometries. *Phys. Chem. Chem. Phys.* **2012**, *14* (15), 5052−5062.
(182) Song, J.; Murphy, R.; Narayan, R.; Davies, G. Biodegradable and compostable alternatives to conventional plastics. *Philos. Trans. R. Soc., B* **2009**, *364* (1526), 2127−2139.
(183) Yates, M. R.; Barlow, C. Y. Life cycle assessments of biodegradable, commercial biopolymers—a critical review. *Resources, Conservation and Recycling* **2013**, *78*, 54−66.
(184) Dickinson, E.; Lorient, D. *Food macromolecules and colloids*; Royal Society of Chemistry, 2007.
(185) Zhang, B.; Sudre, G.; Quintard, G.; Serghei, A.; David, L.; Bernard, J.; Fleury, E.; Charlot, A. Guar gum as biosourced building block to generate highly conductive and elastic ionogels with poly (ionic liquid) and ionic liquid. *Carbohydr. Polym.* **2017**, *157*, 586−595.
(186) Verger, L.; Corre, S.; Poirot, R.; Quintard, G.; Fleury, E.; Charlot, A. Dual guar/ionic liquid gels and biohybrid material thereof: Rheological investigation. *Carbohydr. Polym.* **2014**, *102*, 932−940.
(187) Ariño, R.; Brodin, M.; Boldizar, A.; Westman, G. Thermal and viscoelastic properties of cellulosic gels with different ionic liquids and coagulation agents. *BioResources* **2013**, *8* (2), 2209−2221.
(188) Ziółkowski, B.; Ates, Z.; Gallagher, S.; Byrne, R.; Heise, A.; Fraser, K. J.; Diamond, D. Mechanical Properties and UV Curing Behavior of Poly (N-Isopropylacrylamide) in Phosphonium-Based Ionic Liquids. *Macromol. Chem. Phys.* **2013**, *214* (7), 787−796.
(189) Patel, M.; Gnanavel, M.; Bhattacharyya, A. J. Utilizing an ionic liquid for synthesizing a soft matter polymer "gel" electrolyte for high rate capability lithium-ion batteries. *J. Mater. Chem.* **2011**, *21* (43), 17419−17424.
(190) Hall, C. C.; Zhou, C.; Danielsen, S. P.; Lodge, T. P. Formation of Multicompartment Ion Gels by Stepwise Self-Assembly of a Thermoresponsive ABC Triblock Terpolymer in an Ionic Liquid. *Macromolecules* **2016**, *49* (6), 2298−2306.
(191) Ueki, T.; Nakamura, Y.; Usui, R.; Kitazawa, Y.; So, S.; Lodge, T. P.; Watanabe, M. Photoreversible gelation of a triblock copolymer in an ionic liquid. *Angew. Chem., Int. Ed.* **2015**, *54* (10), 3018−3022.
(192) Kitazawa, Y.; Ueki, T.; Niitsuma, K.; Imaizumi, S.; Lodge, T. P.; Watanabe, M. Thermoreversible high-temperature gelation of an ionic liquid with poly (benzyl methacrylate-b-methyl methacrylate-b-benzyl methacrylate) triblock copolymer. *Soft Matter* **2012**, *8* (31), 8067−8074.
(193) Tamate, R.; Hashimoto, K.; Horii, T.; Hirasawa, M.; Li, X.; Shibayama, M.; Watanabe, M. Self-Healing Micellar Ion Gels Based on Multiple Hydrogen Bonding. *Adv. Mater.* **2018**, *30* (36), 1802792.
(194) Nagasawa, J. i.; Wakahara, S.; Matsumoto, H.; Kihara, H.; Yoshida, M. Effects of polyethylene spacer length in polymeric electrolytes on gelation of ionic liquids and ionogel properties. *J. Polym. Sci., Part A: Polym. Chem.* **2015**, *53* (2), 249−255.
(195) Nagasawa, J. i.; Matsumoto, H.; Yoshida, M. Highly efficient and specific gelation of ionic liquids by polymeric electrolytes to form ionogels with substantially high gel−sol transition temperatures and rheological properties like self-standing ability and rapid recovery. *ACS Macro Lett.* **2012**, *1* (9), 1108−1112.
(196) Ishioka, Y.; Minakuchi, N.; Mizuhata, M.; Maruyama, T. Supramolecular gelators based on benzenetricarboxamides for ionic liquids. *Soft Matter* **2014**, *10* (7), 965−971.
(197) Gravsholt, S. Viscoelasticity in highly dilute aqueous solutions of pure cationic detergents. *J. Colloid Interface Sci.* **1976**, *57* (3), 575−577.
(198) Yang, J. Viscoelastic wormlike micelles and their applications. *Curr. Opin. Colloid Interface Sci.* **2002**, *7* (5), 276−281.
(199) Israelachvili, J. N. *Intermolecular and surface forces*; Academic press: 2011.
(200) Zhou, L.; Tian, T.; Xiao, J.; Wang, T.; Yu, L. Aggregation behavior of pyrrolidinium-based surface active ionic liquids in H2O-EAN binary solvents. *J. Mol. Liq.* **2017**, *225*, 50−55.
(201) Wang, X.; Yang, Q.; Cao, Y.; Zhou, J.; Hao, H.; Liang, Y.; Hao, J. Ionogels of a sugar surfactant in ionic liquids. *Chem. - Asian J.* **2016**, *11* (5), 722−729.
(202) da Silva, M. A.; Dreiss, C. A. Soft nanocomposites: nanoparticles to tune gel properties. *Polym. Int.* **2016**, *65* (3), 268−279.
(203) Trivedi, T. J.; Rao, K. S.; Kumar, A. Facile preparation of agarose−chitosan hybrid materials and nanocomposite ionogels using an ionic liquid via dissolution, regeneration and sol−gel transition. *Green Chem.* **2014**, *16* (1), 320−330.
(204) Sharma, M.; Mondal, D.; Mukesh, C.; Prasad, K. Solvent responsive healing of guar gum and guar gum−multiwalled carbon nanotube nanocomposite gels prepared in an ionic liquid. *RSC Adv.* **2013**, *3* (37), 16509−16515.
(205) Song, H.; Luo, Z.; Zhao, H.; Luo, S.; Wu, X.; Gao, J.; Wang, Z. High tensile strength and high ionic conductivity bionanocomposite ionogels prepared by gelation of cellulose/ionic liquid solutions with nano-silica. *RSC Adv.* **2013**, *3* (29), 11665−11675.
(206) Ramesh, S.; Liew, C.-W. Rheological characterizations of ionic liquid-based gel polymer electrolytes and fumed silica-based composite polymer electrolytes. *Ceram. Int.* **2012**, *38* (4), 3411−3417.
(207) Ponyrko, S.; Donato, R. K.; Matějka, L. Tailored high performance shape memory epoxy−silica nanocomposites. Structure design. *Polym. Chem.* **2016**, *7* (3), 560−572.
(208) Yao, Y.; Xia, X.; Mukuze, K. S.; Zhang, Y.; Wang, H. Study on the temperature-induced sol−gel transition of cellulose/silk fibroin blends in 1-butyl-3-methylimidazolium chloride via rheological behavior. *Cellulose* **2014**, *21* (5), 3737−3743.
(209) Marullo, S.; Rizzo, C.; Dintcheva, N. T.; Giannici, F.; D'Anna, F. Ionic liquids gels: Soft materials for environmental remediation. *J. Colloid Interface Sci.* **2018**, *517*, 182−193.
(210) Pandey, P. K.; Rawat, K.; Aswal, V.; Kohlbrecher, J.; Bohidar, H. Imidazolium based ionic liquid induced DNA gelation at remarkably low concentration. *Colloids Surf., A* **2018**, *538*, 184−191.
(211) Rizzo, C.; Marullo, S.; Campodonico, P. R.; Pibiri, I.; Dintcheva, N. T.; Noto, R.; Millan, D.; D'Anna, F. Self-Sustaining Supramolecular Ionic Liquid Gels for Dye Adsorption. *ACS Sustainable Chem. Eng.* **2018**, *6* (9), 12453−12462.
(212) Billeci, F.; D'Anna, F.; Gunaratne, H. N.; Plechkova, N. V.; Seddon, K. R. Sweet" ionic liquid gels: materials for sweetening of fuels. *Green Chem.* **2018**, *20* (18), 4260−4276.
(213) Taheri, A.; MacFarlane, D. R.; Pozo-Gonzalo, C.; Pringle, J. M. Flexible and non-volatile redox active quasi-solid state ionic liquid based electrolytes for thermal energy harvesting. *Sustainable Energy & Fuels* **2018**, *2* (8), 1806−1812.
(214) Tadros, T. F. *Rheology of dispersions: principles and applications*; John Wiley & Sons, 2011.
(215) Paul, T. C.; Morshed, A.; Fox, E. B.; Khan, J. A. Thermal performance of Al_2O_3 nanoparticle enhanced ionic liquids (NEILs) for concentrated solar power (CSP) applications. *Int. J. Heat Mass Transfer* **2015**, *85*, 585−594.
(216) Asencio, R. n. A. l.; Cranston, E. D.; Atkin, R.; Rutland, M. W. Ionic liquid nanotribology: stiction suppression and surface induced shear thinning. *Langmuir* **2012**, *28* (26), 9967−9976.
(217) Wittmar, A.; Ulbricht, M. Dispersions of various titania nanoparticles in two different ionic liquids. *Ind. Eng. Chem. Res.* **2012**, *51* (25), 8425−8433.
(218) Novak, J.; Britton, M. M. Magnetic resonance imaging of the rheology of ionic liquid colloidal suspensions. *Soft Matter* **2013**, *9* (9), 2730−2737.
(219) Wang, P.; Zakeeruddin, S. M.; Comte, P.; Exnar, I.; Grätzel, M. Gelation of ionic liquid-based electrolytes with silica nanoparticles for quasi-solid-state dye-sensitized solar cells. *J. Am. Chem. Soc.* **2003**, *125* (5), 1166−1167.
(220) Fonseca, G. S.; Umpierre, A. P.; Fichtner, P. F.; Teixeira, S. R.; Dupont, J. The use of imidazolium ionic liquids for the formation and stabilization of Ir0 and Rh0 nanoparticles: efficient catalysts for the hydrogenation of arenes. *Chem. - Eur. J.* **2003**, *9* (14), 3263−3269.

DOI: 10.1021/acssuschemeng.9b02232
ACS Sustainable Chem. Eng. 2019, 7, 13586−13626

(221) Gómez-Ramírez, A.; López-López, M.; González-Caballero, F.; Durán, J. Stability of magnetorheological fluids in ionic liquids. *Smart Mater. Struct.* **2011**, *20* (4), No. 045001.
(222) Gao, J.; Mwasame, P. M.; Wagner, N. J. Thermal rheology and microstructure of shear thickening suspensions of silica nanoparticles dispersed in the ionic liquid $[C_4mim][BF_4]$. *J. Rheol.* **2017**, *61* (3), 525−535.
(223) Smith, J.; Webber, G. B.; Warr, G. G.; Atkin, R. Silica particle stability and settling in protic ionic liquids. *Langmuir* **2014**, *30* (6), 1506−1513.
(224) Wittmar, A.; Gajda, M.; Gautam, D.; Dörfler, U.; Winterer, M.; Ulbricht, M. Influence of the cation alkyl chain length of imidazolium-based room temperature ionic liquids on the dispersibility of TiO_2 nanopowders. *J. Nanopart. Res.* **2013**, *15* (3), 1463−1474.
(225) Rodríguez-Arco, L.; López-López, M. T.; Durán, J. D.; Zubarev, A.; Chirikov, D. Stability and magnetorheological behaviour of magnetic fluids based on ionic liquids. *J. Phys.: Condens. Matter* **2011**, *23* (45), 455101.
(226) Ueno, K.; Sano, Y.; Inaba, A.; Kondoh, M.; Watanabe, M. Soft glassy colloidal arrays in an ionic liquid: colloidal glass transition, ionic transport, and structural color in relation to microstructure. *J. Phys. Chem. B* **2010**, *114* (41), 13095−13103.
(227) Ueno, K.; Imaizumi, S.; Hata, K.; Watanabe, M. Colloidal Interaction in Ionic Liquids: Effects of Ionic Structures and Surface Chemistry on Rheology of Silica Colloidal Dispersions. *Langmuir* **2009**, *25* (2), 825−831.
(228) Ueno, K.; Inaba, A.; Ueki, T.; Kondoh, M.; Watanabe, M. Thermosensitive, Soft Glassy and Structural Colored Colloidal Array in Ionic Liquid: Colloidal Glass to Gel Transition. *Langmuir* **2010**, *26* (23), 18031−18038.
(229) Ueno, K. Soft materials based on colloidal self-assembly in ionic liquids. *Polym. J.* **2018**, *50* (10), 951−958.
(230) Xu, Y.; Zheng, Q.; Song, Y. Comparison studies of rheological and thermal behaviors of ionic liquids and nanoparticle ionic liquids. *Phys. Chem. Chem. Phys.* **2015**, *17* (30), 19815−19819.
(231) Popov, V. N. Carbon nanotubes: properties and application. *Mater. Sci. Eng., R* **2004**, *43* (3), 61−102.
(232) Pamies, R.; Espejo, C.; Carrión, F.; Morina, A.; Neville, A.; Bermúdez, M. Rheological behavior of multiwalled carbon nanotube-imidazolium tosylate ionic liquid dispersions. *J. Rheol.* **2017**, *61* (2), 279−289.
(233) Fukushima, T.; Kosaka, A.; Ishimura, Y.; Yamamoto, T.; Takigawa, T.; Ishii, N.; Aida, T. Molecular Ordering of Organic Molten Salts Triggered by Single-Walled Carbon Nanotubes. *Science* **2003**, *300* (5628), 2072−2074.
(234) Ferreira, A.; Simões, P.; Ferreira, A.; Fonseca, M.; Oliveira, M.; Trino, A. Transport and thermal properties of quaternary phosphonium ionic liquids and IoNanofluids. *J. Chem. Thermodyn.* **2013**, *64*, 80−92.
(235) Wang, B.; Wang, X.; Lou, W.; Hao, J. Rheological and tribological properties of ionic liquid-based nanofluids containing functionalized multi-walled carbon nanotubes. *J. Phys. Chem. C* **2010**, *114* (19), 8749−8754.
(236) Luo, Z.; Wang, A.; Wang, C.; Qin, W.; Zhao, N.; Song, H.; Gao, J. Liquid crystalline phase behavior and fiber spinning of cellulose/ionic liquid/halloysite nanotubes dispersions. *J. Mater. Chem. A* **2014**, *2* (20), 7327−7336.
(237) Zhang, B.; Ning, W.; Zhang, J.; Qiao, X.; Zhang, J.; He, J.; Liu, C.-Y. Stable dispersions of reduced graphene oxide in ionic liquids. *J. Mater. Chem.* **2010**, *20* (26), 5401−5403.
(238) Nasser, M.; Onaizi, S. A.; Hussein, I.; Saad, M.; Al-Marri, M.; Benamor, A. Intercalation of ionic liquids into bentonite: Swelling and rheological behaviors. *Colloids Surf., A* **2016**, *507*, 141−151.
(239) Song, H.-Z.; Luo, Z.-Q.; Wang, C.-Z.; Hao, X.-F.; Gao, J.-G. Preparation and characterization of bionanocomposite fiber based on cellulose and nano-SiO_2 using ionic liquid. *Carbohydr. Polym.* **2013**, *98* (1), 161−167.
(240) Pamies, R.; Avilés, M.; Arias-Pardilla, J.; Espinosa, T.; Carrión, F.; Sanes, J.; Bermúdez, M. Antiwear performance of ionic liquid+graphene dispersions with anomalous viscosity-temperature behavior. *Tribol. Int.* **2018**, *122*, 200−209.
(241) Dutta, B.; Deb, D.; Bhattacharya, S. Ionic liquid-SnO2 nanoparticle hybrid electrolytes for secondary charge storage devices: Physicochemical and electrochemical studies. *Int. J. Hydrogen Energy* **2018**, *43* (8), 4081−4089.
(242) Priyananda, P.; Sabouri, H.; Jain, N.; Hawkett, B. S. Steric Stabilization of γ-Fe_2O_3 Superparamagnetic Nanoparticles in a Hydrophobic Ionic Liquid and the Magnetorheological Behavior of the Ferrofluid. *Langmuir* **2018**, *34* (9), 3068−3075.
(243) Mahalingam, D.; Wang, S.; Nunes, S. P. Graphene Oxide Liquid Crystal Membranes in Protic Ionic Liquid for Nanofiltration. *ACS Applied Nano Materials* **2018**, *1* (9), 4661−4670.
(244) Altin, E.; Gradl, J.; Peukert, W. First Studies on the Rheological Behavior of Suspensions in Ionic Liquids. *Chem. Eng. Technol.* **2006**, *29* (11), 1347−1354.
(245) Pamies, R.; Avilés, M. D.; Arias-Pardilla, J.; Carrión, F. J.; Sanes, J.; Bermúdez, M. D. Rheological study of new dispersions of carbon nanotubes in the ionic liquid 1-ethyl-3-methylimidazolium dicyanamide. *J. Mol. Liq.* **2019**, *278*, 368−375.
(246) Quintana, R.; Persenaire, O.; Lemmouchi, Y.; Sampson, J.; Martin, S.; Bonnaud, L.; Dubois, P. Enhancement of cellulose acetate degradation under accelerated weathering by plasticization with eco-friendly plasticizers. *Polym. Degrad. Stab.* **2013**, *98* (9), 1556−1562.
(247) Schilling, M.; Bouchard, M.; Khanjian, H.; Learner, T.; Phenix, A.; Rivenc, R. Application of chemical and thermal analysis methods for studying cellulose ester plastics. *Acc. Chem. Res.* **2010**, *43* (6), 888−896.
(248) Gan, L.; Liu, J.; Poon, L.; Chew, C.; Gan, L. Microporous polymeric composites from bicontinuous microemulsion polymerization using a polymerizable nonionic surfactant. *Polymer* **1997**, *38* (21), 5339−5345.
(249) Sen, S.; Patil, S.; Argyropoulos, D. S. Thermal properties of lignin in copolymers, blends, and composites: a review. *Green Chem.* **2015**, *17* (11), 4862−4887.
(250) Scott, M. P.; Rahman, M.; Brazel, C. S. Application of ionic liquids as low-volatility plasticizers for PMMA. *Eur. Polym. J.* **2003**, *39* (10), 1947−1953.
(251) Li, Z.; Liu, N.; Yao, Y.; Chen, S.; Wang, H.; Wang, H. Thermal behavior of cellulose diacetate melt using ionic liquids as plasticizers. *RSC Adv.* **2015**, *5* (2), 901−907.
(252) Bendaoud, A.; Chalamet, Y. Plasticizing effect of ionic liquid on cellulose acetate obtained by melt processing. *Carbohydr. Polym.* **2014**, *108*, 75−82.
(253) Tian, Y. C.; Han, K. Q.; Qin, H. L.; Rong, H. P.; Yan, B.; Wang, D.; Liu, S. P.; Yu, M. H. Rheological behaviors of polyacrylonitrile melt using ionic liquids as a plasticizer. *Adv. Mater. Res.* **2012**, *476-478*, 2151−2157.
(254) Marceneiro, S.; Hu, Q.; Dias, A. M.; Lobo, I.; Dias, I.; de Pinho, E.; Rasteiro, M. G.; de Sousa, H. C. Effects of Two Phosphonium-Type Ionic Liquids on the Rheological and Thermomechanical Properties of Emulsion Poly (vinyl chloride)-Based Formulations Plasticized with DINP and CITROFOL. *Ind. Eng. Chem. Res.* **2014**, *53* (41), 16061−16071.
(255) Soares, B. G.; Pontes, K.; Marins, J. A.; Calheiros, L. F.; Livi, S.; Barra, G. M. Poly (vinylidene fluoride-co-hexafluoropropylene)/polyaniline blends assisted by phosphonium−based ionic liquid: dielectric properties and β-phase formation. *Eur. Polym. J.* **2015**, *73*, 65−74.
(256) Liu, D.; Qi, Z.; Zhang, Y.; Xu, J.; Guo, B. Poly (butylene succinate)(PBS)/ionic liquid plasticized starch blends: Preparation, characterization, and properties. *Starch-Stärke* **2015**, *67* (9−10), 802−809.
(257) Yousfi, M.; Livi, S.; Duchet-Rumeau, J. Ionic liquids: A new way for the compatibilization of thermoplastic blends. *Chem. Eng. J.* **2014**, *255*, 513−524.
(258) Soares da Silva, J. P.; Soares, B. G.; Livi, S.; Barra, G. M.O. Phosphonium−based ionic liquid as dispersing agent for MWCNT in melt-mixing polystyrene blends: Rheology, electrical properties and EMI shielding effectiveness. *Mater. Chem. Phys.* **2017**, *189*, 162−168.

DOI: 10.1021/acssuschemeng.9b02232
ACS Sustainable Chem. Eng. 2019, 7, 13586−13626

(259) Ma, H.; Chen, X.; Hsiao, B. S.; Chu, B. Improving toughness of ultra-high molecular weight polyethylene with ionic liquid modified carbon nanofiber. *Polymer* **2014**, *55* (1), 160−165.
(260) Ou, R.; Xie, Y.; Wang, Q.; Sui, S.; Wolcott, M. P. Effects of ionic liquid on the rheological properties of wood flour/high density polyethylene composites. *Composites, Part A* **2014**, *61*, 134−140.
(261) Yang, J.-h.; Xiao, Y.-j.; Yang, C.-j.; Li, S.-t.; Qi, X.-d.; Wang, Y. Multifunctional poly (vinylidene fluoride) nanocomposites via incorporation of ionic liquid coated carbon nanotubes. *Eur. Polym. J.* **2018**, *98*, 375−383.
(262) Chen, G.; Chen, N.; Wang, Q. Preparation of poly (vinyl alcohol)/ionic liquid composites with improved processability and electrical conductivity for fused deposition modeling. *Mater. Des.* **2018**, *157*, 273−283.
(263) Soares, B. G.; Calheiros, L. F.; Silva, A. A.; Indrusiak, T.; Barra, G. M.; Livi, S. Conducting melt blending of polystyrene and EVA copolymer with carbon nanotube assisted by phosphonium-based ionic liquid. *J. Appl. Polym. Sci.* **2018**, *135* (24), 45564.

DOI: 10.1021/acssuschemeng.9b02232
ACS Sustainable Chem. Eng. 2019, 7, 13586−13626